REMARKS

In view of the above amendments and the following remarks, reconsideration of the outstanding office action is respectfully requested.

New claims 37–41 have been added. Support for the subject matter of these claims may be found at paragraphs [0011], [0038], [0055]–[0056], [0059], [0065], and [00104]–[00105]. In addition, accompanying this paper are three exemplary papers that teach measuring membrane potential of a cell to assess activation of a receptor.

For example, monitoring activation of receptors using inside-out patch tests for measuring current flow across kidney cell is disclosed in Dhallan et al., "Primary Structure and Functional Expression of a Cyclic Nucleotide-activated Channel from Olfactory Neurons," *Nature* 347(6289):184–187 (1990) (cyclic-nucleotide-gated channel from olfactory neurons) (attached hereto as Exhibit 1) and Misaka et al., "Taste Buds Have a Cyclic Nucleotide-activated Channel, CNGgust," *J. Bio. Chem.* 272(36):22623–22629 (1997) (CNGgust receptor from rat tongue epithelium) (attached hereto as Exhibit 2). Specifically, Dhallan reports that the electrophysiological properties of a cyclic-nucleotide-gated channel from olfactory neurons were examined by transient expression in a human embryonic kidney cell system. Inside-out patches of plasma membrane were excised from the transfected cells and tested for sensitivity to bath-applied cyclic nucleotides, by measuring membrane currents induced by the nucleotides. Similarly, Misaka reports that CNGgust expressed in human embryonic kidney cells opened upon the addition of cGMP or cAMP. Current was recorded from inside-out patches held in a bath solution containing cGMP or cAMP and subjected to increasing voltages.

Additionally, Altenhofen et al., "Control of Ligand Specificity in Cyclic Nucleotide-gated Channels from Rod Photoreceptors and Olfactory Epithelium," *Proc. Nat'l Acad. Sci. USA* 88:9868–9872 (1991) (attached hereto as Exhibit 3) describes the use of the *Xenopus* oocyte patch test to measure activation of cyclic-nucleotide-gated ionic channels in photoreceptors and olfactory sensory neurons. In particular, macroscopic current measurements on excised inside-out patches were made after injection of mRNA into *Xenopus* oocytes, and were recorded under voltage-clamp conditions. Current-voltage relations were recorded in control and different test solutions containing ligand intermittently.

In light of the disclosure in the present application and the knowledge in the art when the application was filed, one of skill in the art would have known how to measure TRP8 activation by measuring the membrane potential of the cell.

The rejection of claims 17 and 24–36 under 35 U.S.C. § 112 (1st para.) for lack of enablement is respectfully traversed.

The outstanding office action takes the position that one of ordinary skill in the art would not know suitable assays for assessing activation and inhibition of TRP8 and how to correlate the results of such assays and TRP8 activation. In particular, it is asserted that such a skilled artisan would not know whether a particular response indicated activation or inhibition. Applicants respectfully disagree.

The present application (at paragraphs [0011], [0038], [0055]–[0056], [0065], and [0072]) teaches that activation of TRP8 by a bitter tastant results in extracellular calcium entering the cell, thereby activating downstream messengers which, in turn, leads to transmitter release and activation of afferent gustatory nerves. See also page 5, lines 6–13, page 11, lines 1–10, page 18, line 6 through page 19, line 2, page 22, lines 5–11, and page 25, lines 5–17 of the U.S. Provisional Patent Application Serial No. 60/197,491 which the present application claims benefit of. Therefore, activation of TRP8 in the presence of a test compound versus a control is indicated by increased influx of calcium into the cell, as well as increased activation of calcium-induced downstream messengers, increased transmitter release, and increased activation of afferent gustatory nerves.

In conjunction with their Amendment mailed April 4, 2005, applicants submitted references describing various assays (i.e. Gillo et al., "Coexpression of Drosophila TRP and TRP-like Proteins in Xenopus Oocytes Reconstitutes Capacitative Ca2+ Entry," *Proc. Nat'l Acad. Sci. U S A.*, 93(24):14146–14151 (1996) ("Gillo"); Burnashev et al., "Fractional Calcium Currents Through Recombinant GluR Channels of the NMDA, AMPA and Kainate Receptor Subtypes," *J. Physiol.*, 485 (Pt 2):403–418 (1995) ("Burnashev"); and Hu et al., "Appearance of a Novel Ca^{2+} Influx Pathway in Sf9 Insect Cells Following Expression of the Transient Receptor Potential-like (trpl) Protein of Drosophila," *Biochem. Biophys. Res. Commun.*, 201(2):1050–1056 (1994) ("Hu")).

The outstanding office action dismisses these references as not specifically relating to TRP8 activation. While this may be true, it is irrelevant. These references were cited to demonstrate that one of ordinary skill in the art, having read the present application,

would have been able to make and use the present invention. Enablement is thus not analyzed by examination of the cited references alone but in combination with the disclosure of the present application. Properly analyzed, it is clear that the present application fully satisfies the requirements of 35 U.S.C. § 112 (1st para.). In particular, as noted above, the present application teaches that TRP8 activation is indicated by increased influx of calcium into a cell, increased activation of calcium-induced downstream messengers, increased transmitter release, and increased activation of afferent gustatory nerves. Gillo discloses measuring activation of a *Drosophila* TRP channel by monitoring the change in chloride levels and measuring Ca^{2+} entry using Ca^{2+}-sensitive fluorescent dyes. Burnashev discloses studying heterologously expressed ion channels in HEK 293 cells using fluorescent dyes and electrophysiological recordings to monitor Ca^{2+}. Hu teaches monitoring a TRP channel expressed in Sf9 insect cells using the Ca^{2+} indicator dye Fura-2. Thus, these references teach procedures to measure characteristics that the present application teaches can be used to determine whether TRP8 has been activated.

In addition, accompanying this paper are a number of additional papers which demonstrate that the present application fully enables the claimed invention.

Bai et al., "Dimerization of the Extracellular Calcium-sensing Receptor (CaR) on the Cell Surface of CaR-transfected HEK293 Cells," *J. Bio. Chem.* 273(36):23605–23610 (1998) (attached hereto as Exhibit 4) and Chandrashekar et al., "T2Rs Function as Bitter Taste Receptors," *Cell* 100:703–711 (2000) (attached hereto as Exhibit 5) also disclose measuring intracellular calcium levels using fura-2 fluorimetry assays to monitor, e.g., the extracellular calcium-sensing receptor CaR (Bai) and members of the T2R mammalian taste receptor cell family (Chandrashekar). In particular, Bai discloses that activation of the CaR by elevated levels of extracellular calcium stimulates phospholipase C and raises the cytosolic calcium concentration ("$Ca^{2+}{}_i$"). HEK293 cells transfected with CaR cDNAs were loaded with fura-2/AM. The 340/380 excitation ratio of emitted light was then used to calculate $Ca^{2+}{}_i$ after incremental increases in extracellular calcium. Similarly, Chandrashekar reports the expression of putative mammalian taste receptors (T2Rs) with Gα15, a G protein. In this assay, receptor activation reportedly led to increases in intracellular calcium, which was monitored at the single cell level by measuring FURA-2 emission ratios.

Finally, as discussed above, the use of the *Xenopus* oocyte patch test to measure activation of cyclic-nucleotide-gated ionic channels in photoreceptors and olfactory

sensory neurons is described in Altenhofen, and Dhallan and Misaka disclose monitoring activation of receptors using inside-out patch tests for measuring current flow across kidney cell.

Thus, the specification discloses markers of TRP8 activation (e.g., increased intracellular calcium) and assays for these markers were well-known in the art when the application was filed. Accordingly, the rejection for lack of enablement is improper and should be withdrawn.

The rejection of claims 17 and 24–36 under 35 U.S.C. § 112 (1st para.) for lack of written description is respectfully traversed. The PTO's position appears to be that the specification does not correlate the claimed assays to TRP8 activation or bitter taste perception. Applicants respectfully disagree.

Claim 17 expressly correlates assay results (i.e. increased level of TRP8 activation) to what is being measured (i.e. inducing bitter taste perception). In addition to the disclosure identified above in response to the lack of enablement rejection under 35 U.S.C. § 112 (1st para.), the specification expressly correlates TRP8 activation/intracellular calcium (present application at [0060] and U.S. Provisional Patent Application Serial No. 60/197,491 at page 20, lines 8–18) to intracellular cAMP concentration assays (claims 29–33) (present application at [0060] and U.S. Provisional Patent Application Serial No. 60/197,491 at page 20, lines 8–18), and nerve response assays (claim 36) (present application at [0073] and U.S. Provisional Patent Application Serial No. 60/197,491 at page 25, line 18 through page 26, line 3). These specific assays put the public in possession of the genus of TRP8 activation/intracellular calcium assays, demonstrating that claims 17, 25–33, and 36 have written descriptive support. Accordingly, the rejection for lack of written descriptive support under 35 U.S.C. § 112 (1st para.) is improper and should be withdrawn.

The rejection of claims 17 and 24–36 under 35 U.S.C. § 112 (2nd para.) for indefiniteness is respectfully traversed in view of the above amendments. It is the position of the PTO that "TRP8 activation" is not sufficiently defined in the specification, and that the correlation between the claimed assays and TRP8 activation is not delineated in the claims. Applicants respectfully disagree. Claim 17 has now been amended to state that the level of TRP8 activation is measured by measuring the level of intracellular Ca^{2+} in the cell. This is consistent with the present application's teaching on page 23, paragraph [0060] that increased

levels of intracellular Ca^{2+} constitute TRP8 activation. Therefore, the rejection under 35 U.S.C. § 112 (2nd para.) for indefiniteness is improper and should be withdrawn.

In view of all of the foregoing, applicants submit that this case is in condition for allowance and such allowance is earnestly solicited.

Respectfully submitted,

Date: December 20, 2005

Michael L. Goldman
Registration No. 30,727

NIXON PEABODY LLP
Clinton Square, P.O. Box 31051
Rochester, New York 14603-1051
Telephone: (585) 263-1304
Facsimile: (585) 263-1600

CERTIFICATE OF MAILING OR TRANSMISSION [37 CFR 1.8(a)]

I hereby certify that this correspondence is being:

☒ deposited with the United States Postal Service on the date shown below with sufficient postage as first class mail in an envelope addressed to: Mail Stop RCE, Commissioner for Patents, P. O. Box 1450, Alexandria, VA 22313-1450

12/21/05 (Date) Laura Trost (Laura Trost)

21. Monaghan, D. T., Bridges, R. J. & Cotman, C. W. *A. Rev. Pharmac. Tox.* **29**, 365–402 (1989).
22. Bockaert, J. *et al. J. Physiol., Paris* **81**, 219–227 (1986).
23. Sebben, M. *et al. Devl Brain Res.* **52**, 229–239 (1990).
24. Nowak, L., Bregestovski, P., Ascher, P., Herbet, A. & Prochiantz, A. *Nature* **307**, 462–465 (1984).
25. Honoré, T. *et al. Science* **241**, 701–703 (1988).
26. Sugiyama, H., Ito, I. & Watanabe, M. *Neuron* **3**, 129–401 (1988).
27. Yamada, K. A., Dubinsky, J. M. & Rothman, S. M. *J. Neurosci.* **9**, 3230–3236 (1989).
28. Cheng, Y. & Prusoff, W. H. *Biochem. Pharmac.* **22**, 3099–3108 (1973).
29. Manzoni, O. *et al. Neurosci. Lett.* **109**, 146–151 (1990).
30. Pin, J. P., Van Vliet, B. J. & Bockaert, J. *Eur. J. Pharmac.* **172**, 81–91 (1989).
31. Palmer, E., Monaghan, D. T. & Cotman, C. W. *Eur. J. Pharmac.* **166**, 585–587 (1989).
32. Manzoni, O. *et al. Molec. Pharmacol.* (in the press) (1990).
33. Sutherland, C. A. & Amin, D. *J. biol. Chem.* **257**, 14006–14010 (1982).
34. Hebb, D. O. *The Organization of Behavior* (Wiley, New York, 1949).

ACKNOWLEDGEMENTS. We thank A. Turner-Madeuf and M. Passama for help in preparing this manuscript, A. Turner-Madeuf for revising the grammar, and T. Honoré (Ferosam Laboratories) for providing them with CNQX. Support was provided in part by the Centre National de la Recherche Scientifique (CNRS), the Institut National de la Recherche et de la Santé Médicale (INSERM), the Direction des Recherches et Etudes Techniques (DRET) and by Bayer Troponwerke (France and FRG).

Primary structure and functional expression of a cyclic nucleotide-activated channel from olfactory neurons

Ravinder S. Dhallan*, King-Wai Yau†, Karen A. Schrader‡ & Randall R. Reed†‡§

* Department of Biomedical Engineering, † Department of Neuroscience, and ‡ Department of Molecular Biology and Genetics, The Howard Hughes Medical Institute, Johns Hopkins University School of Medicine, Baltimore, Maryland 21205, USA

ODORANT signal transduction occurs in the specialized cilia of the olfactory sensory neurons. Considerable biochemical evidence now indicates that this process could be mediated by a G protein-coupled cascade using cyclic AMP as an intracellular second messenger[1]. A stimulatory G protein α subunit is expressed at high levels in olfactory neurons and is specifically enriched in the cilia[2], as is a novel form of adenylyl cyclase[3]. This implies that the olfactory transduction cascade might involve unique molecular components. Electrophysiological studies have identified a cyclic nucleotide-activated ion channel in olfactory cilia[4]. These observations provide evidence for a model in which odorants increase intracellular cAMP concentration, which in turn activates this channel and depolarizes the sensory neuron. An analogous cascade regulating a cGMP-gated channel mediates visual transduction in photoreceptor cells (see refs 5, 6 for review). The formal similarities between olfactory and visual transduction suggest that the two systems might use homologous channels. Here we report the molecular cloning, functional expression and characterization of a channel that is likely to mediate olfactory transduction.

The coding region of the cGMP-gated channel from bovine rods[7] was isolated and used to screen a rat olfactory complementary DNA library at low stringency (see Fig. 1*a* methods). A single class of recombinant clones was identified. Sequence analysis of the longest of these cDNA clones (clone 3) revealed an open reading frame of 664 amino acids (Fig. 1*a*). The putative protein encoded by this cDNA clone shares considerable homology with the photoreceptor channel (57% identity). One region of sequence divergence occurs at the amino terminus of the two proteins, and is predicted to reside on the cytoplasmic side of the membrane[7]. The remainder of the coding region of these proteins exhibit extensive homology. Notably, the region near the carboxyl terminus implicated as the cyclic nucleotide binding site[7] (overlined region in Fig. 1*a*) is highly conserved. The hydropathicity profile of the rod channel suggests perhaps four or six membrane-spanning regions[7]. The nearly identical hydropathic profiles (Fig. 1*b*) and the high level of overall homology shared by the rod and the olfactory channels do not allow further resolution of possible models for the topological distribution of the membrane-spanning segments proposed previously[7]. In any case, the two channel proteins are likely to have the same topology.

A second full-length independent cDNA clone (clone 2) was also sequenced. The two clones (2 and 3) differ by three nucleotides in length at the 5′ end, the length of the poly(A) tail (13 versus 9 nucleotides) and a single internal position (G versus A at nucleotide 635) that results in a lysine–arginine change in the protein sequence. A third independent cDNA clone contains the A residue, as does clone 3, at this position. The difference could have arisen during cDNA synthesis or as a natural variant in the animal population.

The tissue distribution and abundance of the messenger RNA encoding this putative olfactory channel was determined by northern blot analysis (Fig. 2*a*, right panel). An abundant 3.2-kilobase (kb) message is seen only in RNA from olfactory epithelium. The expression of this message is reduced on elimination of the sensory neurons induced by olfactory bulbectomy[8] (Fig. 2*a*, left panel). These results suggest the channel is expressed in olfactory neurons. A similar pattern of expression is seen for the G protein α-subunit ($G_{olf\alpha}$) specific to olfactory neurons (ref. 2).

The extensive homology shared by the olfactory and the visual channels isolated from different species raised the possibility that they might be derived from the same gene. However, Southern blot analysis of genomic DNA from several species (Fig. 2*b*) revealed unique patterns of hybridization when the coding region of the two channels were used as probes. This observation indicates that the two channels are the products of distinct genes and that they do not have any genomic sequences in common.

The electrophysiological properties of the olfactory channel were examined by transient expression in a human embryonic kidney cell system[9,10]. Inside-out patches of plasma membrane[11] were excised from the transfected cells and tested for sensitivity to bath-applied cyclic nucleotides. At 2 days after transfection, 22 out of 53 patches showed a cyclic-nucleotide-induced current. At earlier times, the frequency of responsive patches was lower, as was the amplitude of the membrane current. In control experiments a total of 50 patches were excised from mock-transfected cells; none of these responded to cyclic nucleotides.

FIG. 1 *a*, The DNA and deduced amino-acid sequences (single-letter code) ► of the rat olfactory channel. The initiating methionine has been assigned position +1. The tandem ATG codons that initiate the open reading frame are preceded by stop codons in all three frames. The second of these methionine residues is in better context for translation initiation[20]. The third row of each line displays the protein sequence of the bovine rod channel[7]; only differences are indicated, and no attempt was made to align the first 150 amino acids of the rod channel. No gaps are required to align the sequences of the two channels, with the exception of a single position at bovine Lys 619, which has no counterpart in the rat olfactory channel; this has been inserted in the displayed sequence as K. The region proposed to bind cyclic nucleotides is overlined. *b*, Hydropathicity comparison of the olfactory and visual channels by the method of Kyte and Doolittle[21]. Hydrophobic regions are shown with positive values.
METHODS. The bovine rod channel probe was obtained using the polymerase chain reaction with oligonucleotides corresponding to the sequences at positions −49–−27 and 2,139–2,166 (ref. 7). The 5′ oligonucleotide contained an *Eco*RI site at the 5′ end. The oligonucleotides were used to prime synthesis from 1 μl of an amplified bovine retinal library (5×10^{10} p.f.u. ml^{-1})[22]. The resulting 2.2-kb fragment was cleaved with *Eco*RI and *Kpn*I at an internal site and cloned into the Bluescript plasmid vector (Stratagene). Purified *Eco*RI–*Kpn*I fragment was subsequently labelled with random hexamers and used to screen 2×10^5 recombinants from a rat olfactory cDNA library. Filters were washed at low stringency (2 × SSC buffer, 1% SDS at 55 °C) as previously described[2]. About 100 hybridizing plaques were obtained and several were analysed further. DNA sequence was determined from both strands using double-stranded templates and specific oligonucleotide primers.

§ To whom correspondence should be addressed.

The following results were obtained from transfections with cDNA clone 3, but no obvious differences were seen with clone 2. Figure 3*a* shows the maximum membrane currents induced in a responsive patch by cAMP (cA), cGMP (cG) and cCMP (cC). Buffered Ringer's solutions with no divalent cations (solution 2 in Fig. 3 legend) were on both sides of the patch. The maximum currents produced by the different ligands were nearly identical, a feature consistent with findings from the native channel in olfactory cilia[4], and distinct from the cyclic-nucleotide-gated channel in rods[12,13]. Figure 3*b* shows the relations between normalized current amplitude and ligand concentration for the three nucleotides at ±40 mV, obtained from the same

a

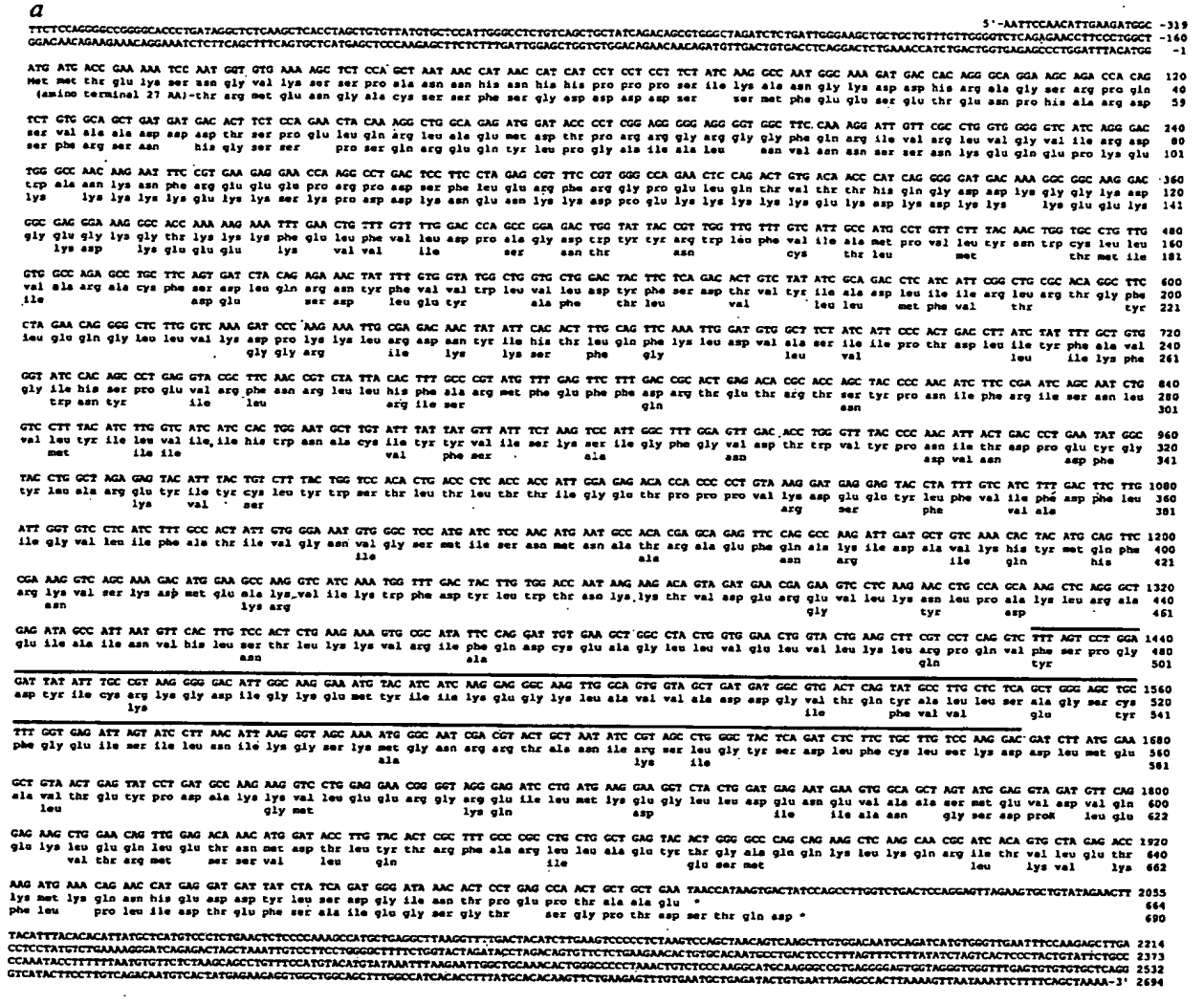

b

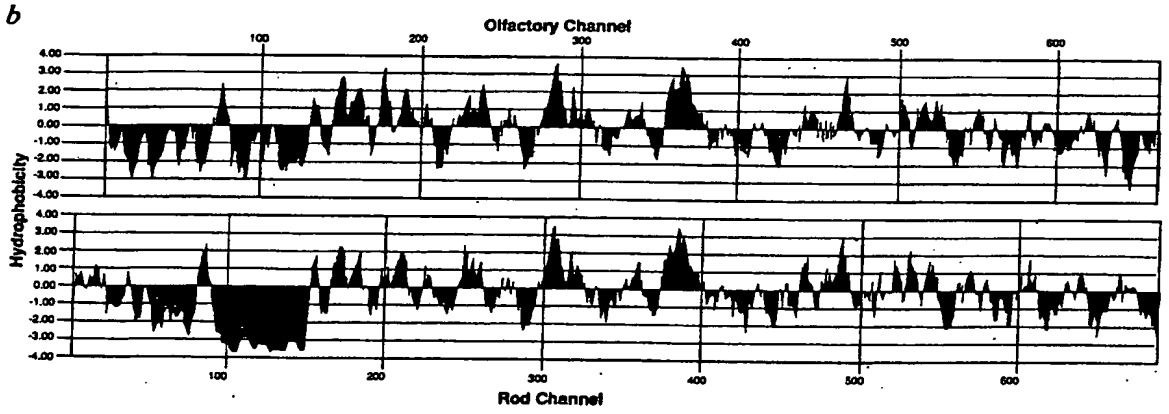

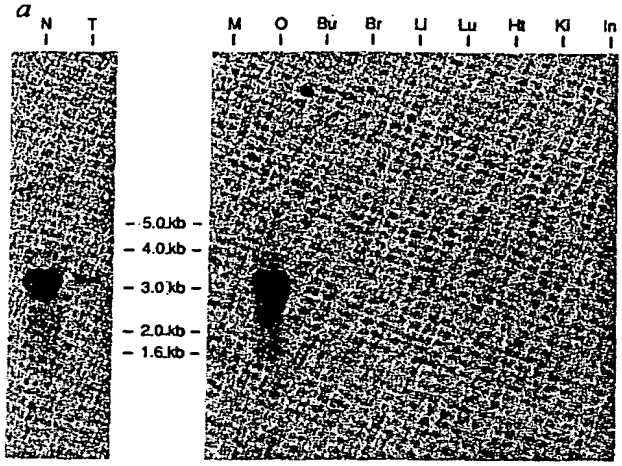

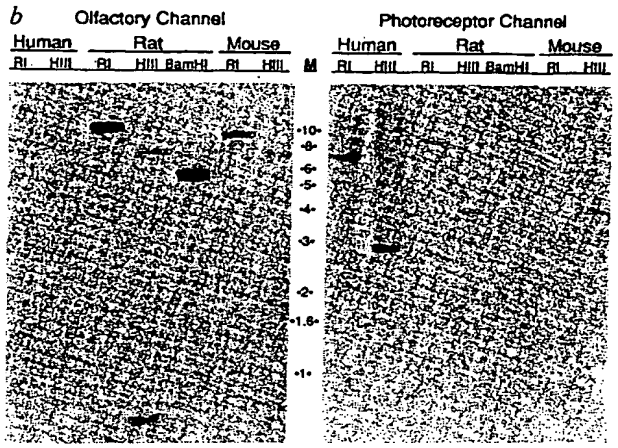

FIG. 2 *a*, Northern analysis of RNA in various tissues. Right panel, the full-length olfactory channel cDNA insert was used to examine the abundance of the corresponding mRNA in several rat tissues. M, markers; O, olfactory; Bu, olfactory bulb; Br, brain; Li, liver; Lu, lung; Ht, heart; Ki, kidney; In, intestine. Left panel, the abundance of the channel mRNA within the olfactory epithelium is seen to decrease when the olfactory neurons are depleted from the tissue. N, RNA derived from normal olfactory epithelium; T, RNA derived from neuron-depleted olfactory epithelium[6]. In a separate experiment, no signal was detected at the same exposure when the olfactory channel probe was hybridized to poly(A)$^+$ rat retinal RNA (0.5 μg) and the filter washed at high stringency (0.1 × SSC and 0.1% SDS) (data not shown) even though the close homology between the two channels might predict a positive hybridization at lower stringencies. *b*, Genomic analysis of fragments that encode the rod channel and the olfactory channel in three species. RI, *Eco*RI; HIII, *Hin*dIII. The only restriction fragments with similar mobility are the rat *Bam*HI fragments.

METHODS. Each lane of the RNA blot analysis contains 10 μg total RNA. Membranes were prepared and hybridized as previously described[23] with ^{32}P-labelled *Eco*RI fragment derived from the full-length cDNA clone. Blots were probed for ribosomal RNA to ascertain that equal amounts of RNA were placed in each lane. For genomic DNA analysis, each lane contained 10 μg digested DNA that was transferred to Hybond membrane (Amersham) and hybridized under the same conditions used to identify the initial olfactory clone (Fig. 1).

FIG. 3 *a*, Membrane currents induced by cyclic nucleotides in an inside-out patch of plasma membranes excised from 293 human embryonic kidney cells transfected with the olfactory channel clone 3 cDNA. Membrane potential was +40 mV, and current flowing from the cytoplasmic to the extracellular side of the membrane is positive. The induced currents were all saturated. The slower decline of the current on removing a solution containing cG was due to the very low activation $K_{1/2}$ for cG. Bandwidth DC-10 Hz. Lower trace shows the time course of solenoid control for the solution changes; there was a lag of about 2 s between solenoid activation and the delivery or removal of cyclic nucleotide (see methods below). The cA + cG solution contained 1 mM of each nucleotide. Base solutions on both sides of patch had composition indicated by solution 2 in methods below. *b*, Normalized dose–response relations between activated current and ligand concentration for the three cyclic nucleotides cA, cG and cC. Same patch as in *a*. Filled symbols, +40 mV; open symbols; −40 mV. Smooth curves are fitted to the filled symbols and are scalings of the Hill equation, $j/j_{max} = C^n/(C^n + K_{1/2}{}^n)$, with a coefficient n of 1.8 and $K_{1/2}$ values of 1.2 μM (cG), 39 μM (cA) and 88 μM (cC), respectively.

METHODS. Transient transfections[9] were performed as follows. The pCIS expression vector contains a cytomegalovirus (CMV) promoter preceding a polylinker site, a simian virus 40 (SV40) polyadenylation site and an SV40 origin of replication. A fragment representing the complete olfactory channel cDNA clone was inserted into the polylinker site of pCIS. The construct RSV-Tag contains the SV40 T antigen under the control of the Rous sarcoma virus (RSV) promoter. Expression vector DNA (5 μg) was mixed with 10 μg of Bluescript carrier DNA and 0.5 μg of RSV-Tag in 250 mM $CaCl_2$ in a volume of 250 μl. This material was added dropwise to 250 μl of 2 × HEPES buffered saline. The solution containing the precipitate was then added to 20% confluent 293 human kidney cells growing in DMEM with 10% FCS, 5% CO_2, and incubation continued for 5 h, at which time the medium was aspirated, the cells washed in PBS and fresh medium added. Incubation then continued as indicated in the text. Cells were mock-transfected as above using the pCIS vector without insert. Electrical recordings were made with a List EPC-7 patch-clamp instrument at bandwidth DC-5 kHz. The recording pipettes were fabricated from borosilicate glass and had tip lumens of ~1 μm. Seal resistance on establishment of a membrane patch was typically

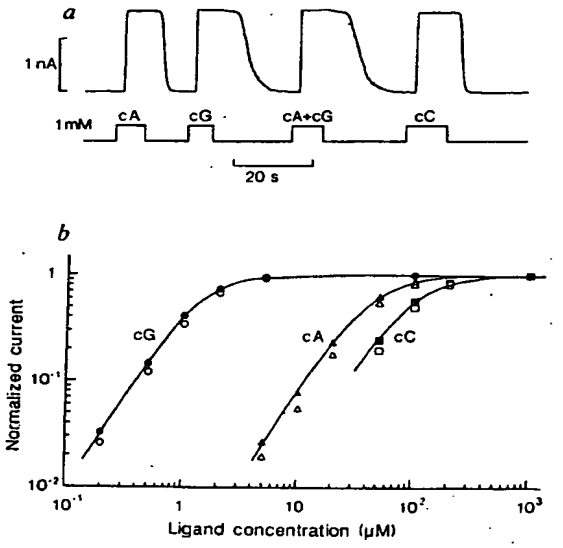

of the order of 10 GΩ. Solutions were at pH [illegible] mM glucose plus the following compositions. Ringer's [illegible] solution 1): 140 mM NaCl, 5 mM KCl, 10 mM sodium HEPES, 2 mM $CaCl_2$, 1 mM $MgCl_2$; Ringer's solution without divalent cations (solution 2): 140 mM NaCl, 5 mM KCl, 10 mM sodium HEPES, 0.5 mM sodium EGTA, 0.5 mM sodium EDTA; pseudointracellular solution (solution 3): 145 mM KCl, 10 mM sodium HEPES, 0.5 mM sodium EGTA, 0.5 mM sodium EDTA. Cyclic nucleotides were bath-applied using a solenoid-controlled rotary valve system[24].

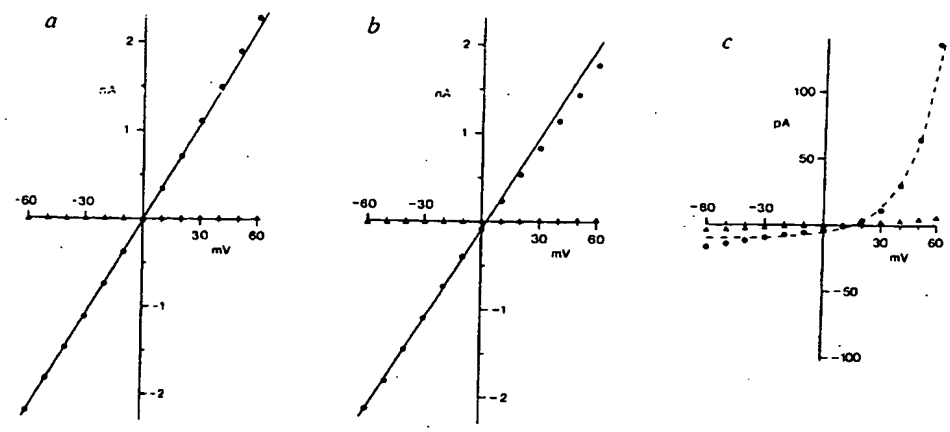

FIG. 4 Steady-state current–voltage relations for the expressed channel under different ionic conditions. In all three cases 1,000 μM cA was present, which fully saturated the current. The experiment consisted of making 1-s voltage pulses at ±10 mV increments from a holding potential of zero, and the current at each voltage was measured at the end of the voltage pulse. ▲, Relation obtained in the absence of ligand (that is, background current); ●, relation induced by ligand (that is, with the background relation already subtracted). *a*, Ringer's solution without divalents (see solution 2 in Fig. 3 legend) on both sides of membrane. Straight line is fitted to points at negative voltages and extrapolated to positive voltages. *b*, Ringer's solution without divalents in pipette and pseudointracellular solution (solution 3 in Fig. 3 legend) in bath. Again, the straight line is fitted to points at negative voltages and extrapolated to positive voltages. Both *a* and *b* represent results from the same patch as in Fig. 3. *c*, Ringer's solution with divalents (solution 1 in Fig. 3 legend) in pipette and pseudointracellular solution in bath. Different patch from *a* and *b*. Dashed curve is a scaling of the equation $j(V)=e^{(V-15)/17.5}-1$ (see text).

patch as in Fig. 3*a*. From two patches, the average half-saturating concentration ($K_{1/2}$) values at +40 mV were 1.2 μM (cG), 38 μM (cA) and 88 μM (cC), and the Hill coefficient was 1.9; at −40 mV, the $K_{1/2}$ values were about 10% higher, but the Hill coefficient was similar. From 12 other patches with physiological concentrations of divalent cations (solution 1 in Fig. 3 legend) on the extracellular side of the membrane, the $K_{1/2}$ values at +40 mV were 2.4 ± 1.1 μM (cG), 68 ± 38 μM (cA) and 123 ± 32 μM (cC), respectively, and the Hill coefficient was 2.0 ± 0.2; at −40 mV, the $K_{1/2}$ values were about 40% higher. These numbers are again broadly consistent with findings from the native channel in olfactory cilia[4], except that the $K_{1/2}$ ratio between cA and cG is about two for the native channel, compared with ~30 for the expressed channel. At nonsaturating ligand concentrations, no desensitization or inactivation of the expressed channel was observed up to 20 s after ligand application at either positive or negative voltages. Finally, *l-cis*-diltiazem[14] at 0.5–1 mM reduced by half the current activated by 100 μM cAMP (four experiments, data not shown).

The current–voltage relation (filled circles) obtained at saturating (1 mM) cA concentration and with symmetrical Ringer's solutions without divalent cations is shown in Fig. 4*a*. Identical relations were obtained with 1 mM cG or cC. The relation is almost linear; the very slight upward curvature probably reflects a small increase in the open probability of the liganded channel at positive voltages, as has been described for the rod channel[15,16]. Figure 4*b* shows, in the same patch, the current–voltage relation when most Na^+ in the bath solution (that is, cytoplasmic side of the membrane) was replaced by K^+ (solution 3, Fig. 3 legend). The current at negative voltages is practically identical to that in Fig. 4*a*, but the outward current at positive voltages is smaller, attributed to a slightly smaller conductance to K^+. The reversal potential in Fig. 4*b* is +3 mV, with a mean of +4.5 mV from two experiments. On the basis of the Goldman–Hodgkin–Katz equation[17], this reversal potential gives a P_K/P_{Na} permeability ratio of 0.82, similar to that observed for the native channel[4,18]. Figure 4*c* shows the current–voltage relation, from a different patch, with physiological Ringer's solution with divalent cations (solution 1) in the patch pipette and pseudointracellular solution (solution 3) in the bath. The relation is nearly linear at negative voltages, but shows outward rectification at voltages positive to the reversal potential, reflecting a voltage-dependent block by divalent cations. The overall relation can be roughly described by a scaling of the function $j(V)=e^{(V-V_r)/V_0}-1$ (dashed curve), where V_r is the reversal potential and V_0 is the slope constant. From four experiments, V_r was 13 ± 2 mV and the best-fit V_0 values was 18 ± 1 mV. This relation with a similar V_0 also describes the behaviour of the cyclic-nucleotide-gated channel in rods under similar ionic conditions[6]. The above characteristics are consistent with observations from the odorant-regulated channel in intact olfactory neurons[18,19], although excised patches from native ciliary membranes[4] give a fairly linear current–voltage relation even at positive voltages.

In summary, the primary structure of a cyclic-nucleotide-gated channel from olfactory neurons has been deduced by cloning and DNA sequence analysis. The homology between this channel and the cyclic-nucleotide-gated channel in retinal rods is consistent with their similar physiological properties. The 30–50-fold higher sensitivity of the olfactory channel[4] to cyclic nucleotides compared to the rod channel[12,13] may result from the amino-acid differences in the putative nucleotide-binding site of the two proteins, though this remains to be examined. We consistently found a $K_{1/2}$ for cAMP of ~40 μM, but the $K_{1/2}$ for cAMP reported by Nakamura and Gold[4] was, curiously, bimodal, being ~2 μM and 40 μM, respectively. Modification of the expressed or the native channel could result in altered nucleotide affinities. In principle one might expect a high $K_{1/2}$ value to be physiologically appropriate, in that this allows the olfactory sensory neuron to be at rest at basal levels of cAMP, and excited when the cAMP concentration rises substantially in response to odorants. □

Received 20 March; accepted 21 June 1990.

1. Pace, U., Hanski, E., Salomon, Y. & Lancet, D. *Nature* **316**, 255–258 (1985).
2. Jones, D. T. & Reed, R. R. *Science* **244**, 730–738 (1989).
3. Pfeuffer, E., Mollner, S., Lancet, D. & Pfeuffer, T. *J. biol. Chem.* **264**, 18803–18807 (1989).
4. Nakamura, T. & Gold, G. H. *Nature* **325**, 442–444 (1987).
5. Stryer, L. *A. Rev. Neurosci.* **9**, 87–119 (1986).
6. Yau, K.-W. & Baylor, D. A. *A. Rev. Neurosci.* **12**, 289–327 (1989).
7. Kaupp, U. B. *et al. Nature* **342**, 762–766 (1989).
8. Jones, D. T., Barbosa, E. & Reed, R. R. *Cold Spring Harb. Symp. quant. Biol.* **53**, 349–353 (1988).
9. Gorman, C. M., Gies, D. R. & McCray, G. *DNA and Protein Engineering Techniques* **2**, 3–9 (1990).
10. Pritchett, D. B. *et al. Science* **242**, 1306–1308 (1988).
11. Hamill, O. P., Marty, A., Neher, E., Sakmann, B. & Sigworth, F. J. *Pflügers Arch.* **391**, 85–100 (1981).
12. Tanaka, J. C., Eccleston, J. F. & Furman, R. E. *Biochemistry* **28**, 2776–2784 (1989).
13. Dhallan, R. S., Haynes, L. W. & Yau, K.-W. *Biophys. J.* **57**, 387a (1990).
14. Koch, K.-W. & Kaupp, U. B. *J. biol. Chem.* **260**, 6788–6800 (1985).
15. Karpen, J. W., Zimmerman, A. L., Stryer, L. & Baylor, D. A. *Proc. natn. Acad. Sci. U.S.A.* **85**, 1287–1291 (1988).
16. Haynes, L. W. & Yau, K.-W. *Biophys. J.* **57**, 366a (1990).
17. Hodgkin, A. L. & Katz, B. *J. Physiol., Lond.* **108**, 37–77 (1949).
18. Kurahashi, T. *J. Physiol., Lond.* **419**, 177–192 (1989).
19. Firestein, S. & Werblin, F. *Science* **244**, 79–81 (1989).
20. Kozak, M. *Nucleic Acids Res.* **12**, 857–872 (1984).
21. Kyte, J. & Doolittle, R. F. *J. Molec. Biol.* **157**, 105–132 (1982).
22. Nathans, J. & Hogness, D. *Cell* **34**, 807–814 (1983).
23. Jones, D. T. & Reed, R. R. *J. biol. Chem.* **262**, 14241–14249 (1987).
24. Nakatani, K. & Yau, K.-W. *J. Physiol., Lond.* **395**, 695–729 (1988).

ACKNOWLEDGEMENTS. We thank J. Nathans and R. Huganir for comments on the manuscript and L. W. Haynes for valuable help. R.D. is supported an NIH training grant.

nature

INTERNATIONAL WEEKLY JOURNAL OF SCIENCE

Volume 347 No. 6289 13 September 1990 $6.95

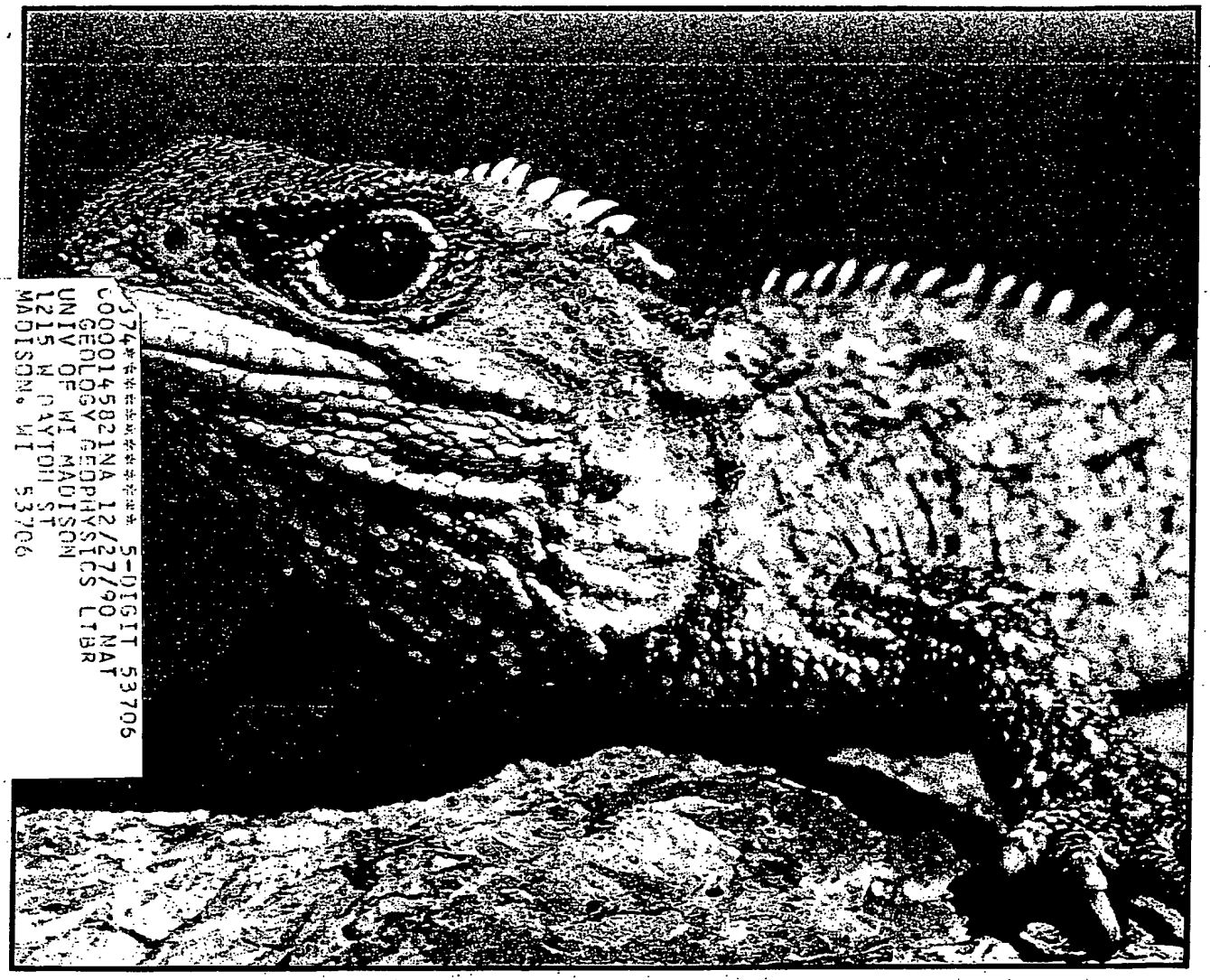

BAD TAXONOMY CAN KILL

A new neuroleptic target

The past and the future in ice cores

BIOTECHNICA product review

THE JOURNAL OF BIOLOGICAL CHEMISTRY
Vol. 272, No. 36, Issue of September 5, pp. 22623–22629, 1997
Printed in U.S.A.

Taste Buds Have a Cyclic Nucleotide-activated Channel, CNGgust*

Takumi Misaka‡, Yuko Kusakabe‡, Yasufumi Emori§, Tohru Gonoi¶, Soichi Arai‡, and Keiko Abe‡‖

(Received for publication, April 17, 1997, and in revised form, June 26, 1997)

From the ‡Department of Applied Biological Chemistry, Graduate School of Agricultural and Life Sciences, The University of Tokyo, 1-1-1 Yayoi, Bunkyo-ku, Tokyo 113; §Department of Biophysics and Biochemistry, Faculty of Science, The University of Tokyo, 7-3-1 Hongo, Bunkyo-ku, Tokyo 113; and ¶Research Center for Pathogenic Fungi and Microbial Toxicoses, Chiba University, 1-8-1 Inohana, Chuo-ku, Chiba 260, Japan

Cyclic nucleotide-gated (CNG) channels have been characterized as important factors involved in physiological processes including sensory reception for vision and olfaction. The possibility thus exists that a certain CNG channel functions in gustation as well. In the present study, we carried out reverse transcription-polymerase chain reaction and genomic DNA cloning and characterized a CNG channel (CNGgust) as a cyclic nucleotide-activated species expressed in rat tongue epithelial tissues where taste reception takes place. Several types of 5′-rapid amplification of cDNA ends clones of CNGgust cDNA were obtained with various 5′-terminal sequences. As the CNGgust gene was a single copy, the formation of such CNGgust variants should result from alternative splicing. The encoded protein was homologous to known vertebrate CNG channels with 50–80% similarities in amino acid sequence, and particularly homologous to bovine testis CNG channel and human cone CNG channel with 82% similarities. CNGgust was functional when expressed in human embryonic kidney cells, where it opened upon the addition of cGMP or cAMP. Immunohistochemical analysis using an antibody raised against a CNGgust peptide demonstrated the channel to be localized on the pore side of each taste bud in the circumvallate papillae, with no signal observed for degenerated taste buds after denervation of the glossopharyngeal nerve. All these results, together with the indication that cyclic nucleotides play a role gustatory signaling pathway(s), strongly suggest the involvement of CNGgust in taste signal transduction.

Vertebrate sensory systems comprise several distinct organs, cell types, and cellular signalings. These systems share many common features in their transmission and amplification of signals intercellularly or intracellularly leading to sense transduction to the central nervous system.

Vision is the most characteristic sensory process in vertebrates. Vision involves membrane receptors (rhodopsins) catching light, signal transducers such as transducin and phosphodiesterase, a soluble second messenger (cGMP), and membrane components such as a cyclic nucleotide-gated (CNG)[1] channel, all of which cooperate in the transduction of light signals to the central nervous system (1). Although this molecular apparatus is thought to be specific to vision, it is believed that similar signaling pathways exist for other sensory processes such as olfaction and gustation (2, 3). In olfactory neuron cells, olfactory receptors encoded by more than 1000 genes (4), a specific GTP-binding protein (G-protein) (Golf) (5), and a CNG channel (6) have been identified. One intriguing fact is that each olfactory neuron expresses one or a few receptor genes from a very large gene family, which strongly suggests that a certain receptor molecule determines the specificity for ligands (odorants) (4).

A similar situation has been implicated in taste chemoreception. We have identified multiple seven-transmembrane receptors similar to olfactory receptors that may participate in gustatory signaling (7). We have also demonstrated by *in situ* hybridization (8) and immunostaining (9) that GUST27, a representative receptor, is closely related to known olfactory receptors with a similarity of about 60% (8) and is expressed exclusively in taste buds and surrounding sites. An independent group has reported similar receptors expressed in taste cells (10–12). McLaughlin *et al.* (13) and Ruiz-Avila *et al.* (14) have confirmed the expression of gustducin, a taste bud-specific G-protein, and transducin in taste cells.

Although many of the molecules present in olfactory and/or gustatory cells have not yet been proved to be involved directly in the intracellular signaling cascade, those that are homologous to the visual signaling process may give rise to olfactory and gustatory sensations. Recently, the functions of various specific molecules have been revealed. Knockout mice lacking the olfactory CNG channel are insensitive to most odors (15), and those lacking gustducin show greatly reduced or sometimes a complete lack of reactivity toward sweet and bitter tastants (16).

As described above, CNG channels may be generally positioned in the middle of the intracellular signaling pathway of a chemosensation. Despite that, there have been no reports of the existence or function of CNG channel(s) in the gustatory system, with the interesting exception that there is a cyclic nucleotide-suppressible conductance/channel in frog taste cells (17).

In the present study, we carried out experiments aimed at

* This study was supported in part by a grant from the Program for the Promotion of Basic Research Activities for Innovation Biosciences. The costs of publication of this article were defrayed in part by the payment of page charges. This article must therefore be hereby marked "*advertisement*" in accordance with 18 U.S.C. Section 1734 solely to indicate this fact.

The nucleotide sequence(s) reported in this paper has been submitted to the GenBank™/EBI Data Bank with accession number(s) AB002801.

‖ To whom correspondence should be addressed: Dept. of Applied Biological Chemistry, Graduate School of Agricultural and Life Sciences, The University of Tokyo, Tokyo 113, Japan. Tel.: 81-3-3812-2111 (ext. 5129); Fax: 81-3-5802-8897.

[1] The abbreviations used are: CNG, cyclic nucleotide gated; nt, nucleotide; RACE, rapid amplification of cDNA ends; HEK, human embryonic kidney; RT, reverse transcription; PCR, polymerase chain reaction; PBS, phosphate-buffered saline; bp, base pair(s); kb, kilobase pair(s).

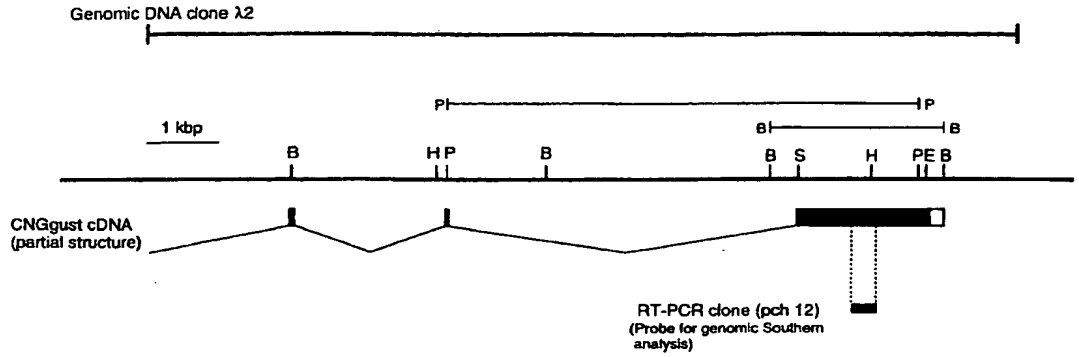

FIG. 1. **Partial restriction map of the CNGgust gene.** Restriction map of the rat gene over the extent of the genomic DNA clone λ2 is shown. Identified exons of the CNGgust gene are *boxed. Filled* and *open boxes* show coding and noncoding regions, respectively. The position of the initially obtained RT-PCR clone (pch 12) is indicated below. *Bam*HI and *Pst*I fragments to be detected by genomic Southern analysis are shown above. *B*, *Bam*HI; *E*, *Eco*RI; *H*, *Hin*dIII; *S*, *Stu*I; and *P*, *Pst*I.

finding and characterizing a mammalian gustatory CNG channel that is activated by cyclic nucleotides. The present report is the first that deals with a CNG channel occurring in taste buds. It also concerns the location of this gustatory CNG channel, CNGgust, on the pore side of each taste bud. Incidentally, it is noted that in this report CNGgust is sometimes specified as cyclic nucleotide-activated channel to distinguish it from the cyclic nucleotide-suppressible one (17).

EXPERIMENTAL PROCEDURES

RT-PCR—Poly(A$^+$) RNA was isolated from the tongue epithelia of rat circumvallate papillae using oligo(dT)-cellulose. A first-strand cDNA was synthesized using oligo(dT) primer and a first-strand cDNA synthesis kit (Pharmacia). Two degenerate oligonucleotide primers, 5′-GGITCIATGAT(ATC)TCIAA(TC)ATGAA(TC)GC-3′ and 5′-AG(TC)-TTICC(TC)TC(TC)TT(GAT)AT(GAT)AT(GA)TACAT(TC)TC(TC)TT-3′, were synthesized according to the amino acid sequences GSMISNMNA and KEMYIIKEGKL, respectively, which are commonly conserved in the COOH-terminal cytosolic region of known CNG channels. PCR amplification was performed using the primers (1 μM each) and rat tongue epithelial cDNA as a template (45 s at 96 °C, 2 min at 45 °C, 3 min at 72 °C, 50 cycles). The amplified DNA fragments of about 380 bp were excised and subcloned into pBluescript KS vector. To obtain clones for CNG channel, another oligonucleotide, 5′-GTCCAIA(GA)(GA)TA-(GA)TC(GA)AACCA(TC)TT(GAT)ATIAC-3′, was prepared as a probe according to the sequence VIKWFDYLW.

Identification of the cDNA for CNG Channel Expressed in Rat Tongue Epithelia, Named CNGgust—To identify the cDNA corresponding to the RT-PCR fragment encoding the CNG channel named CNGgust, genomic DNA cloning and 5′-RACE were carried out. One million plaques from a rat genomic DNA library (kindly supplied by Dr. E. Kominami, Juntendo University School of Medicine, Tokyo) were screened with the ^{32}P-labeled RT-PCR fragment encoding CNGgust. Hybridization was performed at 65 °C and washing at 65 °C in 0.1 × SSC containing 0.1% SDS. The positive clone obtained, designated λ2, was subcloned into pUC18 vector and sequenced.

5′-RACE was carried out to determine the nucleotide sequence of the 5′-end of the CNGgust cDNA as follows. Poly(A$^+$) RNA from rat tongue epithelia was reverse-transcribed into cDNA using the antisense oligonucleotide primer 5′-TGAAGTGCAAGGTC-3′ (+498 to +511 nt in Fig. 2), which is included in the λ2 genomic DNA fragment. An oligo(dA)-tail was added by terminal deoxynucleotidyltransferase. The oligo(dA)-tailed cDNA was amplified (30 s at 94 °C, 1 min at 50 °C, 1 min at 72 °C, 50 cycles) using an oligo(dT) primer, 5′-GAGTCGACTCGAGAATTC-TTTTTTTTTTTTTTTTTT-3′, and a specific primer according to the nucleotide sequence of the λ2 genomic DNA fragment, 5′-GTTTCCA-CAGCCTCTTGG-3′ (+470 to +487 nt, Fig. 2). The products were subcloned into a pUC 18 vector and sequenced.

Amplification of the Open Reading Frame of CNGgust cDNA by RT-PCR—To obtain a full-length open reading frame of CNGgust cDNA, a random primed rat tongue epithelial cDNA was amplified using specific primers, 5′-TTCAGGATGCATCAGATG-3′ (−6 to +12 nt, Fig. 2) of the 5′-RACE clone and 5′-GGATCCAACAACACTCTC-3′ (+2183 to +2200 nt, Fig. 2) of the λ2 genomic DNA fragment (30 s at 94 °C, 1 min at 50 °C, 3 min at 72 °C, 50 cycles).

Genomic Southern Analysis—A 10-μg portion of rat genomic DNA (CLONTECH) was digested with restriction endonuclease, *Eco*RI, *Bam*HI, or *Pst*I, electrophoresed, and transferred to a nylon filter. The filter was hybridized at 65 °C with the ^{32}P-labeled RT-PCR fragment encoding CNGgust (+961 to +1343 nt in Fig. 2) and then washed at 65 °C in 0.1 × SSC containing 0.1% SDS.

Expression of CNGgust in Cultured Cells and Electrophysiological Dissection—CNGgust expression plasmid pSRD-CNG was used for transient expression. pSRD-CNG was constructed as follows. pCNGg1 containing a 2.5 kb-*Bam*HI fragment of λ2 was digested with *Stu*I and *Sal*I, and ligated with a *Stu*I and *Sal*I fragment of a 5′-RACE clone, pCNG5′-1, to generate a 2.2-kb insert encoding the full length of the coding region. The insert (−6 to +1836 nt in Fig. 2) was amplified and subcloned into the pSRD vector, yielding pSRD-CNG.

The transient expression of CNGgust was performed by transfecting the expression plasmid pSRD-CNG into human embryonic kidney (HEK) 293 cells using LipofectAMINE (Life Technologies, Inc.). pAd-VAntage (Promega) and a green fluorescent protein-expressing vector, pS64T-C1 (CLONTECH) were co-transfected with the expression plasmid. Cells were cultured in Dulbecco's modified Eagle's medium supplemented with 10% fetal calf serum for 2 or 3 days. Electrical recordings were performed using green fluorescent protein-expressing cells. The current was recorded from inside-out patches using an EPC-7 amplifier (List Electronic) with the current filtered at 2 kHz. The pipette and bath solution used was 140 mM NaCl, 5 mM KCl, 0.5 mM EDTA, 0.5 mM EGTA, and 10 mM HEPES (pH 7.4). The inside-out patch was held at 0 mV in the bath solution containing cGMP or cAMP and stepped from −75 mV to +90 mV for 30 ms, increasing the voltage by 15 mV every 1 s. The current was measured 5 ms before the ending of the voltage pulse.

Preparation of an Anti-CNGgust Antibody—The COOH-terminal 15-mer peptide of CNGgust, FSPDRENSEDASKAD, was synthesized, and a cysteine residue was added to its NH_2 terminus to conjugate the peptide to keyhole limpet hemocyanin. Rabbit antiserum was prepared by immunizing the synthetic peptide conjugated to hemocyanin. An anti-CNGgust antibody was affinity-purified by a peptide column.

Immunostaining of Circumvallate Papillae—Rats were anesthetized and their tongues were rapidly excised. The excised tongues were immediately embedded in OCT compound (Tissue-Tek, Miles Labs.), frozen in liquid nitrogen, and serially sectioned at 5-μm thickness. Sections containing circumvallate papillae were thaw-mounted onto glass slides, air-dried, and fixed for 10 min in 10% formaldehyde/PBS. The sections were preincubated with normal goat serum and subsequently immunoreacted with a diluted solution of the affinity-purified anti-CNGgust antibody (1:100 in PBS) overnight. After washing with PBS, the slide was incubated with an fluorescein isothiocyanate-conjugated secondary antibody (1:100 in PBS) for 30 min and observed using a fluorescent microscope.

Denervation Treatment—To promote degeneration of the taste buds in circumvallate papillae, the glossopharyngeal nerve was removed. This treatment was performed on 5-week-old male rats by the method described previously (18). Sections containing circumvallate papillae were excised 6 weeks after denervation and used for immunostaining as described above.

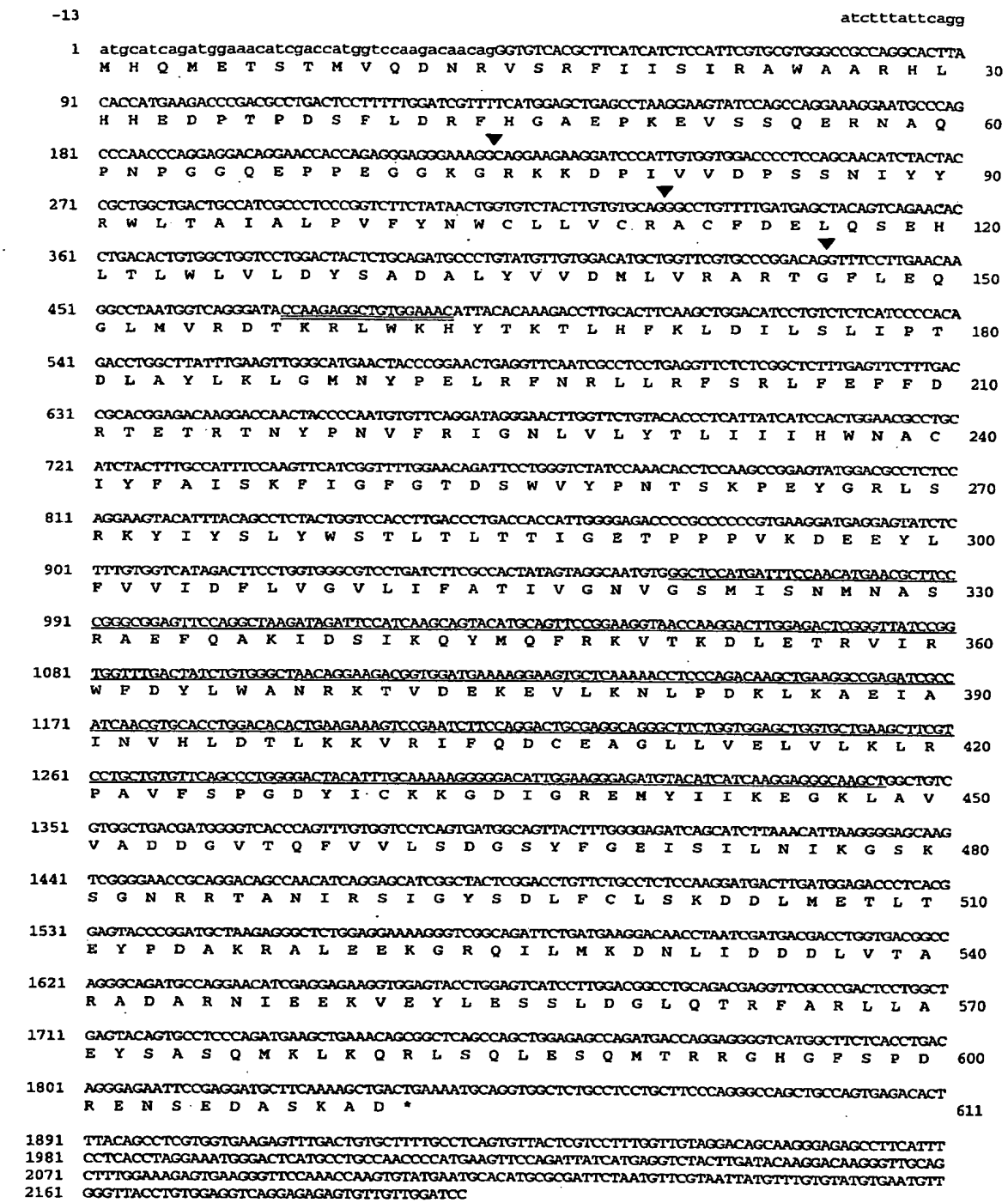

FIG. 2. **Nucleotide and deduced amino acid sequences of CNGgust.** The sequence was obtained from a part of the *Bam*HI fragment of the λ2 genomic DNA clone (+437 to +2200 nt) and one of the 5′-RACE clones (−13 to +487 nt). Nucleotide and amino acid residues are numbered based on the position of the methionine located at the 5′-terminus in the 5′-RACE clone. Established intron positions in the λ2 clone are indicated by *filled triangles*. The nucleotide sequence corresponding to the RT-PCR clone (pch 12) is *underlined*, and the position of the antisense primer for 5′-RACE is *double underlined*. The nucleotide sequence of the 5′-regional 54-bp sequence that varies among 5′-RACE clones is indicated by *lowercase letters*.

RESULTS

A CNG Channel Expressed in Rat Tongue Epithelia—We first tried to obtain cDNA fragments encoding a CNG channel by RT-PCR with mRNA prepared from the epithelia of rat circumvallate papillae. Degenerated oligonucleotide primers corresponding to highly conserved sequences in the COOH-terminal cytosolic regions of known CNG channels were used for the RT-PCR. Resulting products with the expected nucleotide lengths of about 380 bp were subcloned and screened with an internal oligonucleotide probe corresponding to another con-

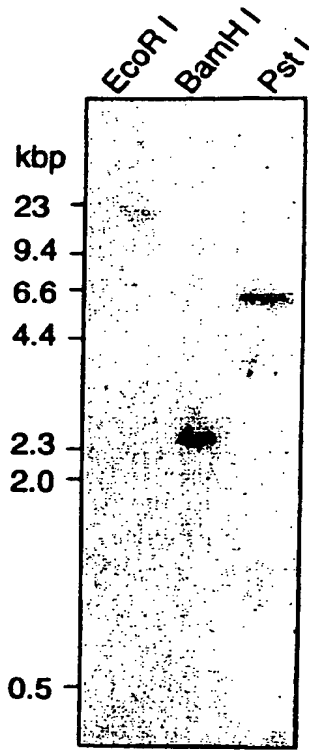

FIG. 3. **Southern blot analysis with the CNGgust cDNA fragment.** Total rat genomic DNA (10 μg) was digested with *Eco*RI, *Bam*HI, or *Pst*I. The blotted membrane was hybridized with the CNGgust cDNA fragment as described under "Experimental Procedures." The positions of the markers used are indicated.

served CNG channel sequence. By this method, we isolated a clone, designated pch 12, encoding a part of the cyclic nucleotide-binding domain (Figs. 1 and 2). From a data base search, the deduced amino acid sequence was found to be part of a CNG channel as a cyclic nucleotide-activated one, and so was named CNGgust.

Determination of the Coding Region of CNGgust cDNA—Next, we tried to obtain a full-length cDNA for CNGgust. Because no appreciable expression of CNGgust mRNA was observed by Northern blot analysis even using 10 μg of poly-(A^+) RNA extracted from rat tongue epithelial tissues (data not shown), it was considered very difficult to obtain any positive cDNA clone from a conventional cDNA library. Therefore, we obtained a genomic DNA fragment to determine a part of the CNGgust cDNA and then carried out 5′-RACE and RT-PCR.

Since it is known that the 3′ two-thirds of the cDNA for the human rod CNG channel consists of a single exon (19), a genomic DNA fragment containing a sequence of the RT-PCR clone (pch 12) was expected to code for the greater part of CNGgust. We then isolated a genomic DNA clone, termed λ2, by screening with pch 12 as a probe. Restriction mapping, Southern hybridization, and sequence analysis indicated that the 2.5-kb *Bam*HI fragment contained a pch 12 sequence (Fig. 1) and that a single exon in this fragment encoded the COOH-terminal part of CNGgust, Phe^{147}–Asp^{611} (Fig. 2). It was also suggested that the fragment contained at least the 3′-noncoding sequence and that exon(s) encoding the NH_2-terminal part should be split by intron(s). To determine the sequence of the 5′-terminal region of the CNGgust cDNA, we next carried out 5′-RACE using a specific antisense primer corresponding to +470 to +487 nt (Fig. 2). As a result, several 5′-RACE clones were obtained. All had the same 3′-regional 446-bp sequence, but their 5′-regional sequences varied (data not shown). This variation was thought to result from alternative splicing, since the CNGgust gene is a single copy as revealed by genomic Southern analysis which yielded a single band under stringent conditions for digestion with *Eco*RI, *Bam*HI, and *Pst*I using the pch 12 insert (+961 to +1343 nt in Fig. 2) as a probe (Fig. 3). The lengths of the DNA fragments detected by genomic Southern analysis were consistent with the restriction map of λ2 (Figs. 1 and 3).

A comparison of the nucleotide sequence of the clone λ2 with that of 5′-RACE clones showed the partial organization of CNGgust gene. Two exons, 108 bp (+222 to +329 nt) and 107 bp (+330 to +436 nt) in length, are located separately (Fig. 1).

Fig. 2 shows the nucleotide and deduced amino acid sequences of CNGgust cDNA. The nucleotide sequence was based on the λ2 genomic DNA clone and the most abundant 5′-RACE clones (−13 to +487 nt). Since the 5′-terminal CNGgust cDNA has not been definitely elucidated, the initiation methionine codon could not be assigned. The methionine residue in the most 5′-terminal region was taken as the starting position for nucleotide and amino acid numbering. Although the 3′-end of the cDNA has not been elucidated, the 2206-nt sequence (−6 to +2200 nt) (Fig. 2) containing the termination codon and part of the 3′-noncoding region was contained in one of the mRNA species, because we obtained a 2206-bp product by RT-PCR using a primer set (−6 to +12 nt and +2183 to +2200 nt in Fig. 2) and random primed cDNA from rat circumvallate papillae.

Structural Characteristics of CNGgust—CNGgust shares an overall structural similarity with other CNG channels. It contains 1) a central hydrophobic region comprising six membrane-spanning segments, 2) a pore-forming region that may determine ion permeability, and 3) a cyclic nucleotide-binding domain near the COOH terminus that locates in the cytosolic region. CNGgust also contains two potential *N*-glycosylation sites (Fig. 4).

Fig. 4 shows an amino acid alignment of CNGgust with known CNG channels. Since the NH_2-terminal sequence of CNGgust has not been definitely determined, a precise comparison of the NH_2-terminal regions is not achieved. In terms of overall homology, CNGgust shows the highest similarity (82%) to bovine testis CNG channel (20, 21) and the same degree of similarity to human cone CNG channel (22). However, it shows lower similarities (50–70%) to other CNG channels: 66% to rat olfactory CNG channel (6) and 63% to rat rod CNG channel (23). As for the central part ranging from the predicted first transmembrane region to the cyclic nucleotide-binding domain, where the highest similarity has generally been observed among known CNG channels, CNGgust has a similarity as high as 85% to the bovine testis and human cone CNG channels, and a similarity of 60–70% to other vertebrate CNG channels. In the NH_2-terminal region, on the other hand, CNGgust lacks the 20–40 amino acids between Gly^{74} and Arg^{75} when compared with bovine testis and human cone CNG channels (Fig. 4). It should be noted that an intron is inserted in this position of the CNGgust cDNA (Fig. 2).

Electrophysiological Function of CNGgust Expressed in HEK 293 Cells—Since known cloned CNG channels are functional when expressed in cultured cells, we expressed CNGgust in HEK 293 cells and investigated CNG channel properties. As shown in Fig. 5, electrophysiological recording of CNGgust-expressing cells showed that the expressed protein in inside-out patches, although it may be missing the NH_2-terminal region, can open when a cyclic nucleotide, cGMP and cAMP, is added. The current-voltage relationship was approximately linear through the change in membrane potential (+90 to −75 mV) at every nucleotide concentration tested (Fig. 5*A*). The

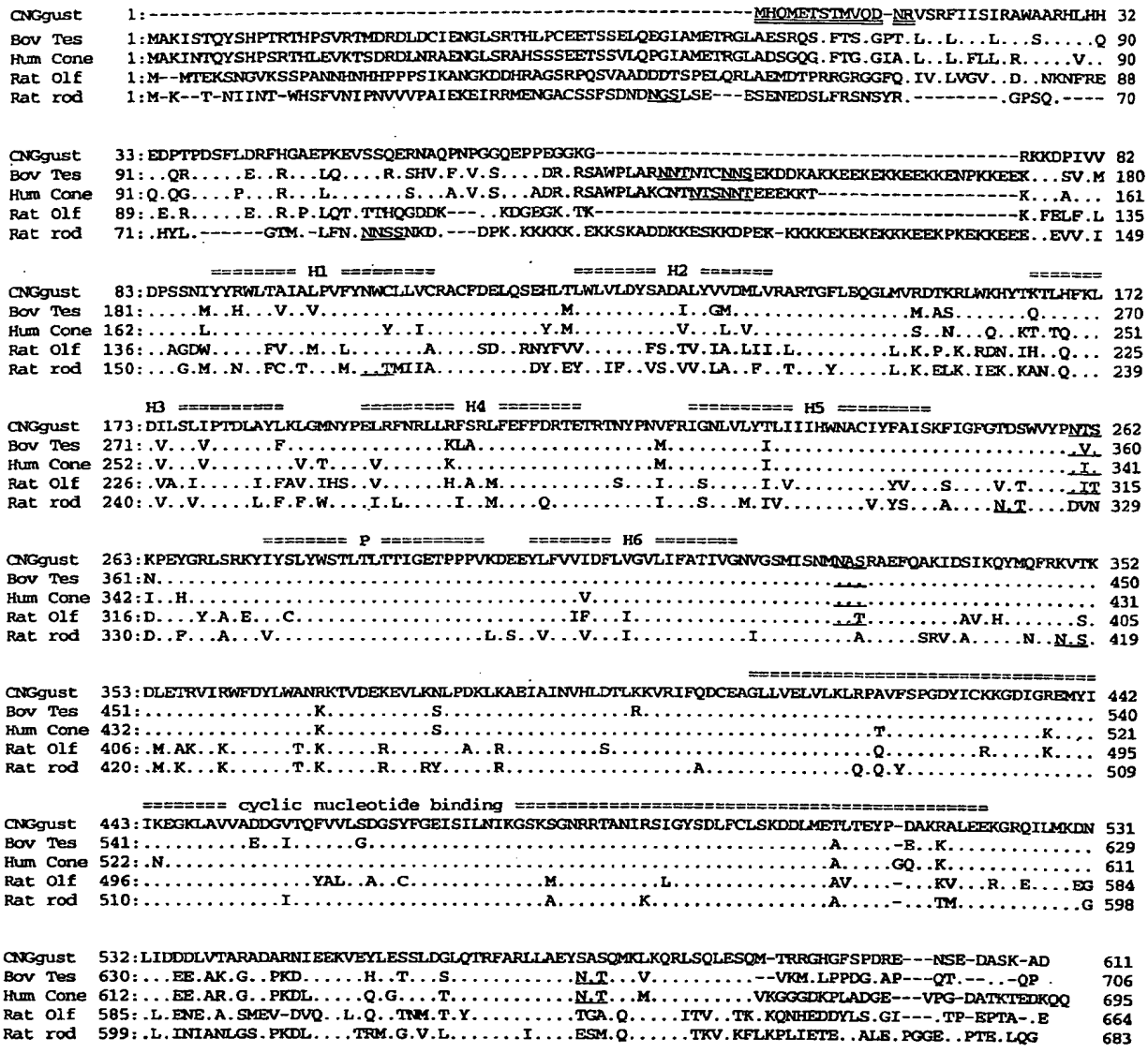

FIG. 4. **Alignment of the amino acid sequences of CNGgust and other known CNG channels.** Gaps are inserted to maximize matching. *Dots* denote amino acid residues identical to CNGgust. Predicted transmembrane domains (*H1–H6*), pore region (*P*), and the cyclic nucleotide-binding domain of the CNGgust protein are *overlined* (*double-dashed lines*). The NH_2-terminal sequence of CNGgust, which varies among 5′-RACE clones, is *double underlined*. The potential *N*-glycosylation sites are *underlined*. Abbreviations are as follows: *Hum Cone*, CNG channel from human retina (22); *Bov Tes*, bovine testis CNG channel (20, 21); *Rat Olf*, rat olfactory CNG channel (6); and *Rat Rod*, rat rod CNG channel (23).

half-maximal activation constant ($K_{1/2}$) at −60 mV was about 3 μM for cGMP, whereas it was about 300 μM for cAMP (Fig. 5*B*). The sensitivity to cGMP is about 100 times higher than it is to cAMP. Further, the current observed with saturating cAMP (10 mM) was 85% of that observed with saturating cGMP (100 μM) (Fig. 5*B*). This ratio is similar to that reported by Biel *et al.* (21) for the bovine testis CNG channel.

CNGgust in Taste Buds—We observed the expression of CNGgust mRNA in the circumvallate papillae by 5′-RACE and RT-PCR. To determine the localization of CNGgust in tissue, immunostaining experiments were carried out using a polyclonal antibody raised against the COOH-terminal peptide. Intense fluorescence was observed in each of the taste buds, especially on the pore side of the apical region where taste reception followed by initial intracellular signaling may occur (Fig. 6, *B* and *C*). To examine whether or not the expression of CNGgust depends on the presence of taste buds, tongue sections from rats whose glossopharyngeal nerves connecting the tongue to the central nervous system had been destroyed were immunostained. The removal of this nerve is known to promote the degeneration of taste buds in the circumvallate papillae since regeneration no longer occurs (24). The taste buds disappeared 6 weeks after denervation, and no CNGgust protein signal was observed in the corresponding region (Fig. 6*D*). These results indicate that our cloned CNGgust is expressed in taste buds.

DISCUSSION

In this study, we report the cloning of a CNG channel (CNGgust) as a cyclic nucleotide-activated one from rat tongue epithelia. This is the first study identifying a CNG channel in mammalian gustatory organs. CNGgust is expressed in taste buds including the taste cells where gustatory reception takes place. Our findings thus strongly indicate the possible involve-

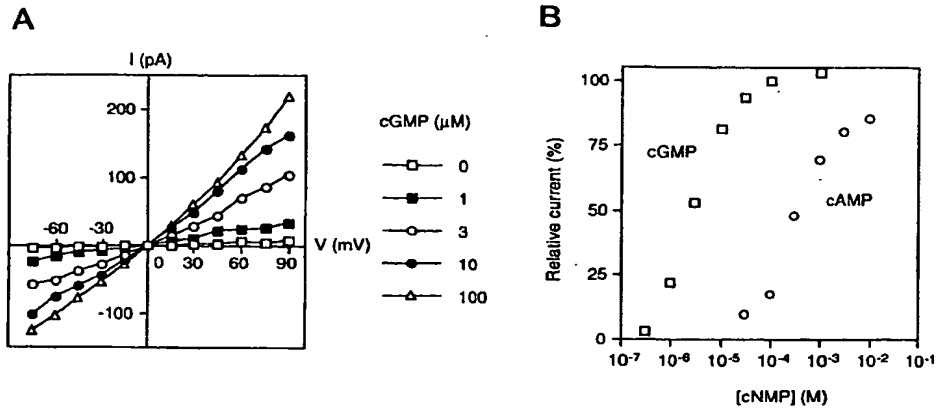

FIG. 5. **Electrophysiological properties of CNGgust.** *A*, macroscopic current-voltage relations obtained by a certain patch at several concentrations of cGMP. Recording from each patch gave almost the same results except for the maximal currents. *B*, dose-response relationships observed at −60 mV for cGMP (□) or cAMP (○). Currents were normalized to that of 100 μM cGMP. All data are mean values obtained from three to five independent experiments.

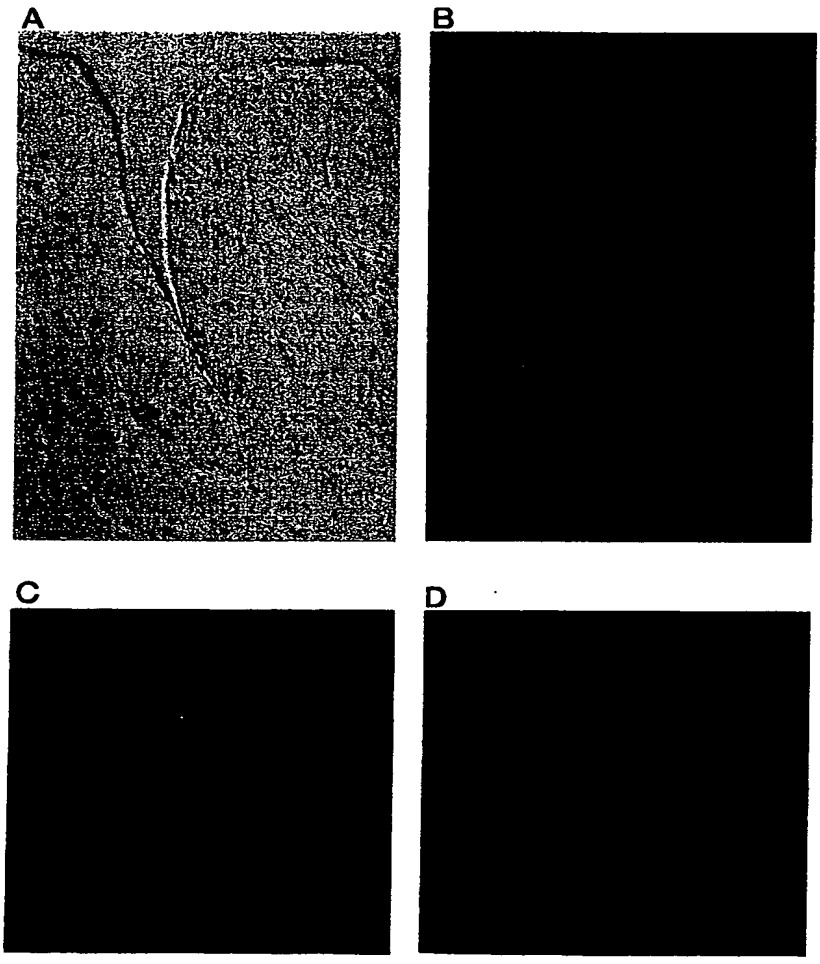

FIG. 6. **Localization of CNGgust in rat tongue circumvallate papillae.** Sections taken from circumvallate papillae were treated with affinity-purified anti-CNGgust antibodies and FITC-conjugated secondary antibody. Bright field (*A*) and fluorescent fields (*B–D*) are indicated. *A–C*, circumvallate papilla from a normal rat (*A* and *B*, low magnification; *C*, high magnification); *D*, circumvallate papilla from a denervated rat without taste buds. CNGgust expression is visible as fluorescent signals in the circumvallate papillae, especially on the pore side of the taste bud (*B* and *C*), but not detected in circumvallate papillae from the denervated rat (*D*).

ment of CNGgust in the intracellular signal transduction of taste cells.

CNGgust may consist of several variants judging from the results of 5′-RACE. Since the CNGgust gene is a single copy gene (Fig. 3), this variation probably results from alternative splicing that gives rise to different 5′-coding regions. Since the CNGgust derived from the most abundant type of 5′-RACE clones was shorter than other CNG channels in the NH_2-terminal region (Fig. 4), a full-length CNGgust species with an additional NH_2 sequence must exist. However, the CNGgust expressed in HEK cells, although not full-length, was functional as a cyclic nucleotide-gated channel (Fig. 5).

Electrophysiological information concerning cloned vertebrate CNG channels is available. It has been reported that cAMP is not capable of activating rod CNG channels even when a high concentration of cAMP (1 mM) is applied (23, 25). On the other hand, cAMP can activate olfactory CNG channels, but the sensitivity for cAMP is about 30 times lower than that for cGMP (6). In our study, we showed that CNGgust responded to cAMP as well as to cGMP, although the sensitivity for cGMP

was about 100 times greater than that for cAMP in terms of the $K_{1/2}$ value (Fig. 5*B*). Recently, a CNG channel has been shown to function as a hetero-oligomer of α- and β-subunits. The α-subunit has been shown to function as a CNG channel in the absence of the β-subunit. On the other hand, the β-subunit, which has been cloned from rod outer segments, olfactory neurons, and testis, does not form any functional channel by itself (26–30). However, it has also been shown that the β-subunit increases the sensitivity for cAMP when coexpressed with the α-subunit (28, 29). Thus the β-subunit is considered to be a modulatory subunit. It is probable that the β-subunit *per se* exists in taste cells to form an α-β hetero-oligomer with the α-subunit (CNGgust), and that the resulting oligomer shows a high sensitivity for cAMP, similar to that for cGMP.

The involvement of CNGgust in the taste signaling process is strongly suggested by the following findings and knowledge. First, CNGgust is expressed specifically on the pore side of each taste bud in the circumvallate papilla (Fig. 6, *B* and *C*). In addition, this site-specific expression is dependent on the existence of taste buds as shown by the denervation experiments (Fig. 6*D*). Second, it has been reported that taste buds contain a series of intrinsic molecules participating in the signal transduction cascade involving cyclic nucleotides. These are exemplified by G-protein-coupled receptors (8, 10–12), gustducin/transducin (13, 14), phosphodiesterase (14, 31), adenylyl cyclase/guanylyl cyclase (32, 33), and rhodopsin kinase (34). Third, it has been reported that the stimulation of taste cells with some sweet tastants increases their intracellular cAMP level (35). Taken together, the CNGgust characterized here may be an essential mediator in cAMP/cGMP-dependent taste signaling.

Recently, Kolesnikov and Margolskee (17) have electrophysiologically demonstrated the occurrence of a cyclic nucleotide-suppressible conductance/channel in frog taste cells. In contrast is our finding that CNGgust, as well as many other CNG channels, is activated in the presence of cyclic nucleotides. It may therefore be appropriate to distinguish CNGgust by designating it as a cyclic nucleotide-activated rather than gated channel. However, it remains unclear whether a similar suppressible channel occurs in rat taste cells or if it is just intrinsic to frogs. If such a channel resides in mammals as well, the possibility exists that both positively and negatively controlled pathways are together involved in mammalian taste signaling, and it will be extremely interesting to define each of them at the molecular level.

Acknowledgments—We express our thanks to Dr. Y. Ninomiya, Asahi University, for performing the denervation treatments, to Dr. S. Seino, Chiba University, for advice concerning the electrophysiological study, and to Dr. K. Sugimoto, Tokyo Medical and Dental University, for pertinent discussion on the histology of taste cells.

REFERENCES

1. Yau, K.-W., and Baylor, D. A. (1989) *Annu. Rev. Neurosci.* **12**, 289–327
2. Buck, L. B. (1996) *Annu. Rev. Neurosci.* **19**, 517–544
3. Kinnamon, S. C., and Margolskee, R. F. (1996) *Curr. Opin. Neurobiol.* **6**, 506–513
4. Ressler, K. J., Sullivan, S. L., and Buck, L. B. (1994) *Curr. Opin. Neurobiol.* **4**, 588–596
5. Jones, D. T., and Reed, R. R. (1989) *Science* **244**, 790–795
6. Dhallan, R. S., Yau, K.-W., Schrader, K. A., and Reed, R. R. (1990) *Nature* **347**, 184–187
7. Abe, K., Kusakabe, Y., Tanemura, K., Emori, Y., and Arai, S. (1993) *FEBS Lett.* **316**, 253–256
8. Abe, K., Kusakabe, Y., Tanemura, K., Emori, Y., and Arai, S. (1993) *J. Biol. Chem.* **268**, 12033–12039
9. Kusakabe, Y., Abe, K., Tanemura, K., Emori, Y., and Arai, S. (1996) *Chem. Senses* **21**, 335–340
10. Matsuoka, I., Mori, T., Aoki, J., Sato, T., and Kurihara, K. (1993) *Biochem. Biophys. Res. Commun.* **194**, 504–511
11. Tal, M., Ammar, D. A., Karpuj, M., Krizhanovsky, V., Naim, M., and Thompson, D. A. (1995) *Biochem. Biophys. Res. Commun.* **209**, 752–759
12. Thomas, M. B., Haines, S. L., and Akeson, R. A. (1996) *Gene (Amst.)* **178**, 1–5
13. McLaughlin, S. K., McKinnon, P. J., and Margolskee, R. F. (1992) *Nature* **357**, 563–569
14. Ruiz-Avila, L., McLaughlin, S. K., Wildman, D., McKinnon, P. J., Robichon, A., Spickofsky, N., and Margolskee, R. F. (1995) *Nature* **376**, 80–85
15. Brunet, L. J., Gold, G. H., and Ngai, J. (1996) *Neuron* **17**, 681–693
16. Wong, G. T., Gannon, K. S., and Margolskee, R. F. (1996) *Nature* **381**, 796–800
17. Kolesnikov, S. S., and Margolskee, R. F. (1995) *Nature* **376**, 85–88
18. Ninomiya, Y., Kajiura, H., Naito, Y., Mochizuki, K., Katsukawa, H., and Torii, K. (1994) *Physiol. Behav.* **56**, 1179–1184
19. Dhallan, R. S., Macke, J. P., Eddy, R. L., Shows, T. B., Reed, R. R., Yau, K.-W., and Nathans, J. (1992) *J. Neurosci.* **12**, 3248–3256
20. Weyand, I., Godde, M., Frings, S., Weiner, J., Müller, F., Altenhofen, W., Hatt, H., and Kaupp, U. B. (1994) *Nature* **368**, 859–863
21. Biel, M., Zong, X., Distler, M., Bosse, E., Klugbauer, N., Murakami, M., Flockerzi, V., and Hofmann, F. (1994) *Proc. Natl. Acad. Sci. U. S. A.* **91**, 3505–3509
22. Yu, W.-P., Grunwald, M. E., and Yau, K.-W. (1996) *FEBS Lett.* **393**, 211–215
23. Barnstable, C. J., and Wei, J.-Y. (1995) *J. Mol. Neurosci.* **6**, 289–302
24. Guth, L. (1957) *Anat. Rec.* **128**, 715–731
25. Kaupp, U. B., Niidome, T., Tanabe, T., Terada, S., Bönigk, W., Stühmer, W., Cook, N. J., Kangawa, K., Matsuo, H., Hirose, T., Miyata, T., and Numa, S. (1989) *Nature* **342**, 762–766
26. Chen, T.-Y., Peng, Y.-W., Dhallan, R. S., Ahamed, B., Reed, R. R., and Yau, K.-W. (1993) *Nature* **362**, 764–767
27. Körschen, H. G., Illing, M., Seifert, R., Sesti, F., Williams, A., Gotzes, S., Colville, C., Müller, F., Dosé, A., Godde, M., Molday, L., Kaupp, U. B., and Molday, R. S. (1995) *Neuron* **15**, 627–636
28. Liman, E. R., and Buck, L. B. (1994) *Neuron* **13**, 611–621
29. Bradley, J., Li, J., Davidson, N., Lester, H. A., and Zinn, K. (1994) *Proc. Natl. Acad. Sci. U. S. A.* **91**, 8890–8894
30. Biel, M., Zong, X., Ludwig, A., Sautter, A., and Hofmann, F. (1996) *J. Biol. Chem.* **271**, 6349–6355
31. McLaughlin, S. K., McKinnon, P. J., Spickofsky, N., Danho, W., and Margolskee, R. F. (1994) *Physiol. Behav.* **56**, 1157–1164
32. Kurihara, K., and Koyama, N. (1972) *Biochem. Biophys. Res. Commun.* **48**, 30–34
33. Asanuma, N., and Nomura, H. (1995) *Chem. Senses* **20**, 231–237
34. Premont, R. T., Koch, W. J., Inglese, J., and Lefkowitz, R. J. (1994) *J. Biol. Chem.* **269**, 6832–6841
35. Striem, B. J., Naim, M., and Lindemann, B. (1991) *Cell. Physiol. Biochem.* **1**, 46–54

GENERAL INFORMATION

This publication is available on-line at http://www.jbc.org. Inquire about availability through your subscription agent or contact: THE JOURNAL OF BIOLOGICAL CHEMISTRY, P.O. Box 830399, BIRMINGHAM, AL 35283-0399, U.S.A. Minireviews are reprinted in January of the succeeding year in a Minireview Compendium. Compendia for 1988 through 1996 are available through the ASBMB office: ASBMB Office, 9650 Rockville Pike, Bethesda, MD 20814, U.S.A.

Submit *all* manuscripts in quadruplicate to

Editor, The Journal of Biological Chemistry
9650 Rockville Pike
Bethesda, MD 20814, U.S.A.

Accepted manuscripts will be published with the implicit understanding that the author(s) will pay a charge per page. Current page charges may be obtained by contacting the JBC office. Under exceptional circumstances, when no source of grant or other support exists, the author(s) may apply, **at the time of submission,** for a grant-in-aid to Chairman, Publications Committee, American Society for Biochemistry and Molecular Biology, Inc., 9650 Rockville Pike, Bethesda, MD 20814. All such applications must be countersigned by an appropriate institutional official stating that no funds are available for page charges.

Queries on matters of general editorial policy, requests for reprints of the "Instructions to Authors," or of the "Editorial Policy and Practices," or for permission to reproduce any part of a previously published article should be directed to the Journal Editorial Office in Bethesda, telephone 301-530-7150; fax 301-571-1824; E-mail jbc@asbmb.faseb.org.

The Journal of Biological Chemistry publishes papers on a broad range of topics of interest to biochemists. The views expressed are those of the author(s) and not of *The Journal of Biological Chemistry* or the American Society for Biochemistry and Molecular Biology.

Address all correspondence and orders relative to subscriptions and back copies to: *The Journal of Biological Chemistry*, P.O. Box 830399, Birmingham, AL 35283-0399, U.S.A., telephone 800-633-4931. Subscriptions are entered on a calendar year basis only. Allow at least six weeks for address changes. Claims for replacement copies must be received within three months of the issue date.

The Journal of Biological Chemistry (ISSN 0021-9258) is published weekly by the American Society for Biochemistry and Molecular Biology, Inc., 9650 Rockville Pike, Bethesda, MD 20814. Volume 272 for 1997: Institutions: United States, $1,400; Foreign, $1,600. Single copies of the Journal are $30. (Note: Maryland and Canada add applicable taxes, unless a tax-exempt certificate number is shown.) The GST number for Canadian subscribers is 13037 0018 RT. C.P.C Int'l Pub Mail # 0060119. Periodicals postage paid at Bethesda, MD 20814, U.S.A. and at additional mailing offices. Printed in the U.S.A. Subscription rates for the on-line JBC are available at http://www.jbc.org. POSTMASTER: Send address changes to THE JOURNAL OF BIOLOGICAL CHEMISTRY at P.O. Box 830399, Birmingham, AL 35283-0399, U.S.A.

ptember 5, 1997 VOLUME 272 NUMBER 36

ISSN 0021-9258
JBCHA3 272(36) 22373–22974 (1997)

THE Journal of Biological Chemistry

Published by the American Society for Biochemistry and Molecular Biology

FOUNDED BY CHRISTIAN A HERTER

AND SUSTAINED IN PART BY THE CHRISTIAN A HERTER MEMORIAL FUND

Proc. Natl. Acad. Sci. USA
Vol. 88, pp. 9868–9872, November 1991
Neurobiology

Control of ligand specificity in cyclic nucleotide-gated channels from rod photoreceptors and olfactory epithelium

(site-directed mutagenesis/ion channels/signal transduction/photoreception/olfaction)

W. ALTENHOFEN, J. LUDWIG, E. EISMANN, W. KRAUS, W. BÖNIGK, AND U. B. KAUPP

Institut für Biologische Informationsverarbeitung, Forschungszentrum Jülich, D-5170 Jülich, Federal Republic of Germany

Communicated by Erwin Neher, July 29, 1991 (received for review June 4, 1991)

ABSTRACT **Cyclic nucleotide-gated ionic channels in photoreceptors and olfactory sensory neurons are activated by binding of cGMP or cAMP to a receptor site on the channel polypeptide. By site-directed mutagenesis and functional expression of bovine wild-type and mutant channels in *Xenopus* oocytes, we have tested the hypothesis that an alanine/threonine difference in the cyclic nucleotide-binding site determines the specificity of ligand binding, as has been proposed for cyclic nucleotide-dependent protein kinases [Weber, I. T., Shabb, J. B. & Corbin, J. D. (1989) *Biochemistry* 28, 6122–6127]. The wild-type olfactory channel is ≈25-fold more sensitive to both cAMP and cGMP than the wild-type rod photoreceptor channel, and both channels are 30- to 40-fold more sensitive to cGMP than to cAMP. Substitution of the respective threonine by alanine in the rod photoreceptor and olfactory channels decreases the cGMP sensitivity of channel activation 30-fold but little affects activation by cAMP. Substitution of threonine by serine, an amino acid that also carries a hydroxyl group, even improves cGMP sensitivity of the wild-type channels 2- to 5-fold. We conclude that the hydroxyl group of Thr-560 (rod) and Thr-537 (olfactory) forms an additional hydrogen bond with cGMP, but not cAMP, and thereby provides the structural basis for ligand discrimination in cyclic nucleotide-gated channels.**

Cation channels that are directly gated by guanosine 3′,5′-cyclic monophosphate (cGMP) control the flow of ions across the surface membrane of vertebrate rod and cone photoreceptor cells (1, 2; for review, see refs. 3 and 4). A similar cation channel exists in vertebrate olfactory sensory neurons (5). Between the rod photoreceptor and the olfactory channel ≈74% of the aligned positions are occupied by identical or conserved amino acid residues (6–8). A single region near the C terminus of the channel polypeptides, comprising ≈80–100 amino acid residues, exhibits significant sequence similarity to both cGMP-binding domains of cGMP-dependent kinases (cGKs) (6). The sequence similarity is less pronounced between the corresponding regions of the channels and of cAMP-dependent kinases (cAKs) or of the catabolite gene activator protein of *Escherichia coli*. The comparison suggests that the channel polypeptides carry a ligand-binding site that is structurally similar to that of other cAMP- or cGMP-binding proteins.

A threonine residue is invariant in the two cGMP-binding domains of all cGKs but is exchanged for an alanine residue in 23 of 24 cAMP-binding sites in cAKs (9). The mammalian rod and olfactory cyclic nucleotide-gated channels contain a threonine residue at this particular position (6–8; Fig. 1). It has been proposed that this alanine/threonine difference might have been important in the evolutionary divergence of cyclic nucleotide-binding sites and that it provides the structural basis for discriminating between cAMP and cGMP (9). We tested the validity of this hypothesis for cyclic nucleotide-gated channels by mutagenesis and expression of wild-type and mutant channels from rod photoreceptors and olfactory epithelium.

MATERIALS AND METHODS

Construction of Recombinant pCHOLF102. PCR (13) was done with pCHOLF100 (8) as template and the following primers: a 5′ adapter primer [containing an *Eco*RV restriction site, a consensus sequence for eukaryotic ribosomal-binding sites (14), and the first nine nucleotides from the coding region of CHOLF100] and a gene-specific 3′ primer. The *Eco*RV/*Dra*III-digested PCR product replaced the corresponding fragment of pCHOLF100 to yield pCHOLF101. The insert of pCHOLF101 was subcloned into a pT7T3 vector to yield pCHOLF102.

Site-Directed Mutagenesis. The point mutations at positions 560 and 537 of the rod and olfactory channel polypeptides, respectively, were introduced by PCR procedure (13) with synthetic oligonucleotides containing the desired nucleotide substitutions.

Rod-channel mutant T560A was constructed by the method of Hemsley *et al.* (15). A circular plasmid with the wild-type rod-channel sequence from pRCG1 (6) was amplified by a pair of primers located "back-to-back" on opposite DNA strands. The resulting PCR product was recircularized and digested with *Nsi* I and *Sty* I. The corresponding *Nsi* I–*Sty* I fragment in pRCG1 was replaced by the mutated fragment to create pT560A. For the construction of rod-channel mutant T560S, we took advantage of a newly introduced *Cla* I restriction site near codon 560 in pT560A. A PCR fragment was produced by using a mutagenic and a complementary primer and linearized pT560A as template. The *Nsi* I–*Cla* I fragment containing the mutation was exchanged for the corresponding *Nsi* I–*Cla* I fragment of pT560A to generate pT560S.

Both olfactory-channel mutants T537A and T537S were constructed by combining two overlapping PCR fragments with the aid of newly introduced restriction sites at the locus of mutation (*Bss*HII for pT537A and *Rsr* II for pT537S) and other suitable restriction sites in the plasmid. pCHOLF102 was used as template. All mutations were verified by sequencing of the entire insert with the dideoxynucleotide chain-termination method.

Functional Expression. mRNA specific for the rod-photoreceptor channel, the olfactory channel, and the mutant channels was synthesized *in vitro* (16) by using the respective linearized plasmid cDNA as template. Transcription was primed with the cap dinucleotide 7-methylguanosine(5′)-triphospho(5′)guanosine (0.6 mM) (17). Macroscopic current measurements on excised inside-out patches (18–20) were made after injection of mRNA into *Xenopus* oocytes (mRNA

The publication costs of this article were defrayed in part by page charge payment. This article must therefore be hereby marked "*advertisement*" in accordance with 18 U.S.C. §1734 solely to indicate this fact.

Abbreviations: cAK, cAMP-dependent kinase; cGK, cGMP-dependent kinase; *I*, current; *I-V*, *I*–voltage; *n*, Hill coefficient; $K_{1/2}$, half-saturating concentration; I_{max}, maximum *I*.

A

		5 6 7 8	
cGMP-channel (rod)	(528)	DGITQFVVLSDGSYFGEISILNIKGSKAGNRRTANIKSIGYSDLFCLS	(575)
cAMP-channel (olf)	(505)	DGVTQYALLSAGSCFGEISILNIKGSKMGNRRTANIRSLGYSDLFCLS	(552)
cGK-bovine (1)	(153)	--GVKLCTMGPGKVFGELAILY------NCTRTATVKTLVNVKLWAID	(192)
cGK-bovine (2)	(275)	EDPVFLRTLGKGDWFGEKALQG------EDVRTANVIAAEAVTCLVID	(316)
cAK-bovine (1)	(186)	--NEWATSVGEGGSFGELALIY------GTPRAATVKAKTNVKLWGID	(225)

B

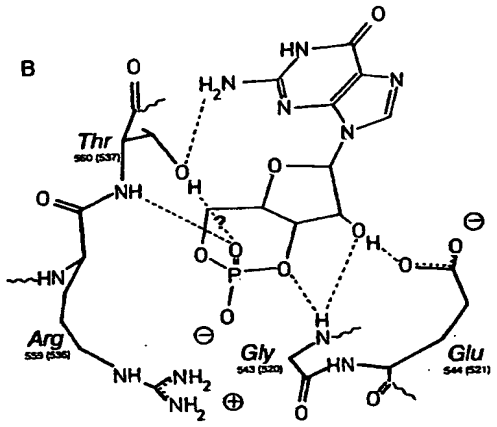

FIG. 1. (*A*) Comparison of the aligned amino acid sequences of parts of the cyclic nucleotide-binding site of several cyclic nucleotide-binding proteins (for details, see ref. 10). The position of the predicted structure of β-strands of the binding-site model in ref. 11 is indicated by bars and numbers. Arrowhead indicates position of the exchanged threonine residue, and asterisks indicate identical residues. Numbers in parentheses refer to binding domain 1 or 2. Sequences are from refs. 6, 8, 9, and 11. (*B*) Predicted sites of contact between cGMP and the binding site in cGKs and cyclic nucleotide-gated channels. Hypothetical hydrogen bonds are indicated by interrupted lines (adapted from ref. 12); numbers refer to position of amino acid residues in the sequence of the photoreceptor (olfactory) channel peptide. The hydrogen bond marked by a question mark most likely is not involved in cAMP or cGMP binding.

concentration, 0.4 μg/μl; average volume injected per oocyte, ≈50 nl) and incubation for 2–3 days in Barth's medium. Oocytes were prepared for recording by standard techniques (20, 21). The solution in the pipette, and the perfusion medium contained 100 mM KCl, 10 mM EGTA·KOH, and 10 mM Hepes·KOH (pH 7.2). Pipettes (2–4 MΩ) gave seal resistances of 0.2–90 GΩ. Macroscopic currents across excised inside-out patches were recorded under voltage-clamp conditions. Voltage ramps were delivered as a triangle (±80 mV, 50–80 mV/sec). Membrane current was low-pass filtered (50 Hz, 8-pole Bessel filter, Frequency Devices, Haverhill, MA) and continuously recorded on-line (pClamp 5.5, Axon Instruments, Burlingame, CA).

The cytoplasmic face of the excised membrane patch was superfused by using one or two concentric arrays of seven fused glass pipettes (i.d., 0.8 mm; Hilgenberg, Malsfeld, F.R.G.) each having an opening diameter of 30–70 μm. Solutions flowed from each port independently (1 ml/min), and a membrane patch could be exposed to a particular solution within ≈100 msec by moving the mouth of the port with a computer-controlled micromanipulator to the patch pipette. The bath temperature was 18–23°C.

Current was measured with a virtual ground current-to-voltage converter (L/M-EPC-7, List Electronics, Darmstadt, F.R.G.). Current–voltage relations (*I–V*) were recorded in the control (leak current) and different test solutions containing ligand intermittently. Leak currents [typically 0.3–20% of maximum current (I_{max})] recorded without ligand were subtracted from currents measured with ligand. Each *I–V* curve represents the average of three consecutive voltage ramps.

RESULTS

Expression of Wild-Type Channel. Photoreceptor channel-specific mRNA derived by *in vitro* transcription from clone pRCG1 of ref. 6 gave rise to cGMP-stimulated channel activity after injection into *Xenopus* oocytes (Fig. 2*A*, *Inset*). cGMP-stimulated currents were not observed in excised patches of uninjected or water-injected control oocytes. mRNA specific for the olfactory channel derived from clone pCHOLF100 of ref. 8 did not produce functional cyclic nucleotide-gated channels in oocytes. However, mRNA derived from recombinant clone pCHOLF102 that lacked the complete 5′ noncoding region and contained a consensus sequence for a eukaryotic ribosomal-binding site (see *Materials and Methods*) gave rise to cyclic nucleotide-stimulated currents (Fig. 2*B*, *Inset*).

Maximum currents at saturating cGMP concentrations typically varied between 2 nA and 13 nA at +80 mV and were largely similar for both channel species. Occasionally, amplitudes of I_{max} could be as low as a few picoamperes, depending mainly on the seasonal or temporal variations in the quality of oocytes. In the rod channel, saturating cAMP concentrations activated a current that was ≤17% of the maximum amplitude of cGMP-stimulated currents, whereas in the olfactory channel both cyclic nucleotides produced the same I_{max} amplitudes. This difference between the rod and olfactory channel with respect to activation by cAMP was qualitatively preserved in all mutant channels. Similar observations have been previously reported for excised patches of amphibian rod-photoreceptor and olfactory channel (22, 23). This result suggests that the open state of the cAMP-liganded rod channel is different from that of the olfactory channel.

Fig. 2 shows the relation between I/I_{max} and cGMP or cAMP concentration for the rod and olfactory wild-type channel. For comparison, half-saturating concentration ($K_{1/2}$) values for cAMP and cGMP of the rod channel are indicated by small arrows in Fig. 2*B*. Mean values of $K_{1/2}$ and Hill coefficient (n) for wild-type and mutant channels are summarized in Table 1. The expressed olfactory channel is ≈22- to 24-fold more sensitive to both cyclic nucleotides than the rod channel; and both channel types are ≈40-fold less sensitive to cAMP than to cGMP (see Table 1). We consistently found a higher degree of cooperativity for the olfactory channel (n_{cGMP} = 2.4, n_{cAMP} = 2.6) than for the rod-photoreceptor channel (n_{cGMP} = 1.7, n_{cAMP} = 1.8). The difference is statistically significant on the 5% level.

Replacement of Thr-560 (Rod) and Thr-537 (Olfactory) by Alanine. Both channel mutants T560A (rod) and T537A (olfactory) were functional when expressed in *Xenopus* oocytes. The mean of the maximum cGMP-stimulated current amplitude in the T560A [I_{mean} = 2831 ± 2232 pA (number of experiments, x = 9)] and T537A [I_{mean} = 2037 ± 1035 pA (x = 8)] mutant channels was ≈2-fold smaller than that seen for wild-type channel [I_{mean} = 5203 ± 3064 pA (x = 11) (rod) and 5614 ± 1168 pA (x = 15) (olfactory)]. The *I–V* relationships of the mutant channels were not significantly different

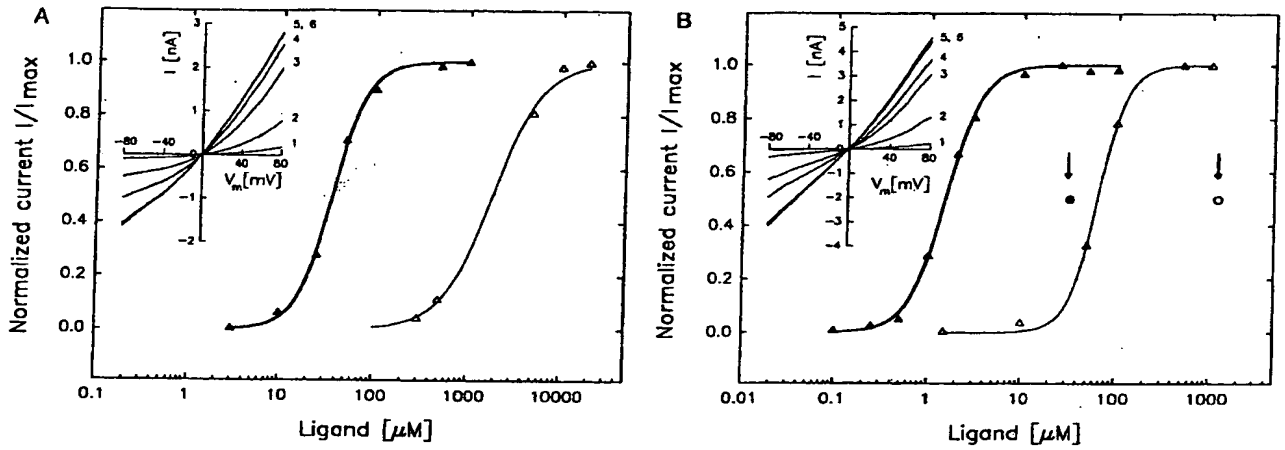

FIG. 2. Ligand sensitivity of normalized currents I/I_{max} of wild-type channels. Smooth curves represent a least-square-fit of the Hill equation $I/I_{max} = c^n/(c^n + K_{1/2}^n)$ to the experimental data, where c = concentration of the ligand. Normalized currents I/I_{max} were determined from current amplitudes at +80 mV of *I–V* curves similar to those shown in *Insets*. (*A*) Rod-photoreceptor channel; ▲, cGMP; △, cAMP. $K_{1/2}$ (cGMP) = 28.0 ± 1.0 μM; n = 2.0 ± 0.1; $K_{1/2}$ (cAMP) = 1849 ± 200 μM; n = 1.64 ± 0.1; data points for cAMP come from two different patches. (*B*) Olfactory channel; ▲, cGMP; △, cAMP; $K_{1/2}$ (cGMP) = 1.5 ± 0.03 μM; n = 2.2 ± 0.1; $K_{1/2}$ (cAMP) = 64 ± 1.8 μM; n = 2.9 ± 0.2. Arrows indicate the $K_{1/2}$ constants for cGMP (●) and cAMP (○) of the rod channel. (*Insets*) Series of *I–V* recordings in the presence of different cGMP concentrations. (*A*) Trace 1, 10 μM; trace 2, 25 μM; trace 3, 50 μM; trace 4, 100 μM; trace 5, 500 μM; and trace 6, 1000 μM; pipette resistance 4 MΩ. (*B*) Trace 1, 0.5 μM; trace 2, 1 μM; trace 3, 2 μM; trace 4, 3 μM; trace 5, 10 μM; and trace 6, 25 μM; pipette resistance, 3.5 MΩ.

from those of the wild-type channels (Fig. 3*B*, *Inset*), suggesting that the electrical and the underlying structural properties of the channels are preserved by these mutations. However, we have not yet tested the electrical properties on a single-channel level.

Upon replacement of Thr-560 by alanine in the rod channel, the $K_{1/2}$ constant for the activation by cGMP increased ≈30-fold (from 32.6 to 939 μM), whereas the activation by cAMP remained almost constant (Fig. 3*A*). The n values of activation were not significantly changed. The T537A mutant of the olfactory channel behaved similarly: the cGMP sensitivity of channel activation was decreased ≈40-fold (from 1.4 to 53.0 μM), whereas the cAMP sensitivity increased 2- to 3-fold (Fig. 3*B*). Again, the cooperativity of the channel activation was not influenced by the threonine/alanine exchange (see Table 1). The $K_{1/2}$ constants for activation by cGMP in the T537A (olfactory) mutant and by cAMP in the wild-type channel became identical (compare thick line/filled symbols with thin line/no symbols in Fig. 3*B*).

Replacement of Thr-560 (Rod) and Thr-537 (Olfactory) by Serine. If the hydroxyl group of the 560 or 537 residue is of critical importance, replacement of Thr-560 or Thr-537 by a serine residue should yield mutant channels with a ligand specificity similar to that of the respective wild-type channels. Surprisingly, the T560S mutant of the rod channel was activated at 5- to 6-fold lower cGMP concentrations ($K_{1/2}$ = 6.4 μM) than the wild-type rod channel (see Table 1). The T537S mutant of the olfactory channel was also 2-fold more sensitive to cGMP than the wild-type channel. The cAMP sensitivity of T560S was slightly decreased, and that of T537S was slightly increased. These results support the notion that a hydroxyl function in the amino acid residue at position 560 (and 537) is important for recognition of cGMP but not of cAMP.

DISCUSSION

The rod-photoreceptor channel is more sensitive to cGMP than to cAMP and contains a threonine residue at a particular

Table 1. $K_{1/2}$ and n of wild types and mutants

	Rod-photoreceptor channel		Olfactory channel	
	$K_{1/2}$, μM	n	$K_{1/2}$, μM	n
WT				
cGMP	32.63 ± 13.32 [15.67–53.57 (11)]	1.66 ± 0.56 [0.95–2.65]	1.36 ± 0.37 [0.89–2.39 (15)]	2.40 ± 0.64 [1.42–3.43]
cAMP	1210 ± 300 [850–1580 (3)]	1.81 ± 0.93 [1.05–3.12]	53.73 ± 15.05 [28.24–72.78 (6)]	2.59 ± 0.87 [1.81–4.23]
Thr → Ala				
cGMP	940 ± 140 [755–1265 (9)]	1.73 ± 0.44 [1.35–2.78]	53.03 ± 16.04 [33.38–77.74 (8)]	1.98 ± 0.56 [1.25–2.89]
cAMP	2750 ± 910 [1980–4030 (3)]	1.60 ± 0.27 [1.28–1.94]	16.29 ± 3.69 [10.90–25.94 (15)]	2.07 ± 0.54 [1.36–3.44]
Thr → Ser				
cGMP	6.40 ± 1.01 [4.68–8.23 (8)]	2.29 ± 0.19 [1.94–2.58]	0.69 ± 0.15 [0.55–0.95 (6)]	2.59 ± 0.54 [1.46–3.07]
cAMP	2240 ± 330 [1900–2690 (3)]	1.93 ± 0.10 [1.79–2.02]	13.87 ± 3.73 [10.17–18.98 (3)]	1.51 ± 0.37 [1.23–2.03]

Data are presented as means ± SDs. Ranges are in brackets; number of experiments are in parentheses.

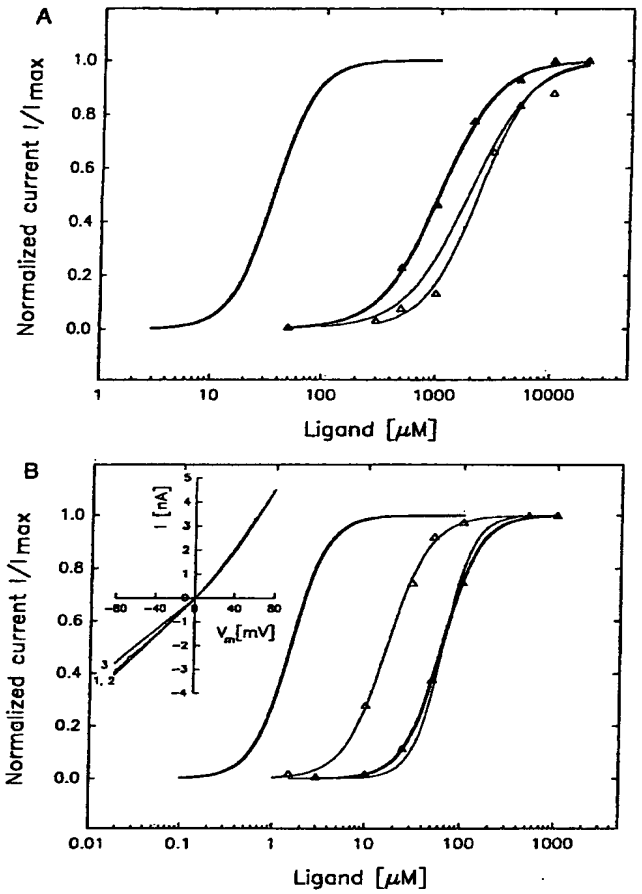

FIG. 3. Ligand sensitivity of normalized currents I/I_{max} of mutant channels. The smooth lines without symbols represent the fitted dose–response curves of wild-type channels for cGMP (thick lines) and cAMP (thin lines). (*A*) T560A rod mutant: ▲, cGMP; △, cAMP. $K_{1/2}$ (cGMP) = 1038 ± 30 μM, n = 1.8 ± 0.1; $K_{1/2}$ (cAMP) = 2250 ± 150 μM, n = 1.9 ± 0.2. (*B*) T537A olfactory mutant: ▲, cGMP; △, cAMP. $K_{1/2}$ (cGMP) = 62.2 ± 0.3 μM, n = 2.3 ± 0.03; $K_{1/2}$ (cAMP) = 16.4 ± 1.3 μM, n = 2.0 ± 0.3. (*Inset*) *I–V* curves from olfactory wild type (trace 1), T537A mutant (trace 2), and T537S mutant (trace 3) at saturating cGMP concentrations (scaled to *I–V* of wild type at +80 mV).

position in the cyclic nucleotide-binding site that is also conserved in cGKs but not in cAKs. Thus, the rod-photoreceptor channel by these criteria is a cGMP-gated channel. Surprisingly, the expressed olfactory channels from rat (7) and bovine tissue (this paper) are also much more sensitive to cGMP than to cAMP and exhibit a higher degree of sequence similarity to the cGMP-binding region of the rod channel and of cGKs than to the respective cAMP-binding domain of cAKs. Thus, by these criteria the olfactory channel has also a cGMP-specific binding site, even though cAMP most likely represents the physiologic ligand of the olfactory channel (24, 25). The available evidence does not support a similar role for cGMP in olfactory transduction (26).

The hypothesis by Weber *et al.* (9) predicts that a threonine residue enhances cGMP binding by forming a hydrogen bond with the guanine 2-amino group of cGMP, whereas no such interaction can occur with cAMP. Specifically, the $K_{1/2}$ constants for cGMP and cAMP should become similar in the threonine/alanine mutant channels if the difference in binding affinity is caused by the threonine–ligand interaction alone. The experimental results described in this paper are consistent with these basic features of the hypothesis. The similar cAMP sensitivity of wild-type and mutant channels argues against the possibility that the decrease in cGMP sensitivity in the threonine/alanine mutants might be caused by some unintended structural perturbations that propagate through the entire binding site.

Optimal hydrogen bonding requires the collinear alignment of the donor and acceptor group -O-H· · ·N (27). The methyl group at C_β in threonine might restrict rotational freedom around the C_α—C_β axis of the amino acid and thereby prevent optimal alignment of the atoms that form the hydrogen bond. Serine contains a hydrogen atom instead of a methyl group at C_β, and formation of a collinear hydrogen bond might be facilitated.

From the ratio of half-saturating cGMP concentrations $K_{1/2}$ between a binding site that can form an "optimal" hydrogen bond (T560S mutant) and a binding site that lacks this possibility altogether (T560A mutant), a difference in the incremental Gibbs free energy ΔG_b of ≈−3.0 kcal/mol is calculated according to the equation:

$$\Delta G_b = RT \ln[K_{1/2}\ (\text{T560S})/K_{1/2}\ (\text{T560A})].$$

This difference is quantitatively similar to the free energy of hydrogen bond formation (>3–6 kcal/mol), supporting the notion, but not proving it, that the higher cGMP sensitivity results from an additional hydrogen bond.

Experiments similar to those presented here have not yet been performed in other cGMP-binding proteins—for example, cGK. Shabb *et al.* (12), however, reported an increase in cGMP binding by introducing a threonine for an alanine residue in one of the two cyclic nucleotide-binding sites of the regulatory subunit of cAK—i.e., the reverse of the mutations introduced into the channel proteins. Our results are qualitatively similar to those obtained in cAK but differ in some quantitative aspects. For example, a mutant of cAK in which an alanine was replaced by serine, does not bind cGMP as strongly as the respective alanine/threonine mutant (12), and the alanine/threonine mutant still prefers binding of cAMP over cGMP.

Functional expression of mutant cyclic nucleotide-gated channels is particularly suitable for the study of structural features of the ligand-binding site. These channels are homo-oligomers (28) that contain only one cyclic nucleotide-binding domain per monomer (6), whereas the regulatory subunits of cAK and cGK contain two kinetically different ligand-binding sites. The cyclic nucleotide sensitivity and specificity of mutant binding sites in channels can be accurately determined *in situ* in excised membrane patches, whereas the regulatory subunit-cAK mutants need to be purified after expression for a functional or a binding assay (12).

The threonine/alanine difference is only one among several factors that determine the absolute binding affinity. Apparently, there are at least two different levels of structural organization of cyclic nucleotide-binding sites. The first level involves an invariant sequence pattern of amino acids shared by all cyclic nucleotide-binding sites (10): [NDEQRK]G[DEA]X[AG]XXX[FY]XXXXG{15–35}GE{5–20}R[ATSQ]A. X can be any amino acid, letters in brackets denote alternative amino acid residues at the relevant position, and numbers indicate the variable number of intervening residues. We define this sequence motif as the "core" of the binding site. The highly conserved arginine and glutamate residues (see Fig. 1) have been shown in catabolite gene activator protein to interact with the cyclic phosphodiester and the ribose moiety, respectively. At this level, a threonine residue increases cGMP affinity by formation of an additional hydrogen bond. In contrast, binding of cAMP to cAK does not involve hydrogen bonds with the adenine ring but differ-

ent mechanisms such as stacking interactions or van der Waals forces (for review, see ref. 29). Depending on the relative contribution of each interaction mechanism, it is conceivable that cyclic nucleotide-binding sites might exist that contain a threonine residue but which are more sensitive to cAMP than to cGMP. In this respect it will be interesting to determine the amino acid sequence of cAMP-specific channels (30, 31). For the rod-photoreceptor and olfactory channel, however, we were able to show that the threonine/alanine exchange is sufficient to establish the physiological range of nucleotide selectivity.

At a second level, interaction between the core of the ligand-binding site and other parts of the same or a neighboring subunit mediates activation of the channel. It affects the activation constant independently of the ligand species and might account for the absolute difference in sensitivity between the rod-photoreceptor and the olfactory channel. In fact, the $K_{1/2}$ constant of a chimeric rod channel that contains the binding region of the olfactory channel is identical with that of the wild-type rod channel. An analogous result was obtained with the respective olfactory channel chimera (unpublished observation). The importance of interactions between the binding site and other parts of the polypeptide for binding and activation has been also demonstrated in cAK, cGK, and catabolite gene activator protein (11, 32–35).

We are particularly grateful to Dr. W. Stühmer (Max-Planck-Institut, Göttingen, F.R.G.) for help and advice with the oocyte expression system and for critical reading of the manuscript. We also thank A. Eckert and M. Bruns for preparing many versions of the manuscript. This work was supported by a grant from the Deutsche Forschungsgemeinschaft Ka 545/6-2 and by the Fonds der Chemischen Industrie.

1. Fesenko, E. E., Kolesnikov, S. S. & Lyubarsky, A. L. (1985) *Nature (London)* **313**, 310–313.
2. Haynes, L. W. & Yau, K.-W. (1985) *Nature (London)* **317**, 61–64.
3. Yau, K.-W. & Baylor, D. A. (1989) *Annu. Rev. Neurosci.* **12**, 289–327.
4. Kaupp, U. B. (1991) *Trends Neurosci.* **14**, 150–157.
5. Nakamura, T. & Gold, G. H. (1987) *Nature (London)* **325**, 442–444.
6. Kaupp, U. B., Niidome, T., Tanabe, T., Terada, S., Bönigk, W., Stühmer, W., Cook, N. J., Kangawa, K., Matsuo, H., Hirose, T., Miyata, T. & Numa, S. (1989) *Nature (London)* **342**, 762–766.
7. Dhallan, R. S., Yau, K.-W., Schrader, K. A. & Reed, R. R. (1990) *Nature (London)* **347**, 184–187.
8. Ludwig, J., Margalit, T., Eismann, E., Lancet, D. & Kaupp, U. B. (1990) *FEBS Lett.* **270**, 24–29.
9. Weber, I. T., Shabb, J. B. & Corbin, J. D. (1989) *Biochemistry* **28**, 6122–6127.
10. Kaupp, U. B., Vingron, M., Altenhofen, W., Bönigk, W., Eismann, E. & Ludwig, J. (1991) in *Signal Transduction in Photoreceptor Cells* (Springer, Heidelberg), in press.
11. Weber, I. T., Steitz, T. A., Bubis, J. & Taylor, S. S. (1987) *Biochemistry* **26**, 343–351.
12. Shabb, J. B., Ng, L. & Corbin, J. D. (1990) *J. Biol. Chem.* **265**, 16031–16034.
13. Saiki, R. K., Gelfand, D. H., Stoffel, S., Scharf, S. J., Higuchi, R., Horn, G. T., Mullis, K. B. & Erlich, H. A. (1988) *Science* **239**, 487–491.
14. Kozak, M. (1984) *Nucleic Acids Res.* **12**, 857–872.
15. Hemsley, A., Arnheim, N., Toney, M. D., Cortopassi, G. & Galas, D. J. (1989) *Nucleic Acids Res.* **17**, 6545–6551.
16. Melton, D. A., Krieg, P. A., Rebagliati, M. R., Maniatis, T., Zinn, K. & Green, M. R. (1984) *Nucleic Acids Res.* **12**, 7035–7056.
17. Konarska, M. M., Padgett, R. A. & Sharp, P. A. (1984) *Cell* **38**, 731–736.
18. Hamill, O. P., Marty, A., Neher, E., Sakmann, B. & Sigworth, F. J. (1981) *Pflügers Arch.* **391**, 85–100.
19. Stühmer, W., Methfessel, C., Sakmann, B., Noda, M. & Numa, S. (1987) *Eur. Biophys. J.* **14**, 131–138.
20. Methfessel, C., Witzemann, V., Takahashi, T., Mishina, M., Numa, S. & Sakmann, B. (1986) *Pflügers Arch.* **407**, 577–588.
21. Kushner, L., Lerma, J., Bennett, M. V. L. & Zukin, R. S. (1989) in *Methods in Neurosciences*, ed. Conn, P. M. (Academic, New York), Vol. 1, pp. 3–29.
22. Tanaka, J. C., Eccleston, J. F. & Furman, R. E. (1989) *Biochemistry* **28**, 2776–2784.
23. Zufall, F., Firestein, S. & Shepherd, G. M. (1991) *J. Neurosci.*, in press.
24. Lancet, D. & Pace, U. (1987) *Trends Biochem. Sci.* **12**, 63–66.
25. Breer, H., Boekhoff, I. & Tareilus, E. (1990) *Nature (London)* **345**, 65–68.
26. Shirley, S. G., Robinson, J., Dickinson, K., Aujla, R. & Dodd, G. H. (1986) *Biochem. J.* **240**, 605–607.
27. Baker, E. N. & Hubbard, R. E. (1984) *Prog. Biophys. Mol. Biol.* **44**, 97–179.
28. Cook, N. J., Hanke, W. & Kaupp, U. B. (1987) *Proc. Natl. Acad. Sci. USA* **84**, 585–589.
29. Taylor, S. S., Buechler, J. A. & Yonemoto, W. (1990) *Annu. Rev. Biochem.* **59**, 971–1005.
30. Delgado, R., Hidalgo, P., Diaz, F., Latorre, R. & Labarca, P. (1991) *Proc. Natl. Acad. Sci. USA* **88**, 557–560.
31. DiFrancesco, D. & Tortora, P. (1991) *Nature (London)* **351**, 145–147.
32. Landgraf, W. & Hofmann, F. (1989) *Eur. J. Biochem.* **181**, 643–650.
33. Chan, V., Juang, L. C., Romero, G., Biltonen, R. L. & Huang, C. (1980) *Biochemistry* **19**, 924–928.
34. McKay, D. B., Weber, I. T. & Steitz, T. A. (1982) *J. Biol. Chem.* **257**, 9518–9524.
35. Garges, S. & Adhya, S. (1985) *Cell* **41**, 745–751.

Proceedings
OF THE
National Academy of Sciences
OF THE UNITED STATES OF AMERICA

Editorial correspondence: PROCEEDINGS OF THE NATIONAL ACADEMY OF SCIENCES, 2101 Constitution Avenue, Washington, DC 20418.

Business correspondence: Circulation Office of the PROCEEDINGS, National Academy of Sciences, 2101 Constitution Avenue, Washington, DC 20418.

Information for Contributors: See p. i (of this issue) and pp. i–viii of issue number 1, January 1, 1991.

Subscriptions: All correspondence concerning subscriptions should be addressed to the Circulation Office of the PROCEEDINGS. Subscriptions are entered on a calendar year basis only. For 1992, subscription rates are as follows—in the United States: student/postdoctoral, $50; personal, $210; institutional, $380; elsewhere by surface mail: student/postdoctoral, $145; personal, $305; institutional, $475; elsewhere by Air Cargo at a surcharge of $192. Information regarding other air mail postage rates is available from the Circulation Office. Subscribers are requested to notify the Circulation Office of the PROCEEDINGS 6 weeks in advance of any change of address; also the local postmaster. The Academy is not responsible for nonreceipt of issues because of an improper address unless a change of address is on file. The notice of address change should list both the old and new addresses. Claims for replacement copies will not be honored more than 60 days after the issue date for domestic subscribers and not more than 90 days after the issue date for foreign subscribers.

Back Issues: Volumes 83–87, January 1986 and thereafter, are available from the Circulation Office of the PROCEEDINGS. The price of a single issue is $20.00.

Second class postage paid at Washington, DC, and at additional mailing offices. PRINTED IN THE USA

PROCEEDINGS OF THE NATIONAL ACADEMY OF SCIENCES OF THE UNITED STATES OF AMERICA (ISSN-0027-8424) *is published semimonthly by* THE NATIONAL ACADEMY OF SCIENCES, *2101 Constitution Avenue, Washington, DC 20418.*

POSTMASTER: Send address changes to: PROCEEDINGS OF THE NATIONAL ACADEMY OF SCIENCES OF THE UNITED STATES OF AMERICA, 2101 Constitution Ave., Washington, DC 20418.

NOVEMBER 1, 1991
VOLUME 88
NUMBER 21

Proceedings
OF THE
National Academy of Sciences
OF THE UNITED STATES OF AMERICA

THE JOURNAL OF BIOLOGICAL CHEMISTRY Vol. 273, No. 36, Issue of September 4, pp. 23605–23610, 1998

Printed in U.S.A.

Dimerization of the Extracellular Calcium-sensing Receptor (CaR) on the Cell Surface of CaR-transfected HEK293 Cells*

(Received for publication, June 4, 1998)

Mei Bai‡, Sunita Trivedi, and Edward M. Brown

From the Endocrine-Hypertension Division, Department of Medicine, Brigham and Women's Hospital and Harvard Medical School, Boston, Massachusetts 02115

The extracellular calcium (Ca^{2+}_o)-sensing receptor (CaR) is a G protein-coupled receptor that plays important roles in calcium homeostasis. In this study, we employed epitope tagging, cell-surface biotinylation, and immunoprecipitation techniques to demonstrate that the CaR is expressed mostly in the form of a dimer on the surface of transfected human embryonic kidney (HEK293) cells. Western analysis of cell-surface proteins under nonreducing conditions showed that the CaR exists in several forms with molecular masses greater than 200 kDa. Most of these high molecular mass forms of the receptor could be converted to a single monomeric species at 160 kDa under reducing conditions. This result suggests that the CaR forms dimers or even higher oligomers on the cell surface through intermolecular disulfide bonds that are sensitive to reducing agents. Consistent with this hypothesis, use of a cell-surface cross-linking agent substantially increases the proportion of the putative dimeric CaR at 280 kDa relative to the monomeric form of the receptor at 160 kDa under reducing conditions. Dimerization of the CaR in intact cells was further demonstrated when we co-transfected and co-immunoprecipitated the wild type, full-length receptor and a truncated form of the CaR lacking its cytoplasmic tail. Taken together, we conclude from these results that the functional CaR resides on the cell surface of transfected HEK293 cells in the form of a dimer.

The extracellular calcium (Ca^{2+}_o)-sensing receptor (CaR)[1] is a G protein-coupled receptor (GPCR) (1). Activation of the CaR by elevated levels of Ca^{2+}_o stimulates phospholipase C and raises the cytosolic calcium concentration (Ca^{2+}_i). The physiological importance of the CaR in determining the level at which Ca^{2+}_o is set *in vivo* has been documented by the characterization of human syndromes resulting from activating or inactivating mutations of the CaR, which alter the function of parathyroid and kidney so as to produce hypo- or hypercalcemia, respectively (2, 3).

The function and expression of the CaR have been assessed in transiently transfected human embryonic kidney cells (HEK293) (4–9). CaR-transfected HEK293 cells respond to Ca^{2+}_o with an EC_{50} of 4.1 ± 0.1 mM (the effective concentration of Ca^{2+}_o producing one-half of the maximal Ca^{2+}_i response). The concentration-response curve for the Ca^{2+}_o-elicited Ca^{2+}_i responses in CaR-transfected HEK293 cells exhibits a relatively high Hill coefficient of about 3. This large Hill coefficient suggests a substantial degree of positive cooperativity in the binding of ligand and/or G protein by the CaR, which may involve intra- or intermolecular interactions (*e.g.* via formation of homodimers); namely, binding of the first ligand or G protein increases the affinity of the second ligand or G protein. Intermolecular interactions leading to cooperativity, for example, could result from dimerization of GPCRs (*e.g.* as for the muscarinic receptor and rhodopsin), which has been suggested as the molecular basis for cooperativity in the binding of their respective agonists (10, 11) or G proteins (12, 13).

Our earlier biochemical studies had shown the presence of considerable amounts of CaR-specific, high molecular mass immunoreactivity by Western analysis, in addition to the putative monomeric form of the receptor, in membrane proteins prepared from both CaR-transfected HEK293 cells and native parathyroid cells (4). These high molecular mass species likely correspond to dimeric and trimeric CaRs. The presence of dimeric forms of the CaR has also recently been described in detergent extracts prepared with the inner medulla of the rat kidney (14).

A structurally related GPCR, mGluR5, forms homodimers via intermolecular disulfide linkages within the amino-terminal extracellular domain. The extracellular domains of mGluR5 and the CaR share 17 cysteines in equivalent positions, raising the possibility that the CaR could also dimerize in this manner (15). In addition, several less structurally related GPCRs have been demonstrated to form homodimers, including the muscarinic receptor (16), β_2-adrenergic receptor (17, 18), glucagon receptor (19), and δ-opioid receptor (20). A noncovalent hydrophobic dimerization motif has been suggested to mediate homodimerization of the β_2-adrenergic receptor (18), which was also present in the CaR. Therefore, the CaR can potentially dimerize through two distinct types of intermolecular interactions, *i.e.* noncovalent hydrophobic interactions and formation of covalent intermolecular disulfide bonds.

In this report, using molecular and biochemical approaches, we show that the functional CaR normally resides on the cell surface mostly as a homodimer. The unusually high degree of cooperativity in the activation of the CaR by its polycationic agonists suggests that dimerization of the CaR is likely to have functional implications.

EXPERIMENTAL PROCEDURES

Site-directed Mutagenesis to Produce Tail-truncated Receptors—Site-directed mutagenesis was performed using the approach described by Kunkel (21). The *dut-1 ung-1* strain of *Escherichia coli*, CJ236, was transformed with cassette VI of a reconstructed CaR containing unique restriction sites introduced into the wild type human CaR as silent point mutations as described previously (4). Uracil-containing, single-stranded DNA was produced by infecting the cells with the helper

* This work was supported in part by National Institutes of Health Grant DK09436 (to M.B.) and The St. Giles Foundation (to E.M.B.). The costs of publication of this article were defrayed in part by the payment of page charges. This article must therefore be hereby marked "*advertisement*" in accordance with 18 U.S.C. Section 1734 solely to indicate this fact.

‡ To whom correspondence should be addressed: Endocrine-Hypertension Division, Brigham and Women's Hospital, 221 Longwood Ave., Boston, MA 02115. Tel.: 617-732-4093; Fax: 617-732-5764.

[1] The abbreviations used are: CaR, calcium (Ca^{2+}_o)-sensing receptor; GPCR; G protein-coupled receptor; PAGE, polyacrylamide gel electrophoresis; DTT, dithiothreitol; BS^3, bis(sulfosuccinimidyl) suberate.

phage, VCSM13. The single-stranded DNA was then annealed to a mutagenesis primer, which contained a stop codon at the desired position and was flanked on both sides by a wild type sequence. The primer was then extended around the entire single-stranded DNA and ligated to generate closed circular heteroduplex DNA. DH5α-competent cells were transformed with the DNA heteroduplex, and incorporation of the desired mutation was confirmed in all cases by sequencing the entire cassette. Finally, the mutated cassette VIs were cloned into the *Xho*I and *Xba*I sites of the reconstructed CaR (4).

Construction of Flag-tagged CaRs—Cassette III in each of the mutant receptors was replaced with that in the Flag-tagged wild type receptor (9) by double restriction digestion with *Afl*II and *Nhe*I followed by ligation of the larger restriction fragments containing point mutations and the smaller restriction fragment containing the Flag-tag.

Transient Expression of CaRs in HEK293 Cells—The DNA for transfection was prepared using the Midi Plasmid Kit (QIAGEN). LipofectAMINE (Life Technologies, Inc.) was employed as a DNA carrier for transfection (22) according to the manufacturer's procedures. The HEK293 cells used for transient transfection were provided by NPS Pharmaceuticals, Inc. (Salt Lake City, UT) and cultured in Dulbecco's modified Eagle's medium (Life Technologies, Inc.) with 10% fetal bovine serum (Hyclone). The DNA-liposome complex was prepared by mixing DNA and LipofectAMINE in Opti-MEM I Reduced Serum Medium (Life Technologies, Inc.) and incubating the mixture at room temperature for 30 min. The DNA-LipofectAMINE mixture was then diluted with Opti-MEM I Reduced Serum Medium and added to 90% confluent HEK293 cells plated on 13.5 × 20.1 mm glass coverslips using 0.625 μg of DNA (for measurement of Ca^{2+}_i) or in 100-mm Petri dishes using 3.75 μg of DNA (for obtaining protein for immunoprecipitation and Western analysis). After 5 h of incubation at 37 °C, equivalent amounts of Opti-MEM I Reduced Serum Medium with 20% fetal bovine serum were added to the medium overlying the transfected cells, and the latter was replaced with fresh Dulbecco's modified Eagle's medium containing 10% fetal bovine serum at 24 h after transfection. The expressed Ca^{2+}_o-sensing receptor protein was assayed 48 h after the start of transfection. To perform co-expression of two receptors, 0.625 μg each of the two cDNAs were mixed and used to transfect HEK293 cells.

Biotinylation of Cell-surface Forms of the CaR and Cross-linking of Multimeric Receptors—Prior to preparing whole cell lysates, intact HEK293 cells transiently transfected with Flag-tagged CaR were rinsed twice with phosphate-buffered saline and treated with 1 mM ImmunoPure Sulfo-NHS-Biotin (Pierce), a membrane-impermeant biotinylation reagent, at room temperature with constant agitation for 30 min to biotinylate the proteins on the cell surface. The reaction was then quenched by incubating the cells in 0.5 M Tris-HCl, pH 7.5, for 5 min. For cross-linking experiments, we added an appropriate amount of Bis(sulfosuccinimidyl) suberate (BS^3), a noncleavable, membrane-impermeant cross-linker, into the labeling solution with ImmunoPure Sulfo-NHS-Biotin.

Preparation of Whole Cell Lysates—The surface-biotinylated and/or cross-linked HEK293 cells were rinsed twice with phosphate-buffered saline and solubilized with 1% Triton X-100, 0.5% Nonidet P-40, 150 mM NaCl, 10 mM Tris, pH 7.4, 2 mM EDTA, 1 mM EGTA, protease inhibitors, including 83 μg/ml aprotinin, 30 μg/ml leupeptin, 1 mg/ml Pefabloc, 50 μg/ml calpain inhibitor, 50 μg/ml bestatin, and 5 μg/ml pepstatin (1 × immunoprecipitation buffer), at room temperature. Insoluble material was removed by centrifuging the cell lysates at 15,000 rpm for 15 min at 4 °C. The supernatants were collected as total cell lysates. The protein concentration was determined using the BCA protein assay (Pierce).

Immunoprecipitation of Flag-tagged CaRs—First, 5 μg of anti-Flag M2 monoclonal antibody (VWR), 400 μl of H_2O, 500 μl of 2 × immunoprecipitation buffer (see above), and 100 μl of total lysate containing approximately 500 μg of protein were added to a microcentrifuge tube. The mixture was incubated at 4 °C for 1 h. Then, 5 μl of an alkaline phosphatase-conjugated, anti-mouse IgG (Sigma) was added to the mixture. The incubation was continued for an additional 30 min at 4 °C. Subsequently, 50 μl of 10% Protein A-agarose (Life Technologies, Inc.) was added to the mixture for an additional 30-min incubation at 4 °C. The Protein A-agarose was washed three times with 1 × immunoprecipitation buffer, and the immunoreactive species were subsequently eluted in 60 μl of 2 × electrophoresis sample buffer at 65 °C for 30 min. The receptor of interest was detected by Western analysis.

Western Analysis of the Human CaR Expressed in Whole Cells and on the Cell Surface—An appropriate amount of immunoprecipitated proteins from CaR-transfected HEK293 cells was subjected to SDS-containing polyacrylamide gel electrophoresis (PAGE) (23) using a linear gradient of polyacrylamide (3–10%). The proteins on the gel were subsequently electrotransferred to a nitrocellulose membrane. After blocking with 5% milk, the forms of the receptor present on the cell surface were detected using an avidin-horseradish peroxidase conjugate (Bio-Rad) followed by visualization of the biotinylated bands with an enhanced chemiluminescence system (Amersham Pharmacia Biotech). After removal of the avidin using the recommended procedure for stripping the blots (Amersham Pharmacia Biotech), all forms of the CaR on the same blot were detected using anti-CaR antiserum (4641, a polyclonal antiserum raised against a peptide within the extracellular domain of the CaR, kindly provided by Drs. Forrest Fuller and Rachel Simin at NPS) followed by a secondary, horseradish peroxidase-conjugated goat anti-rabbit antibody and then an Enhanced Chemiluminescence system (Amersham Pharmacia Biotech).

Measurement of Ca^{2+}_i by Fluorimetry in Cell Populations—Coverslips with nearly confluent HEK293 cells previously transfected with the appropriate CaR cDNAs were loaded for 2 h at room temperature with fura-2/AM in 20 mM HEPES, pH 7.4, containing 125 mM NaCl, 4 mM KCl, 1.25 mM $CaCl_2$, 1 mM $MgSO_4$, 1 mM NaH_2PO_4, 0.1% bovine serum albumin, and 0.1% dextrose and were then washed once with a bath solution (20 mM HEPES, pH 7.4, containing 125 mM NaCl, 4 mM KCl, 0.5 mM $CaCl_2$, 0.5 mM $MgCl_2$, 0.1% dextrose, and 0.1% bovine serum albumin) at 37 °C for 20 min. The coverslips were then placed diagonally in a thermostatted quartz cuvette containing the bath solution, using a modification of the technique employed previously in this laboratory (24). Extracellular calcium was increased stepwise to give the desired final concentrations with additions of Ca^{2+}_o in increments of 1 mM that were followed by 5 mM increments after achieving a level of 5.5 mM Ca^{2+}_o and 10 mM increments after reaching a level of 20 mM Ca^{2+}_o. Excitation monochrometers were centered at 340 nm and 380 nm with emission light collected at 510 ± 40 nm through a wide band emission filter. The 340/380 excitation ratio of emitted light was used to calculate Ca^{2+}_i as described previously (24).

Statistics—The mean EC_{50} values for the wild type or truncated receptors determined in response to increasing concentrations of Ca^{2+}_o were calculated from the EC_{50} values for all of the individual experiments and were expressed with the standard error of the mean (S.E.) as the index of dispersion. Comparison of the EC_{50} values was performed using analysis of variance or Duncan's multiple comparison test (25) ($p \leq 0.05$). Each of the experiments described above in the experimental protocols was generally performed at least four times.

RESULTS

To detect cell-surface expression of the CaR, we introduced the Flag epitope tag into the extracellular domain of CaR. The function as well as the pattern and overall level of expression of the Flag-tagged CaR are identical to those of the wild type receptor, as assessed by high Ca^{2+}_o-evoked Ca^{2+}_i responses and Western analysis, respectively (9). Proteins on the cell surface of HEK293 cells transiently transfected with the Flag-tagged CaR or empty vector were first labeled with membrane-impermeant, Sulfo-NHS-Biotin prior to lysing the cells. The CaR was then immunoprecipitated with anti-Flag monoclonal antibody and eluted with SDS-sample buffer containing dithiothreitol (DTT) or no DTT. The free thiol groups of the native CaR were prevented from forming nonspecific disulfide bonds during protein preparation by including 100 mM iodoacetamide in the lysis buffer (see below). The immunopurified CaR was first detected with an avidin-horseradish peroxidase conjugate to visualize the forms of the receptor expressed on the cell surface. After removal of the avidin from the blot, the CaR was detected with a polyclonal anti-CaR antiserum (4), 4641, to detect both cell-surface and intracellular forms of the immunopurified receptor.

Identification of Cell-Surface Forms of the CaR—On reduced SDS-PAGE, using avidin for detection we identified a major band at 160 kDa (the expected position of the mature monomeric CaR) in the sample immunoprecipitated with anti-Flag antibody and reduced with DTT (Fig. 1*A*, *lane 2*). When we detected with anti-CaR antiserum, in contrast, two immunoreactive bands (*i.e.* a doublet) were observed at the expected positions of the monomeric as well as the putative dimeric and higher multimeric CaRs (Fig. 1*B*, *lane 2*). The surface forms of the monomeric receptor corresponded to the upper band of the

FIG. 1. **Determination of cell-surface expression of the CaR.** HEK293 cells were transfected with either Flag-tagged CaR (*lane 2*) or a vector with no CaR insert (*lane 1*). Proteins on the cell surface were treated with Sulfo-NHS-Biotin prior to lysing the cells in the presence of 100 mM iodoacetamide. The CaR was immunoprecipitated with anti-Flag antibody. The immunopurified protein samples were eluted with SDS-sample buffer containing 100 mM DTT and subjected to SDS-PAGE (3–10%). The surface expression of the CaR was detected with avidin (*panel A*). Both surface and intracellular forms of the CaR were then detected with anti-CaR antibody (4641) after removal of the avidin (*panel B*).

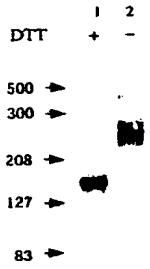

FIG. 2. **Detection of thiol-sensitive CaR homodimers in the absence of DTT.** HEK293 cells were singly transfected with Flag-tagged wild type CaR. Proteins on the cell surface were treated with Sulfo-NHS-Biotin prior to lysing the cells in the presence of 100 mM iodoacetamide. The CaR was immunoprecipitated with anti-Flag antibody. The immunopurified protein samples were eluted with SDS-sample buffer containing DTT (*lane 1*) or no DTT (*lane 2*) and subjected to SDS-PAGE (3–10%). Expression of the CaRs on the cell surface was determined using avidin.

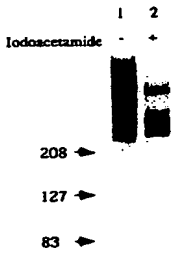

FIG. 3. **The inclusion of iodoacetamide blocks the formation of thiol-sensitive aggregates during protein preparation.** The transfected cells were lysed in the absence (*lane 1*) or presence (*lane 2*) of 100 mM iodoacetamide. The sample buffer for SDS-PAGE (3–10%) contained no DTT. The CaR in whole-cell lysate, 15 μg, was detected with anti-CaR antibody (4641).

doublet. With both methods of detection, the CaR-specific bands were not present in cells transfected with vector alone (Fig. 1, *A* and *B*, *lane 1*). Therefore, the observed bands are specific for the CaR.

The CaR Self-dimerizes through Disulfide Bonds—To preserve specific intermolecular disulfide linkages, we surface-biotinylated and immunoprecipitated the CaR, but eluted the immunoprecipitated receptor with SDS-sample buffer lacking DTT. The monomeric CaR observed in Fig. 1*A*, *lane 2*, was completely absent when nonreduced conditions were employed (see Fig. 2, *lane 2*). Instead, we detected two major bands between 200 and 300 kDa with avidin as well as one higher molecular mass species between 300 and 500 kDa for the wild type CaR (Fig. 2, *lane 2*). In this experiment, the control with DTT in Fig. 2, *lane 1*, showed a trace amount of a high molecular mass species at 280 kDa (the expected position of the dimeric CaR) in addition to the monomeric species. This 280-kDa band in Fig. 2, *lane 1*, lined up with the upper band of doublet observed between 200 and 300 kDa in Fig. 2, *lane 2*. It is likely that this 280-kDa band in Fig. 2, *lanes 1* and *2*, represents a more denatured dimeric receptor than the lower band at 250 kDa in Fig. 2, *lane 2*, if both bands are homodimeric receptors.

Next, to determine whether the dimerization is agonist-dependent, we preincubated the intact cells with high Ca^{2+}_o, *e.g.* 5 mM in 1 mM phosphate buffer, at 37 °C for 6 min prior to surface labeling. Under nonreducing conditions, the patterns of surface expression of the CaR were the same in cells stimulated and nonstimulated with high Ca^{2+}_o (data not shown), suggesting that activation of the receptor does not alter its degree of dimerization.

It was important in these studies to prevent the formation of nonspecific disulfide linkages during protein preparation by including 100 mM iodoacetamide in the lysis buffer. Iodoacetamide is a compound chemically reactive with the sulfhydryls on cysteines and prevents the latter from forming disulfide bonds. As shown in Fig. 3, *lane 2*, inclusion of 100 mM iodoacetamide in the lysis buffer prevented the formation of a smear of CaR immunoreactivity (Fig. 3, *lane 1*) that otherwise was evident in Western blots performed using the CaR-specific antiserum. Therefore, the high molecular species observed in Figs. 2 and 3, *lane 2*, are not the artifacts because of formation of nonspecific disulfide bonds.

To show that the putative dimers of the CaR observed on the cell surface were not artifacts of other types of nonspecific aggregation occurring during protein preparation, we stabilized pre-existing multimeric forms of the receptor on the cell surface by covalently linking them with BS^3, a noncleavable, membrane-impermeant cross-linker, while we surface-labeled the cells with the Sulfo-NHS-Biotin. The surface-biotinylated and cross-linked cells were then lysed in the presence of iodoacetamide. The Flag-tagged wild type receptor was immunoprecipitated, and the immunoprecipitated CaR was eluted with DTT-containing, SDS-sample buffer. When we increased the concentration of cross-linker, the ratios of dimer to monomer increased progressively (Fig. 4*A*). Without cross-linker, the monomer is the principal CaR species identified on the cell surface (Fig. 4*A*, *lane 1*) while with 5 mM BS^3, the dimer becomes the major species visible on the blot (Fig. 4*A*, *lane 4*). This result confirms that the dimeric receptor is the principal species present on the cell surface. The reduction in intensities of overall surface labeling by the Sulfo-NHS-Biotin in the presence of BS^3 occurs because both reagents form covalent bonds with the same pool of primary amines on the receptor.

When we employed anti-CaR antiserum to detect CaR-immunoreactive proteins to assess sample loading after removal of the avidin, we found that the sample loaded in Fig. 4, *lane 1*, was somewhat less than others based on the CaR immunoreactivities of the intracellular species, *i.e.* the lower band at 140 kDa in Fig. 4*B*, *lane 1*. Of interest, we found that the cross-linker did not change CaR immunoreactivity at 160 kDa in Fig.

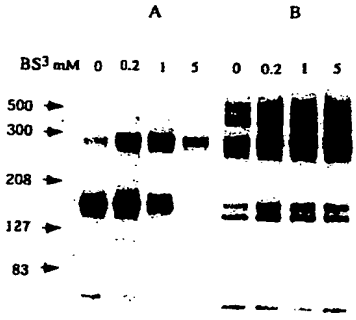

FIG. 4. **Stabilization of oligomers of the CaR on the cell surface using a noncleavable, membrane-impermeant cross-linker.** HEK293 cells were transfected with Flag-tagged CaR. Proteins on the cell surface were treated with both Sulfo-NHS-Biotin and varying concentrations of BS^3, a cross-linker, in millimolar, prior to lysing the cells. The CaR was then immunoprecipitated with anti-Flag antibody. The immunopurified protein samples were eluted with DTT-containing SDS buffer and subjected to SDS-PAGE (3–10%). Surface expression of the CaR was detected with avidin (*panel A*). Both surface and intracellular forms of the CaR were then detected with anti-CaR antibody (4641) after removal of the avidin (*panel B*).

FIG. 5. **Dimerization of CaRs truncated in their carboxyl-terminal tails.** HEK293 cells were transfected with Flag-tagged full-length CaR or CaRs truncated in their carboxyl termini at positions 863, 877, or 892. Proteins on the cell surface were treated with Sulfo-NHS-Biotin prior to lysing the cells in the presence of 100 mM iodoacetamide. The CaR was immunoprecipitated with anti-Flag antibody. The immunopurified protein samples were eluted with SDS-sample buffer containing no DTT and subjected to SDS-PAGE on a linear gradient running gel of 3–10%. The surface expression of the CaR was detected with avidin.

4*B*, unlike what we observed for the surface expression of the CaR in Fig. 4*A*, and all CaR-immunoreactive bands had similar ratios of monomers relative to dimers or oligomers (Fig. 4*B*). Therefore, the amount of the receptor on the cell surface must be sufficiently small that any changes in surface distribution between the monomeric and oligomeric forms as a result of cell-surface cross-linking does not produce any readily detectable alterations in the ratios of the intensities of the various CaR-immunoreactive bands when detected with anti-CaR antibody.

The Cytoplasmic Tail of the CaR Is Not Required for Dimerization—To examine the role of the CaR cytoplasmic tail in dimerization, several receptors with varying degrees of truncation of their carboxyl-terminal tails were constructed. We introduced stop codons at amino acid positions 863 (located at the beginning of the cytoplasmic tail), 877, and 892; the respective receptors are referred to below as K863Stop, A877Stop, and S892Stop. The truncated receptors, K863Stop (data not shown), similar to a slightly longer receptor terminated at position 865 that has been documented to be inactive by Ray *et al.* (26), and A877Stop (9), were functionally inactive, whereas S892Stop was not only active but also had a lower EC_{50} of 3.2 ± 0.1 mM (n = 6) for high $Ca^{2+}{}_o$-evoked increases in $Ca^{2+}{}_i$ than did the full-length wild type receptor (4.0 ± 0.2 mM, n = 4).

We then transfected HEK293 cells with the truncated receptors, surface-biotinylated the cells, and immunoprecipitated as above. Western analysis showed that the levels of expression of the truncated receptors were either similar to (K863Stop) or more than (A877Stop and S892Stop) that of the wild type receptor, and all three truncated receptors formed homodimers on the cell surface similar to the full-length, wild type receptor (Fig. 5) under nonreducing conditions. This result raised the possibility that the truncated receptors could form heterodimers with the full-length receptor when the two receptors were co-transfected, if high molecular weight species detected in nonreducing conditions (Fig. 5) were truly homodimers. Therefore, we next undertook studies to prove that the high molecular weight species of the various CaRs observed in Figs. 2 and 5, *i.e.* the wild type receptor and the truncated receptors, are indeed homodimers.

Co-transfection of Full-length Wild Type and Tail-truncated CaRs Produce Heterodimers in Addition to the Respective Homodimers—To determine whether the full-length and truncated receptors associate, we co-transfected the nontagged truncated receptors with a Flag-tagged full-length receptor or Flag-tagged truncated receptors with a nontagged full-length receptor and immunoprecipitated the tagged receptors. If the nontagged and tagged receptors formed heterodimers, we would be able to co-immunoprecipite nontagged receptors with tagged receptors. Because monomeric full-length and truncated receptors can be resolved under reducing conditions on SDS-PAGE, we would be able to determine the relative amounts of tagged and nontagged receptors, which were associated during immunopurification prior to elution with SDS-sample buffer containing DTT, on Western blot using avidin as a probe if we surface-biotinylated the co-transfected cells. Subsequently, we would be able to determine the nature of the association, namely dimers or higher oligomers, on nonreduced SDS-PAGE.

Fig. 6*A*, *lanes 2, 4, 6, 9, 11,* and *13*, shows that surface forms of nontagged receptors in co-transfected cells were co-immunoprecipitated using the anti-Flag antibody, which was resolved from co-transfected tagged receptors on a reduced SDS-PAGE and detected with avidin. As a control, the nontagged receptors isolated from singly transfected cells could not be immunoprecipitated by anti-Flag antibody (Fig. 6*A*, *lanes 1, 10, 12,* and *14*). On nonreduced PAGE, only oligomers (mostly dimers) were detected, and no monomeric forms of either full-length or truncated receptors were detected on the surface of co-transfected cells (Fig. 6*B*). As shown in Fig. 6*A*, the intensity of the Flag-tagged receptor was higher than that of the nontagged receptor, indicating that besides the heterodimers, there were substantial amounts of the homodimers of each of the co-transfected receptors. Of interest, the expression of the full-length receptor was significantly increased in cells co-transfected with S892Stop (Fig. 6*A*, *lane 13*) compared with that in cells transfected with the full-length receptor alone (Fig. 6*A*, *lane 8*).

DISCUSSION

The cross-linking and co-immunoprecipitation experiments carried out in the present study, together with Western analysis of cell-surface CaR under nonreducing conditions, clearly demonstrate that the CaR resides on the cell surface mostly as a dimer and possibly as higher oligomers but hardly at all as a monomer. Formation of homodimers between cytoplasmic tail-truncated receptors suggests that the cytoplasmic tail is not necessary for homodimerization. Unlike epidermal growth factors, platelet-derived growth factor and fibroblast growth factor

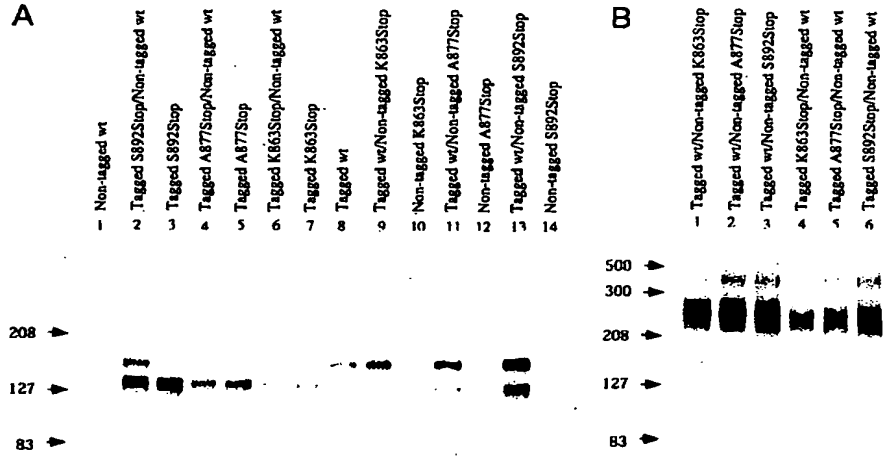

FIG. 6. **Co-immunoprecipitation of the nontagged wild type with Flag-tagged truncated receptors or nontagged truncated receptors with the Flag-tagged wild type receptor.** HEK293 cells transfected singly or doubly with Flag-tagged or nontagged CaRs, as indicated in the figure, were biotinylated prior to lysing the cells in the presence of 100 mM iodoacetamide. After immunoprecipitation with anti-Flag antibody, elution with SDS sample buffer containing DTT (*panel A*) or no DTT (*panel B*) and SDS-PAGE (3–10%), CaR surface expression was detected with avidin.

receptors, which undergo ligand-induced dimerization upon activation (27), the dimerization of the CaR is not agonist-dependent.

Fig. 3 shows that iodoacetamide blocks nonspecific aggregation of the CaR in whole cell lysates. Because iodoacetamide blocks the thiol groups on free cysteines from forming disulfide bonds with other free cysteines in the vicinity, the aggregates formed in the absence of iodoacetamide were most probably because of oxidation of the three cysteines that are present in the cytoplasmic tail of the CaR during the preparation of cellular proteins for gel electrophoresis. In the intact cell, these intracellular cysteines likely remain in a reduced form because of the strongly reducing intracellular environment maintained by the glutathione system (28). Indeed, no such nonspecific aggregation was observed with a mutant CaR in which the entire carboxyl-terminal tail was deleted, even in the absence of iodoacetamide.[2]

The majority of the surface dimeric form of the CaR and higher oligomers of the receptor observed under nonreducing conditions is readily converted to a single form of the monomeric receptors with a molecular mass of 160 kDa under reducing conditions (Fig. 2). Our earlier biochemical studies had shown that there are three monomeric forms of the CaR in crude membrane preparations of CaR-transfected HEK293 cells with molecular masses of 120, 140, and 160 kDa on reduced SDS-PAGE. These forms of the receptor represent the nonglycosylated CaR and receptors with varying types and extent of glycosylation (4), respectively. The 160-kDa species contains *N*-linked complex carbohydrates that we refer to as the mature form, whereas the 140-kDa species contains *N*-linked, high mannose-containing carbohydrates. The exclusive conversion of the surface CaR to a single form of monomeric receptor (160 kDa, Fig. 2, *lane 1*) suggests that only the CaR *N*-glycosylated with complex carbohydrate reaches the cell surface. In other words, biosynthetic intermediates, such as the immature forms of the CaR *N*-glycosylated with high mannose (140 kDa), fail to arrive at the cell surface.

The sensitivity of the dimeric receptor to reducing agents suggests that one type of intermolecular interaction mediating dimerization is intermolecular disulfide bonds. It is likely that the cysteine(s) involved in the intermolecular disulfide bond(s) of the CaR are located in the same general region identified in mGluR5 (15), because mGluR5 and the CaR share the relative positions of 20 cysteines. These shared cysteines may form either intramolecular disulfide bonds that are involved in the correct folding of both the CaR and mGluRs or intermolecular disulfide bonds for dimerization of these two receptors. It has been shown that the cysteine(s) involved in the intermolecular disulfide linkage of dimeric mGluR5 are located within about 17 kDa of the amino terminus (15). In this region, the CaR has six cysteines, including two within the putative signal peptide that are likely cleaved off by signal peptidase during biosynthesis of the receptor. Therefore, one or more of the four cysteines located within 17 kDa of the amino terminus and/or some of the nonconserved cysteines present in CaR may be involved in forming intermolecular disulfide bonds.

Moreover, we noted putative dimers even in the presence of reducing agents when we detected the CaR with either avidin, to detect cell-surface expression (Figs. 2 and 4*A*), or an anti-CaR antiserum (4641) to assess the overall level of CaR protein expression (Figs. 1*B* and 4*B*), including both the mature and immature forms. It has been suggested that a noncovalent hydrophobic dimerization motif in the β_2-adrenergic receptor (18) mediates the formation of a functionally important homodimer that is SDS-resistant. Interestingly, this consensus dimerization motif for noncovalent hydrophobic interactions is also present in the CaR within TM5 (LMALGFLIGYTCL, note that the conserved amino acids forming the putative intermolecular interface are underlined). Molecular modeling of GPCRs has suggested that TM5 is one of the most membrane-exposed of all the transmembrane segments, likely making this motif in one receptor molecule accessible to the same motif in another receptor molecule (29). Our previous studies showed that P747frameshift (a mutation identified in familial hypocalciuric hypercalcemia syndrome with a single-base deletion as well as a separate transversion in codon 747, which normally encodes proline, thereby resulting in a frameshift and a truncated CaR lacking TM5 and the rest of carboxyl terminus) can no longer form an SDS-resistant dimer in the presence of 100 mM DTT (5). Thus, the CaR's putative dimerization motif in TM5 could contribute to the formation of dimers of the receptor

[2] M. Bai, unpublished observation.

and/or stabilization of dimeric CaR during post-translational processing.

In conclusion, we have demonstrated that the CaR resides on the cell surface as homodimers that likely represent the active form of the receptor and contribute to the high degree of apparent cooperativity observed for the CaR. It is likely that the wild type and mutant CaRs form heterodimers in familial hypocalciuric hypercalcemia patients carrying a normal CaR on one allele and an abnormal CaR on the other. Furthermore, dominant negative phenotypes present in some familial hypocalciuric hypercalcemia patients suggest that formation of heterodimers between wild type and mutant receptors may negatively affect the function of the normal receptor in the heterodimeric complex. For example, a purely random association of the mutant receptor with either wild type CaRs or with other mutant receptors in the heterozygous state in familial hypocalciuric hypercalcemia could potentially reduce the level of the wild type homodimer to approximately one-quarter of that present in normal individuals.

Acknowledgments—We thank Dr. O. Kifor for helpful advice and Drs. J. E. Garrett, I. V. Capuano, A. Paruhar, F. Fuller, R. T. Simin, and K. V. Rogers for providing us with the HEK293 cells and the 4641 antibody.

REFERENCES

1. Brown, E. M., Gamba, G., Riccardi, D., Lombardi, M., Butters, R., Kifor, O., Sun, A., Hediger, M. A., Lytton, J., and Hebert, S. C. (1993) *Nature* **366**, 575–580
2. Pollak, M. R., Brown, E. M., Chou, Y. H., Hebert, S. C., Marx, S. J., Steinmann, B., Levi, T., Seidman, C. E., and Seidman, J. G. (1993) *Cell* **75**, 1297–1303
3. Pollak, M. R., Brown, E. M., Estep, H. L., McLaine, P. N., Kifor, O., Park, J., Hebert, S. C., Seidman, C. E., and Seidman, J. G. (1994) *Nat. Genet.* **8**, 303–307
4. Bai, M., Quinn, S., Trivedi, S., Kifor, O., Pearce, S. H. S., Pollak, M. R., Krapcho, K., Hebert, S. C., and Brown, E. M. (1996) *J. Biol. Chem.* **271**, 19537–19545
5. Pearce, S. H., Bai, M., Quinn, S. J., Kifor, O., Brown, E. M., and Thakker, R. V. (1996) *J. Clin. Invest.* **98**, 1860–1866
6. Pearce, S. H., Williamson, C., Kifor, O., Bai, M., Coulthard, M. G., Davies, M., Lewis-Barned, N., McCredie, D., Powell, H., Kendall-Taylor, P., Brown, E. M., and Thakker, R. V. (1996) *New Engl. J. Med.* **335**, 1115–1122
7. Bai, M., Pearce, S. H., Kifor, O., Trivedi, S., Stauffer, U. G., Thakker, R. V., Brown, E. M., and Steinmann, B. (1997) *J. Clin. Invest.* **99**, 88–96
8. De Luca, F., Ray, K., Mancilla, E. E., Fan, G. F., Winer, K. K., Gore, P., Spiegel, A. M., and Baron, J. (1997) *J. Clin. Endocrinol. Metab.* **82**, 2710–2715
9. Bai, M., Janicic, N., Trivedi, S., Quinn, S. J., Cole, D. E. C., Brown, E. M., and Hendy, G. N. (1997) *J. Clin. Invest.* **99**, 1917–1925
10. Potter, L. T., Ballesteros, L. A., Bichajian, L. H., Ferrendelli, C. A., Fisher, A., Hanchett, H. E., and Zhang, R. (1991) *Mol. Pharmacol.* **39**, 211–221
11. Hirschberg, B. T., and Schimerlik, M. I. (1994) *J. Biol. Chem.* **269**, 26127–26135
12. Wessling-Resnick, M., and Johnson, G. L. (1987) *J. Biol. Chem.* **262**, 3697–3705
13. Willardson, B. M., Pou, B., Yoshida, T., and Bitensky, M. W. (1993) *J. Biol. Chem.* **268**, 6371–6382
14. Ward, D. T., Brown, E. M., and Harris, H. W. (1998) *J. Biol. Chem.* **273**, 14476–14483
15. Romano, C., Yang, W. L., and O'Malley, K. L. (1996) *J. Biol. Chem.* **271**, 28612–28616
16. Avissar, S., Amitai, G., and Sokolovsky, M. (1983) *Proc. Natl. Acad. Sci. U. S. A.* **80**, 156–159
17. Venter, J. C., and Fraser, C. M. (1983) *Fed. Proc.* **42**, 273–278
18. Hebert, T. E., Moffett, S., Morello, J. P., Loisel, T. P., Bichet, D. G., Barret, C., and Bouvier, M. (1996) *J. Biol. Chem.* **271**, 16384–16392
19. Herberg, J. T., Codina, J., Rich, K. A., Rojas, F. J., and Iyengar, R. (1984) *J. Biol. Chem.* **259**, 9285–9294
20. Cvejic, S., and Devi, L. A. (1997) *J. Biol. Chem.* **272**, 26959–26964
21. Kunkel, T. A. (1985) *Proc. Natl. Acad. Sci. U. S. A.* **82**, 488–492
22. Hawley-Nelson, P., Ciccarone, V., Gebeyehu, G., Jessee, J., and Felgner, P. L. (1993) *Focus* **15**, 73–79
23. Laemmli, U. K. (1970) *Nature* **227**, 680–685
24. Fajtova, V. T., Quinn, S. J., and Brown, E. M. (1991) *Am. J. Physiol.* **261**, E151–E158
25. Duncan, D. B. (1955) *Biometrics* **11**, 1–42
26. Ray, K., Fan, G. F., Goldsmith, P. K., and Spiegel, A. M. (1997) *J. Biol. Chem.* **272**, 31355–31361
27. Heldin, C. H. (1995) *Cell* **80**, 213–223
28. Schulz, G. E., and Schirmer, R. H. (1985) *Principles of Protein Structure* (Cantor, C. R., ed) 1st Ed., pp. 53–55, Springer-Verlag New York Inc., New York
29. Baldwin, J. M. (1993) *EMBO J.* **12**, 1693–1703

GENERAL INFORMATION

This publication is available on-line at http://www.jbc.org. Inquire about availability through your subscription agent or contact: The Journal of Biological Chemistry, P.O. Box 830399, Birmingham, AL 35283-0399, U.S.A. Minireviews are reprinted in January of the succeeding year in a Minireview Compendium. Compendia for 1988 through 1997 are available through the ASBMB office: ASBMB Office, 9650 Rockville Pike, Bethesda, MD 20814, U.S.A.

Submit *all* manuscripts in quadruplicate to

Editor, The Journal of Biological Chemistry
9650 Rockville Pike
Bethesda, MD 20814, U.S.A.

Accepted manuscripts will be published with the implicit understanding that the author(s) will pay a charge per page. Current page charges may be obtained by contacting the JBC office. Under exceptional circumstances, when no source of grant or other support exists, the author(s) may apply, at the time of submission, for a grant-in-aid to Chairman, Publications Committee, American Society for Biochemistry and Molecular Biology, Inc., 9650 Rockville Pike, Bethesda, MD 20814. All such applications must be countersigned by an appropriate institutional official stating that no funds are available for page charges.

Queries on matters of general editorial policy, requests for reprints of the "Instructions to Authors," or of the "Editorial Policy and Practices," or for permission to reproduce any part of a previously published article should be directed to the Journal Editorial Office in Bethesda, telephone 301-530-7150; fax 301-571-1824; E-mail jbc@asbmb.faseb.org.

The Journal of Biological Chemistry publishes papers on a broad range of topics of interest to biochemists. The views expressed are those of the author(s) and not of *The Journal of Biological Chemistry* or the American Society for Biochemistry and Molecular Biology.

Address all correspondence and orders relative to subscriptions and back copies to: *The Journal of Biological Chemistry,* P.O. Box 830399, Birmingham, AL 35283-0399, U.S.A., telephone 800-633-4931. Subscriptions are entered on a calendar year basis only. Allow at least six weeks for address changes. Claims for replacement copies must be received within three months of the issue date.

The Journal of Biological Chemistry (ISSN 0021-9258) is published weekly by the American Society for Biochemistry and Molecular Biology, Inc., 9650 Rockville Pike, Bethesda, MD 20814. Volume 273 for 1998: Institutions: United States, $1,500; Foreign, $1,750. Single copies of the Journal are $30. (Note: Maryland and Canada add applicable taxes, unless a tax-exempt certificate number is shown.) The GST number for Canadian subscribers is 13037 0018 RT. C.P.C Int'l Pub Mail # 0060119. Periodicals postage paid at Bethesda, MD 20814, U.S.A. and at additional mailing offices. Printed in the U.S.A. Subscription rates for the on-line JBC are available at http://www.jbc.org. POSTMASTER: Send address changes to The Journal of Biological Chemistry at P.O. Box 830399, Birmingham, AL 35283-0399, U.S.A.

tember 4, 1998 VOLUME 273 NUMBER 36

0021-9258 (Print)
1083-351x (Electronic)
JBC 273(36) 22857–23616 (1998)

THE Journal of Biological Chemistry

Published by the American Society for Biochemistry and Molecular Biology

FOUNDED BY CHRISTIAN A HERTER

AND SUSTAINED IN PART BY THE CHRISTIAN A HERTER MEMORIAL FUND

Cell, Vol. 100, 703–711, March 17, 2000, Copyright ©2000 by Cell Press

T2Rs Function as Bitter Taste Receptors

Jayaram Chandrashekar,* Ken L. Mueller,*
Mark A. Hoon,† Elliot Adler,† Luxin Feng,‡ Wei Guo,*
Charles S. Zuker,*§ and Nicholas J. P. Ryba†§
*Howard Hughes Medical Institute and
Department of Biology
Department of Neurosciences
University of California, San Diego
La Jolla, California 92093
†National Institute of Dental and Craniofacial Research
National Institutes of Health
Bethesda, Maryland 20892
‡Aurora Biosciences
11010 Torreyana Road
La Jolla, California 92121

Summary

Bitter taste perception provides animals with critical protection against ingestion of poisonous compounds. In the accompanying paper, we report the characterization of a large family of putative mammalian taste receptors (T2Rs). Here we use a heterologous expression system to show that specific T2Rs function as bitter taste receptors. A mouse T2R (mT2R-5) responds to the bitter tastant cycloheximide, and a human and a mouse receptor (hT2R-4 and mT2R-8) responded to denatonium and 6-*n*-propyl-2-thiouracil. Mice strains deficient in their ability to detect cycloheximide have amino acid substitutions in the *mT2R-5* gene; these changes render the receptor significantly less responsive to cycloheximide. We also expressed mT2R-5 in insect cells and demonstrate specific tastant-dependent activation of gustducin, a G protein implicated in bitter signaling. Since a single taste receptor cell expresses a large repertoire of T2Rs, these findings provide a plausible explanation for the uniform bitter taste that is evoked by many structurally unrelated toxic compounds.

Introduction

Mammals can perceive and distinguish between sweet, sour, bitter, and salty tastes (Kinnamon and Cummings, 1992; Lindemann, 1996a; Stewart et al., 1997). Of these four modalities, bitter perception has a particularly important role: many naturally poisonous substances taste bitter to humans, and virtually all animal species show an aversive response to such tastants (Garcia and Hankins, 1975; Glendinning, 1994; Glendinning et al., 1999), suggesting that bitter transduction evolved as a key defense mechanism against the ingestion of harmful substances.

The biology of bitter perception is very poorly understood; neither the sensory receptor cells nor the receptor molecules have been physiologically or molecularly defined (Lindemann, 1996b). However, several biochemical and physiological studies have suggested that bitter transduction in mammalian taste receptor cells is mediated by G proteins and G protein–coupled receptors (GPCRs) (Lindemann, 1996a; Wong et al., 1996). Because the universe of chemical compounds that evoke a bitter taste is structurally diverse, we reasoned that bitter receptors might encompass a large GPCR family with significant sequence variation. In the accompanying paper (Adler et al., 2000 [this issue of *Cell*]), we described the isolation of a novel family of 40–80 divergent GPCRs, T2Rs, selectively expressed in subsets of taste receptor cells of the tongue and palate epithelium. T2Rs in humans and mice are genetically linked to loci associated with bitter perception (Conneally et al., 1976; Capeless et al., 1992; Reed et al., 1999), and are selectively expressed in taste receptor cells that contain gustducin, a G protein α subunit implicated in bitter transduction (Wong et al., 1996; Ming et al., 1998). While the genetics, expression profile, and diversity of the T2R family support the proposal that T2Rs are taste receptors, rigorous demonstration of their role in taste transduction requires functional validation. Here we use a heterologous expression system to demonstrate that T2Rs function as receptors for bitter tastants. We analyzed mouse strains that differ in their recognition of various bitter compounds and show that mice that do not perceive low concentrations of cycloheximide contain missense mutations in the *mT2R-5* gene. These amino acid changes significantly reduce the sensitivity of the mT2R-5 receptor to cycloheximide. Notably, this sensitivity shift measured in cell-based assays closely mirrors the behavioral phenotype of the *Cyx*-deficient mice (Lush and Holland, 1988). The discovery of mammalian bitter receptors will help understand the biology of bitter perception, from transduction pathways in receptor cells to coding of bitter signals through the afferent sensory pathway.

Results and Discussion

Functional Expression of T2Rs

A difficulty in generating a cell-based reporter system to measure T2R activity is our poor understanding of the native signaling pathway. We therefore expressed T2Rs with Gα15, a G protein α subunit that has been shown to couple a wide range of receptors to phospholipase Cβ (Offermanns and Simon, 1995; Krautwurst et al., 1998). In this system, receptor activation leads to increases in intracellular calcium ($[Ca^{2+}]_i$, which can be monitored at the single cell level using the FURA-2 calcium-indicator dye (Tsien et al., 1985). To test and optimize Gα15 coupling, we used two different GPCRs, a Gαi-coupled μ opioid receptor (Reisine, 1995) and a Gαq-coupled mGluR1 receptor (Masu et al., 1991). Transfection of these receptors into HEK-293 cells produced robust, agonist-selective, and Gα15-dependent Ca^{2+} responses (Figure 1). To assay T2R function, we initially generated four expression constructs containing epi-

§To whom correspondence should be addressed (e-mail: nr13k@nih.gov [N. J. P. R.], czuker@flyeye.ucsd.edu [C. S. Z.]).

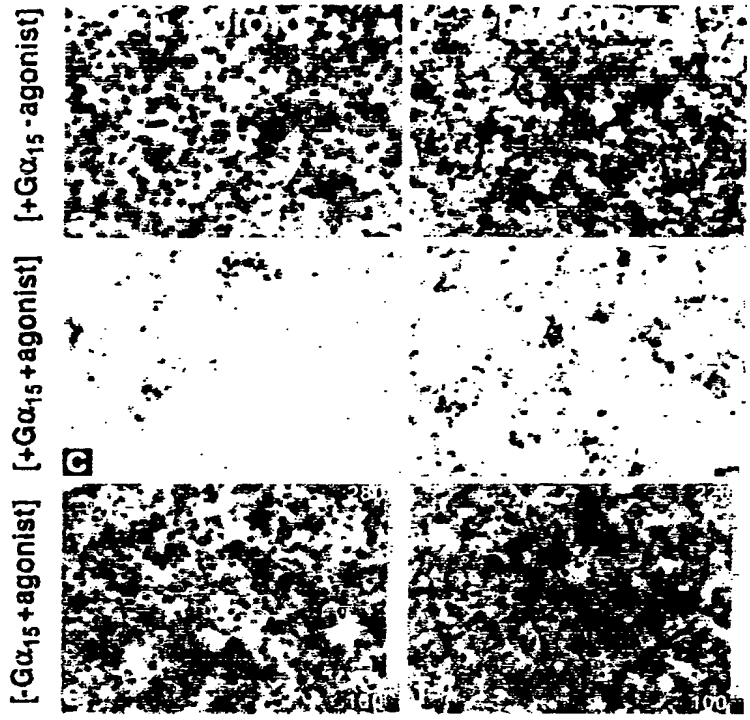

Figure 1. Gα15 Couples Activation of μ Opioid Receptor and mGluR1 Receptor to Release of Intracellular Calcium

HEK-293 cells were transiently transfected with the Gαi-coupled μ opioid receptor or the Gαq-coupled mGluR1 receptor. Transfected cells containing Gα15 were assayed for increases in $[Ca^{2+}]_i$ before (a and b) and after (c and d) the addition of receptor agonists: (c) 10 μM DAMGO and (d) 20 μM trans (±) 1-amino-1,3 cyclopentane dicarboxylic acid (ACPD). Ligand- and receptor-dependent increases in $[Ca^{2+}]_i$ were dependent on Gα15 (e and f). Scales indicate $[Ca^{2+}]_i$ (nM) determined from FURA-2 emission ratios.

tope-tagged hT2R-3, hT2R-5, hT2R-10, and hT2R-16 (see Adler et al., 2000). However, none of the receptors was efficiently targeted to the plasma membrane.

A number of studies have shown that many GPCRs, in particular sensory receptors, require specific "chaperones" for maturation and targeting through the secretory pathway (Baker et al., 1994; Dwyer et al., 1998). Recently, Krautwurst et al. (1998) generated chimeric receptors consisting of the first 20 amino acids of rhodopsin and various rodent olfactory receptors. These were targeted to the plasma membrane and functioned as odorant receptors in HEK-293 cells. We constructed rhodopsin-T2R chimeras (rho-T2Rs) and determined that the first 39 amino acids of bovine rhodopsin are very effective in targeting T2Rs to the plasma membrane of HEK-293 cells (Figure 2). Similar results were obtained with 11 human and 16 rodent T2Rs (see below). Inclusion of this N-terminal sequence also increased membrane expression of control mGluR1 receptors, and significantly augmented their Gα15-mediated responses (data not shown). To further enhance the level of T2R expression, rho-T2Rs were placed under the control of a strong EF-

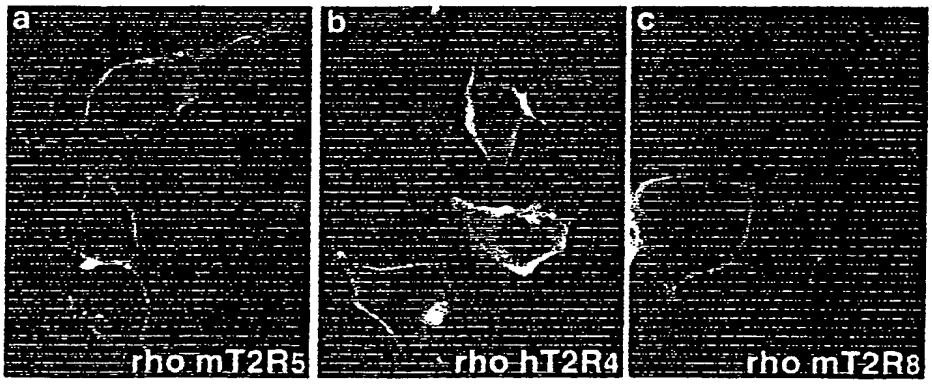

Figure 2. Rho-T2R Fusions Are Targeted to the Plasma Membrane

The first 39 amino acids of bovine rhodopsin effectively targeted T2Rs to the plasma membrane of HEK-293 cells. Immunofluorescence staining of nonpermeabilized cells transfected with representative rho-T2R fusions was detected using an anti-rhodopsin mAb B6–30.

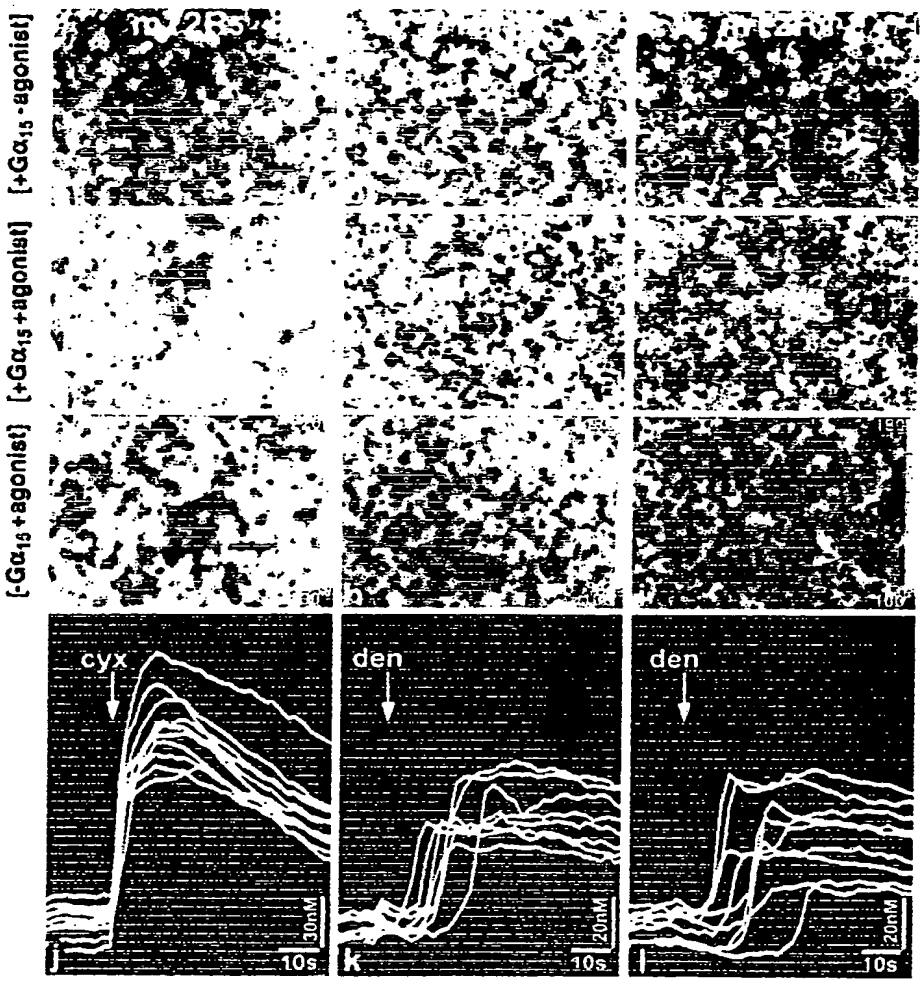

Figure 3. T2R Receptors Are Stimulated by Bitter Compounds

HEK-293 cells were transfected with rho-mT2R-5 (a, d, and g), rho-hT2R-4 (b, e, and h), and rho-mT2R-8 (c, f, and i). Cells expressing mT2R-5 were stimulated using 1.5 μM cycloheximide (d and g) and those expressing hT2R-4 and mT2R-8 with 1.5 mM denatonium (e, f, h, and i). No increase in $[Ca^{2+}]_i$ was observed in the absence of Gα15 (g–i); in contrast robust Gα15-dependent responses were observed in the presence of tastants (d–f); scales indicate $[Ca^{2+}]_i$ (nM) determined from FURA-2 emission ratios. Line traces (j–l) show the kinetics of the $[Ca^{2+}]_i$ changes for representative cells from panels (d–f); arrows indicate addition of tastants.

1α promoter and introduced as episomal plasmids into modified HEK-293 cells expressing Gα15 (PEAK^{rapid} cells; see Experimental Procedures).

We employed two parallel strategies to identify ligands for T2Rs. In one, we chose a random set of human, rat, and mouse T2R receptors, and individually tested them against a collection of 55 bitter and sweet tastants (see Experimental Procedures). We expected functional coupling to meet four criteria: tastant selectivity, temporal specificity, and receptor- and G protein-dependence. In the other, we used data on the genetics of bitter perception in mice to link candidate receptors with specific tastants.

Nearly 30 years ago, it was first reported that various inbred strains of mice differ in their sensitivity to the bitter compound sucrose-octaacetate (Warren and Lewis, 1970). Subsequently, a number of studies demonstrated that this strain difference was due to allelic variation at a single genetic locus (*Soa*) (Whitney and Harder, 1986; Capeless et al., 1992). These findings were extended to additional loci influencing sensitivity to various bitter tastants, including raffinose undecaacetate (*Rua*), cycloheximide (*Cyx*), copper glycinate (*Glb*), and quinine (*Qui*) (Lush, 1984, 1986; Lush and Holland, 1988). Genetic mapping experiments showed that the *Soa, Rua, Cyx, Qui,* and *Glb* loci are clustered at the distal end of chromosome 6 (Lush and Holland, 1988; Capeless et al., 1992). In the accompanying paper, we show that at least 25 mT2Rs colocalize with this mouse chromosome 6 bitter cluster (Adler et al., 2000). Therefore, we selected

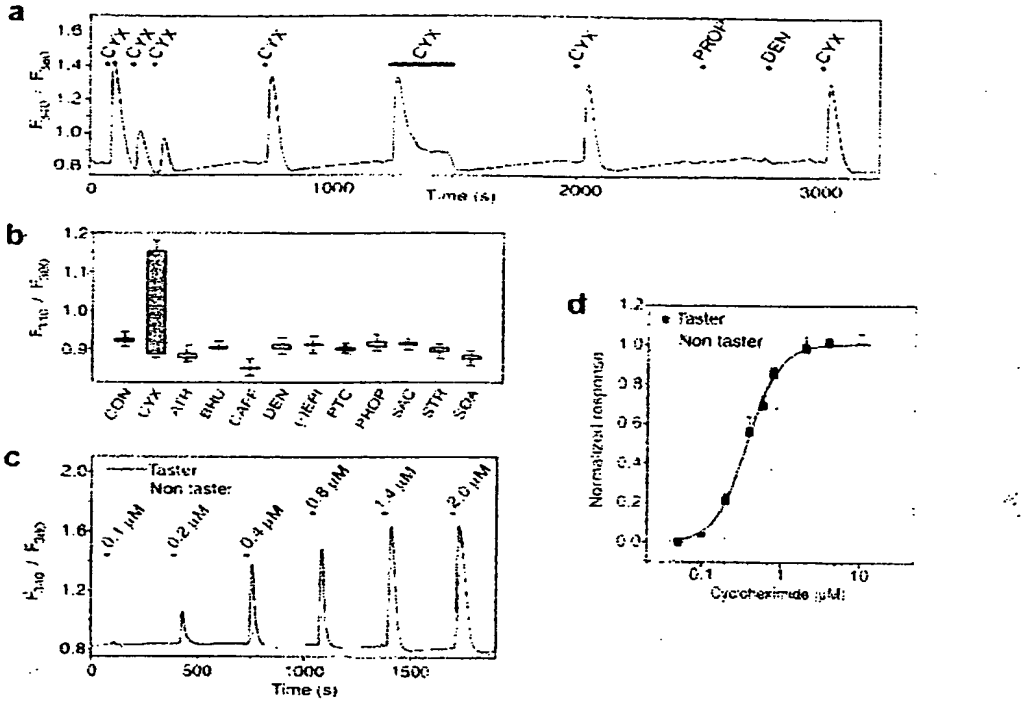

Figure 4. mT2R-5 Is a Taste Receptor for Cycloheximide

(a) HEK-293 cells expressing Gα15 and rho-mT2R-5 were challenged with multiple pulses of 2 μM cycloheximide (CYX), 3 mM 6-n-propyl thiouracil (PROP), or 5 mM denatonium (DEN); dots and horizontal bars above the traces indicate the time and duration of tastant pulses. Cycloheximide triggers robust receptor activation. This experiment also illustrates desensitization to repeated stimulation or during sustained application of the stimulus. The data shown here were derived from 50 responding cells on a high-density plate. Equivalent results were obtained in HEK-293 cell plated at high (confluent) or low density. (b) Responses to cycloheximide are highly specific and are not observed after addition of buffer (CON) or high concentrations of other tastants. Abbreviations and concentrations used are: cycloheximide, CYX (5 μM); atropine, ATR (3 mM); brucine, BRU (5 mM); caffeic acid, CAFF (2 mM); denatonium, DEN (5 mM); epicatechin, (−)EPI (3 mM); phenyl thiocarbamide, PTC (3 mM); 6-n-propyl thiouracil, PROP (10 mM); saccharin, SAC (10 mM); strychnine, STR (5 mM); sucrose octaacetate, SOA (3 mM). Columns represent the mean ± SE of at least six independent experiments. (c) The mT2R-5 gene from taster (DBA/2-allele) and nontaster (C57BL/6-allele) strains mediate differential $[Ca^{2+}]_i$ changes to pulses of cycloheximide. Horizontal bars depict the time and duration of the stimulus. We waited 200 s between stimuli to ensure that cells were not desensitized due to the successive application of cycloheximide. (d) Cycloheximide dose response of mT2R-5. Changes in $[Ca^{2+}]_i$ are shown as FURA-2 (F_{340}/F_{380}) ratios normalized to the response at 30 μM cycloheximide; points represent the mean ± SE of at least six determinations. The nontaster allele shows a marked decrease in cycloheximide sensitivity relative to the taster allele. The data shown in panels (a), (c), and (d) were obtained from measurements of $[Ca^{2+}]_i$ from 50 individual responding cells. Because HEK-293 cells plated at high density may form functional gap junctions, our quantitative studies were based on recordings from isolated cells (see Experimental Procedures). Qualitatively similar data was obtained in whole-field recordings.

T2R receptors from this array, constructed the corresponding rho-mT2R chimeras and individually transfected them into HEK-293 cells expressing the promiscuous Gα15 protein. After loading the cells with FURA-2, we assayed for responses to sucrose octaacetate, raffinose undecaacetate, copper glycinate, quinine, and cycloheximide. As controls for transfection efficiencies, we used a CMV-GFP construct, and as a control for Gα15 signaling a set of plates was cotransfected with rho-mGluR1 and assayed for responses to the mGluR1-agonist ACPD.

Cells expressing mT2R-5 specifically responded to cycloheximide (Figure 3). The response occurred in nearly all transfected cells and was receptor- and Gα15-dependent because cells lacking either of these components did not trigger $[Ca^{2+}]_i$ changes (Figure 3g), even at 5000-fold higher cycloheximide concentration. As expected for this coupling system, the tastant-induced increase in $[Ca^{2+}]_i$ was due to release from internal stores, since analogous results were obtained in nominally zero $[Ca^{2+}]_{out}$ (data not shown). The activation of mT2R-5 by cycloheximide is very selective; this receptor did not respond to any other tastants (Figures 4a and 4b), even at concentrations that far exceeded their biologically relevant range of action (Saroli, 1984; Glendinning, 1994). While cycloheximide is only moderately bitter to humans (Lush and Holland, 1988), it is strongly aversive to rodents with a sensitivity threshold of ~0.25 μM (Kusano et al., 1971; Lush and Holland, 1988). In our cell-based assay, the concentration of cycloheximide required to induce half-maximal response of mT2R-5 was 0.5 μM, and the threshold was ~0.2 μM (Figures

4c and 4d). Notably, this dose response closely matches the sensitivity range of cycloheximide tasting in mice (Lush and Holland, 1988; see next section).

To examine the kinetics of the cycloheximide response, rho-mT2R-5 transfected cells were placed on a microperfusion chamber and superfused with test solutions under various conditions. Figure 4a shows robust transient responses to micromolar concentrations of cycloheximide that closely follow application of the stimulus (latency <1 s). As expected, when the tastant was removed, $[Ca^{2+}]_i$ returned to baseline. A prolonged exposure to cycloheximide (>10 s) resulted in adaptation: a fast increase of $[Ca^{2+}]_i$ followed by a gradual, but incomplete decline to the resting level (Figure 4a). Similarly, successive applications of cycloheximide led to significantly reduced responses, indicative of desensitization (Lefkowitz et al., 1992). This is likely to occur at the level of receptor, since responses of a cotransfected mGluR1 were not altered during the period of cycloheximide desensitization (data not shown).

Are other T2Rs also activated by bitter compounds? We assayed 11 rhodopsin-tagged human T2R receptors by individually transfecting them into HEK-293 cells expressing Gα15. Each transfected line was tested against a battery of bitter and sweet tastants, including amino acids, peptides, and other natural and synthetic compounds (see Experimental Procedures). We found that the intensely bitter tastant denatonium induced a significant transient increase in $[Ca^{2+}]_i$ in cells transfected with one of the human candidate taste receptors, hT2R-4, but not in control untransfected cells (Figure 3), or in cells transfected with other hT2Rs. The denatonium response had a strong dose dependency with a threshold of ~100 μM. While this response met the criteria of tastant selectivity, temporal specificity, and receptor- and Gα15-dependency, the threshold for activation was over two orders of magnitude higher than the human psychophysical threshold for denatonium (Saroli, 1984). This could be due to poor functioning of this receptor in the heterologous expression system, or perhaps humans express another higher affinity denatonium receptor. Interestingly, hT2R-4 displayed a limited range of promiscuity since it also responded to high concentrations of the bitter tastant 6-n-propyl-2-thiouracil (PROP; Figure 5).

If the responses of hT2R-4 reflect the in vivo function of this receptor, we hypothesized that similarly tuned receptors might be found in other species. The mouse receptor mT2R-8 is a likely ortholog of hT2R-4: they share ~70% identity, while the next closest receptor is only 40% identical; these two genes are contained in homologous genomic intervals (Adler et al., 2000). We generated a rho-mT2R-8 chimeric receptor and examined its response to a wide range of tastants. Indeed, mT2R-8, like its human counterpart, is activated by denatonium and by high concentrations of PROP (Figures 3 and 5). No other tastants elicited significant responses from cells expressing mT2R-8. Because these two receptors share only 70% identity, the similarity in their responses to bitter compounds attests to their role as orthologous bitter taste receptors.

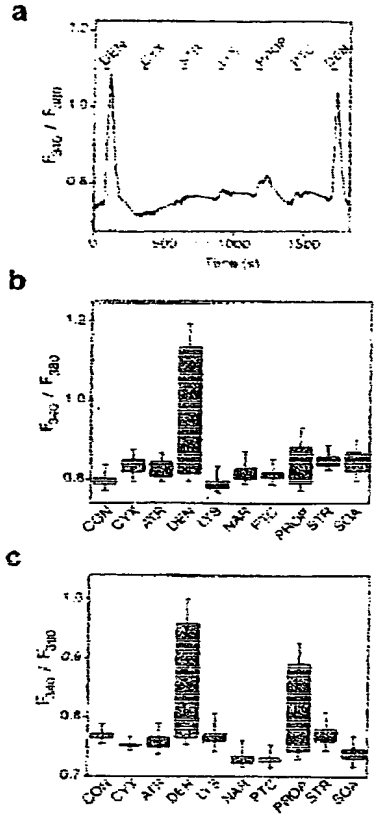

Figure 5. hT2R-4 and mT2R-8 Respond to Denatonium

HEK-293 cells expressing Gα15 were transiently transfected with hT2R-4 or mT2R-8 receptors and $[Ca^{2+}]_i$ was monitored as shown in Figure 3. (a) An increase in $[Ca^{2+}]_i$ could be induced by stimulation with denatonium but not by various other bitter compounds. Response profiles of (b) hT2R-4 and (c) mT2R-8 to a set of nine out of 55 different bitter and sweet tastants (see Experimental Procedures) are shown. CON refers to control buffer addition, NAR to 2 mM naringin and LYS to 5 mM lysine. Other abbreviations and concentrations are as reported in Figure 4. The mean FURA-2 fluorescence ratio (F_{340}/F_{380}) before and after ligand addition was obtained from 100 equal-sized areas that included all responding cells. The values represent the mean ± SE of at least six experiments.

Cycloheximide Nontaster Mice Have Mutations in the mT2R-5 Taste Receptor

Our demonstration that mT2R-5 functions as a high-affinity receptor for cycloheximide suggested that the *mT2R-5* gene might correspond to the *Cyx* locus. If this is true, we expected that either the expression profile or sequence of mT2R-5 might differ between strains categorized as *Cyx* tasters (DBA/2J) and nontasters (C57BL/6J) (Lush and Holland, 1988). In situ hybridizations to tissue sections demonstrated that the expression profile of mT2R-5 is indistinguishable between taster and nontaster strains (Figure 6). To determine the linkage between mT2R-5 and the *Cyx* locus, we identified polymorphisms in the *mT2R-5* gene and determined their distribution in a recombinant inbred panel

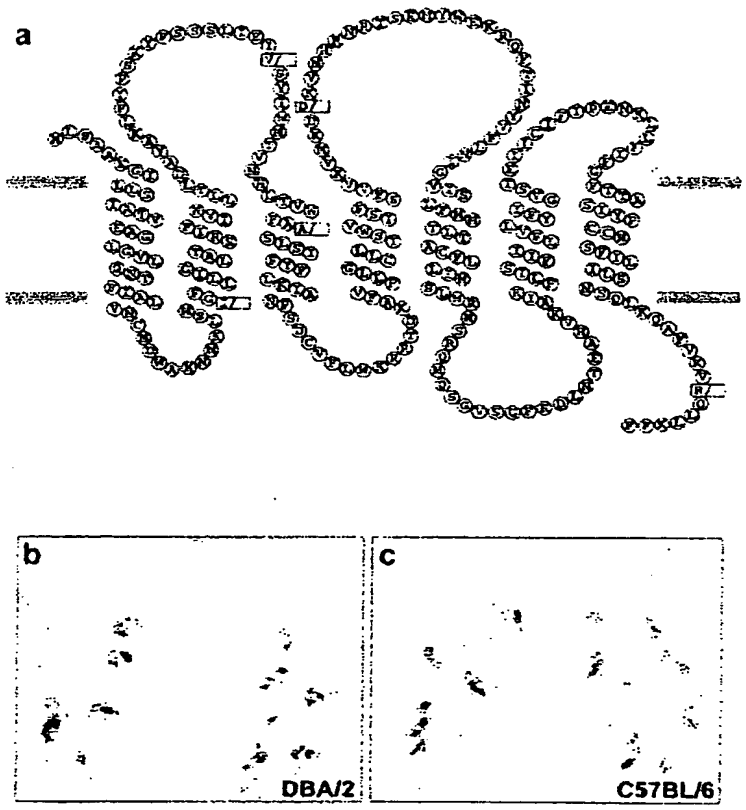

Figure 6. Cycloheximide Taster and Nontaster Strains Express Different Alleles of mT2R5

(a) Predicted transmembrane topology of mT2R-5; amino acid substitutions in the allele from nontaster strains are highlighted in red. The presence of only two alleles at this locus is not unexpected because the strains that share the same polymorphisms were derived from a common founder (Beck et al., 2000). In situ hybridization showing expression of mT2R-5 in subsets of cells in the circumvallate papilla of (b) a cycloheximide taster strain (DBA/2) and (c) a nontaster strain (C57BL/6); no strain specific differences in expression pattern were detected in taste buds from other regions of the oral cavity.

from a C57BL/6J (nontaster) × DBA/2J (taster) cross. We found tight linkage between mT2R-5 and the *Cyx* locus but not perfect concordance in their strain distribution pattern (data not shown). We believe that this is due to the reported ambiguity in the original designation of the cycloheximide phenotype of the recombinant inbred panel progeny and parental lines (Lush and Holland, 1988). We therefore isolated the *mT2R-5* gene from several additional well-characterized cycloheximide taster (CBA/Ca, BALB/c, C3H/He) and nontaster (129/Sv) strains and determined their nucleotide sequences. Indeed, as would be expected if mT2R-5 functions as the cycloheximide receptor in these strains, all the tasters share the same *mT2R-5* allele as DBA/2J, while the nontasters share the C57BL/6 allele, which carries missense mutations (Figure 6), including three nonconservative amino acid substitutions (T44I, G155D and L294R).

If the *mT2R-5* C57BL/6 allele is responsible for the taste deficiency of *Cyx* mutants, its cycloheximide dose response might recapitulate the sensitivity shift seen in *Cyx* mutant strains. Two-bottle preference tests have shown that *Cyx* taster strains avoid cycloheximide with a threshold of 0.25 μM (Lush and Holland, 1988), while nontasters have an ~8-fold decrease in sensitivity (e.g., they are nontasters at 1 μM, but strongly avoid cycloheximide at 8 μM). We constructed a rho-mT2R-5 fusion with the *mT2R-5* gene from a nontaster strain and compared its dose response with that of the receptor from taster strains. To prevent bias due to differences in receptor numbers in the heterologous cells, we measured surface expression and assayed mT2R-5 function from the same transfection experiments (see Experimental Procedures). Remarkably, mT2R-5 from the nontaster strains displays a shift in cycloheximide sensitivity (Figure 4d) that resembles the sensitivity of these strains to this bitter tastant. Taken together, these results validate mT2R-5 as a cycloheximide receptor and strongly suggest that mT2R-5 corresponds to the *Cyx* locus. Formal proof that mT2R-5 is *Cyx* will require the knockout of this gene in taster strains, or the phenotypic rescue of nontaster animals with an mT2R-5 transgene.

T2Rs Couple to Gustducin

In the accompanying paper (Adler et al., 2000), we demonstrated that T2Rs are coexpressed with gustducin, suggesting that T2Rs may activate this G protein in response to bitter tastants. To investigate the selectivity of T2R–G protein coupling, we chose to study mT2R-5 because its activation by cycloheximide recapitulates mouse taste responses. Because of the need to assay several G proteins and the lack of a cell-based gustducin assay, we used a cell-free system. Rho-tagged mT2R-5

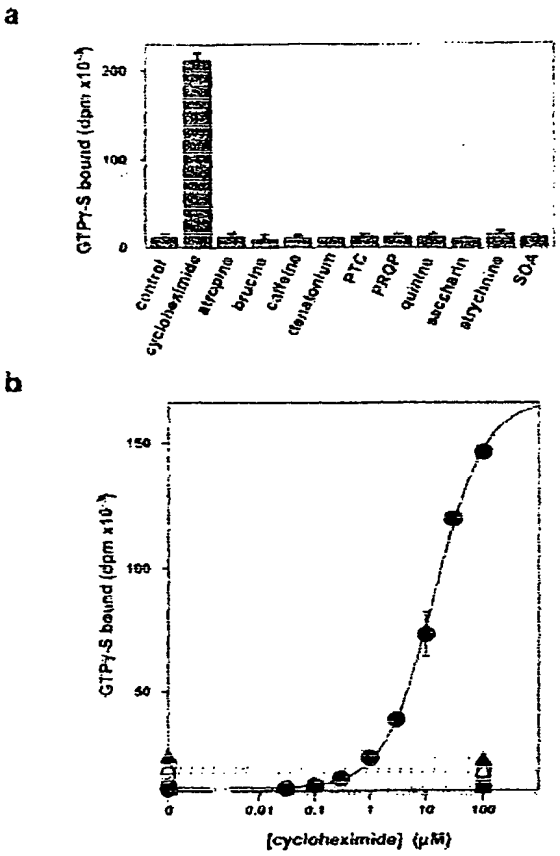

Figure 7. mT2R-5 Activates Gustducin in Response to Cycloheximide

(a) Insect larval cell membranes containing mT2R-5 activate gustducin in the presence 300 μM cycloheximide but not without ligand (control) or in the presence of 1 mM atropine, brucine, caffeine, denatonium, phenylthiocarbamide, 6-n-propyl thiouracil, quinine, saccharin, strychnine, sucrose octaacetate. (b) Cycloheximide concentration dependence of gustducin activation by mT2R-5 (filled circle) was fitted by single-site binding (K_a = 14.8 ± 0.9 μM). No cycloheximide-induced activity was detected in the presence of Gαo (filled triangle), Gαi (open triangle), Gαs (open square), or Gαq (filled square).

and gustducin were prepared using a baculovirus expression system. We incubated mT2R-5-containing membranes with various purified G proteins, including gustducin, and measured tastant-induced GTPγS binding (Hoon et al., 1995). Figure 7 shows the results of GTPγS binding assays, demonstrating exquisite cycloheximide-dependent coupling of mT2R-5 to gustducin. In contrast, no coupling was seen with Gαs, Gαi, Gαq, or Gαo. No significant GTPγS binding was observed in the absence of receptor, gustducin, or βγ heterodimers (data not shown). The high selectivity of T2R-5 for gustducin, and the exclusive expression of T2Rs in taste receptor cells that contain gustducin (Adler et al., 2000), affirm the hypothesis that T2Rs function as gustducin-linked taste receptors.

Concluding Remarks

To date, many putative taste receptors have been reported (Abe et al., 1993; Matsuoka et al., 1993; Ming et al., 1998; Hoon et al., 1999; Chaudhari et al., 2000). However, none have satisfied the requirements of rigorous biological verification: (1) demonstrated tissue and cell-specific expression, (2) functional validation, and (3) genetic corroboration. The T2R receptors presented in this and the accompanying paper were examined for all three criteria. First, we showed that T2Rs are selectively expressed in subsets of taste receptor cells of the tongue and palate epithelium. Second, three T2Rs (mT2R-5, hT2R-8, and mT2R-4) functioned as receptors for bitter tastants in heterologous cells. Third, polymorphisms in the mT2R-5 receptor were found to be associated with changes in bitter taste sensitivity to cycloheximide, both in vivo and in vitro. Thus, mT2R-5 is a strong candidate for *Cyx*. Furthermore, mT2R-5 selectively couples to gustducin, which has been implicated biochemically and genetically in taste transduction (Wong et al., 1996; Ming et al., 1998). Together, these results demonstrate that the T2R gene family contains functionally defined bitter taste receptors.

At present, we do not know what fraction of the available human and rodent receptors function in bitter transduction. However, our demonstration that all T2R-positive taste cells express multiple receptors suggests that T2R receptors may function in a similar taste modality. This is consistent with the observation that mammals can recognize a large number of bitter compounds, but do not discriminate between them (McBurney and Gent, 1979). Indeed, the two mouse receptors presented in this study (mT2R-5 and mT2R-8) respond to different bitter tastants and are expressed in combination with a number of other T2Rs in overlapping taste receptor cells (data not shown). Alternatively, if T2Rs respond to more than one modality, for example bitter and sweet then these cells would have to functionally segregate T2R receptors so as to maintain specificity and selectivity of signaling (Tsunoda et al., 1998).

A number of studies have shown that the oral cavity displays regional differences in sensitivity to the various taste modalities (Frank et al., 1983; Nejad, 1986; Frank, 1991). Our demonstration that T2Rs are expressed in all taste buds of circumvallate, foliate, and palate taste buds indicates that if there are significant differences in bitter sensitivity between these three regions, they may reflect events distal to tastant recognition.

The discovery of bitter taste receptors makes it possible to experimentally approach and elucidate critical aspects of the logic of bitter coding. For instance, it should be possible to genetically mark mT2R-expressing cells and examine their physiology and connectivity patterns. Similarly, it will be possible to knock out selective subsets of mT2R receptors and study the impact on bitter taste perception.

Taste receptor cells turn over throughout life (Beidler and Smallman, 1965). Therefore, synapses need to be continuously reestablished. It will be interesting to determine how this is achieved and whether nerve terminals provide any instructive signals for the expression of T2R receptors. The observation that taste buds degenerate when denervated and regenerate when the gustatory

epithelium is reinnervated provides a tractable experimental paradigm to address this question. Finally, the identification of human bitter receptors makes it possible to use high-throughput screening strategies to identify bitter antagonists, and in a small but significant way, eliminate bitterness from the world.

Experimental Procedures

Generation, Expression, and Immunostaining of Chimeric Receptors

A bridge overlap PCR extension technique was used to generate rho-T2R chimeras, which contain the first 39 amino acids of bovine rhodopsin in frame with human and rodent T2R coding sequences (Mehta and Singh, 1999). The rhodopsin segment was amplified from a bovine cDNA clone kindly provided by Dr. J. Nathans. All receptors were cloned into a pEAK10 mammalian expression vector (Edge Biosystems, MD). The rho-mGluR1 chimeras were constructed using a similar strategy.

Modified HEK-293 cells (PEAK^{rapid} cells; Edge BioSystems, MD) were grown and maintained at 37°C in UltraCulture medium (Bio Whittaker) supplemented with 5% fetal bovine serum, 100 μg/ml Gentamycin sulphate (Fisher), 1 μg/ml Amphotericin B, and 2 mM GlutaMax I (Lifetechnologies). For transfection, cells were seeded onto matrigel-coated 24-well culture plates or 35 mm recording chambers. After 24 hr at 37°C, cells were washed in OptiMEM medium (Lifetechnologies) and transfected using LipofectAMINE reagent (Lifetechnologies). Transfection efficiencies were estimated by cotransfection of a GFP reporter plasmid and were typically >70%. Immunofluoresence staining and activity assays were performed 36–48 hr after transfection.

For immunostaining transfected cells were grown on coated glass coverslips, fixed for 20 min in ice-cold 2% paraformaldehyde, blocked with 1% BSA, and incubated for 4–6 hr at 4°C in blocking buffer containing a 1:1000 dilution of anti-rhodopsin mAb B6–30 (Hargrave et al., 1986). Chimeric receptor expression was visualized using FITC-coupled donkey anti-mouse secondary antibody (Jackson Immunochemical). Surface expression of *mT2R-5* alleles was estimated by ELISA measurements using antibodies against the rhodopsin N-terminal tag. Transfected cells were seeded in 96-well dishes (~4 × 10^4 cells per well) for ELISA experiments and in 35 mm recording chambers for parallel functional assays. Nonpermeabilized cells were fixed in cold 2% paraformaldehyde for 20 min, washed, blocked with PBS + 1% BSA, and incubated with the B6–30 anti-rhodopsin antibody. Surface receptors were detected using peroxidase-conjugated goat anti-mouse antibodies and quantified using a Kinetic microplate reader (Molecular Devices, CA). In all cases, similar numbers of cells were examined. The ratio of surface expression of nontaster/taster alleles was found to be 1.34 ± 0.19 (n = 144 wells in 3 independent transfections). In situ hybridization was carried out as described previously (Hoon et al., 1999).

Calcium Imaging

Transfected cells were washed once in Hank's balanced salt solution with 1 mM sodium pyruvate and 10 mM HEPES, pH 7.4 (assay buffer), and loaded with 2 μM FURA-2 AM (Molecular Probes) for 1 hr at room temperature. The loading solution was removed and cells were incubated in 200 μl of assay buffer for 1 hr to allow the cleavage of the AM ester. For most experiments, 24-well tissue culture plates containing cells expressing a single rho-T2R were stimulated with 200 μl of a 2× tastant solution (see next section). $[Ca^{2+}]_i$ changes were monitored using a Nikon Diaphot 200 microscope equipped with a 10×/0.5 fluor objective with the TILL imaging system (T.I.L.L. Photonics GmbH). Acquisition and analysis of the fluorescence images used TILL-Vision software. Generally, $[Ca^{2+}]_i$ was measured for 80–120 s by sequentially illuminating cells for 200 ms at 340 nm and 380 nm and monitoring the fluorescence emission at 510 nm using a cooled CCD camera. The F_{340}/F_{380} ratio was analyzed to measure $[Ca^{2+}]_i$. Kinetics of activation and deactivation were measured using a bath perfusion system. Cells were seeded onto a 150 μl microperfusion chamber, and test solutions were pressure-ejected with a picospritzer apparatus (General Valve, Inc.). Flow-rate was adjusted to ensure complete exchange of the bath solution within 4–5 s. In the case of mT2R-5, we either measured responses from 50 individual responding cells, or the entire camera field since >70% of the cells responded to cycloheximide. For mT2R-8 and hT2R-4, we averaged 100 areas of interest in each experiment.

List of Tastants

The following tastants were tested (maximum concentrations): 5 mM aristolochic acid, 5 mM atropine, 5 mM brucine, 5 mM caffeic acid, 10 mM caffeine, 1 mM chloroquine, 5 mM cycloheximide, 10 mM denatonium benzoate, 5 mM (−) epicatechin, 10 mM L-leucine, 10 mM L-lysine, 10 mM $MgCl_2$, 5 mM naringin, 10 mM nicotine, 2.5 mM papavarine hydrochloride, 3 mM phenyl thiocarbamide, 10 mM 6-n-propyl thiouracil, 1 mM quinacrine, 1 mM quinine hydrochloride, 800 μM raffinose undecaacetate, 3 mM salicin, 5 mM sparteine, 5 mM strychnine nitrate, 3 mM sucrose octaacetate, 2 mM tetraethyl ammonium chloride, 10 mM L-tyrosine, 5 mM yohimbine, 10 mM each of glycine, L-alanine, D-tryptophan, L-phenylalanine, L-arginine, sodium saccharin, aspartame, sodium cyclamate, acesulfame K, 150 mM each of sucrose, lactose, maltose, D-glucose, D-fructose, D-galactose, D-sorbitol, 0.1% monellin, 0.1% thaumatin. Additional sweet tastants were 150 μM alitame, 1.8 mM dulcin, 800 μM stevioside, 1.9 mM cyanosulfan, 600 μM neohesperidin dihydrochalcone, 10 mM xylitol, 9.7 mM H-Asp-D-Ala-OTMCP, 70 μM N-Dmb-L-Asp-L-Phe-Ome, 12 μM N-Dmb-L-Asp-D-Val-(S)-α methylbenzylamide, kindly provided by Dr. M. Goodman.

Recombinant Inbred Typing

The mT2R-5 coding sequence from the parental and each of the 26 C57BL/6J × DBA/2J (BXD) recombinant inbred lines (Research Genetics; Huntsville, AL) was amplified by PCR using primers flanking the coding sequence. Products were either sequenced, or analyzed for restriction site polymorphism at position 414 (+1 being the start of translation), which contains an AluI site in the DBA/2 allele, but not the C57BL/6 allele. In addition a similar strategy was used to analyze the sequence of mT2R-5 from other strains.

In Vitro Coupling of mT2R-5 to Gustducin

Infectious Bacmid containing rhodopsin-tagged mT2R-5 (DBA/2-allele) was produced using the Bac-to-Bac system (Lifetechnologies, MD). Insect larval cells were infected for 60 hr with recombinant Bacmid and membranes were prepared as described previously (Ryba and Tirindelli, 1995). Peripheral proteins were removed by treatment with 8 M urea and membranes were resuspended in 10 mM HEPES pH 7.5, 1 mM EDTA, and 1 mM DTT. The expression of rho-mT2R-5 was assessed by Western blot using mAb B6–30 and quantitated by comparison with known amounts of rhodopsin. Approximately 300 pmol of rho-mT2R-5 could be obtained from 2 × 10^8 infected cells. Gustducin and $G\beta_1\gamma_8$ heterodimers were isolated as described previously (Hoon et al., 1995; Ryba and Tirindelli, 1995). Recombinant Gαs, Gαq, and Gαi and bovine brain Gαo were generously provided by Dr. Elliott Ross. Receptor-catalyzed exchange of GDP for GTPγS on gustducin and other G protein α subunits was measured in the presence of 10 nM rho-mT2R-5, 100 μM GDP, and 20 μM $G\beta_1\gamma_8$ (Hoon et al., 1995). All measurements were made at 15 min time points and reflect the initial rate of GTPγS binding.

Acknowledgments

We thank Dr. Paul Negulescu from Aurora Biosciences (La Jolla, CA) for helpful discussions on orphan receptors and heterologous expression systems. We are particularly grateful to Laramiya Phillips for expert technical assistance with cells and cultures, and Dr. Elliott Ross for the generous gift of Gαs, Gαi, Gαo, and Gαq subunits. We also thank D. Cowan for great help with DNA sequencing, Dong Cao for help with Gα15 cells, and Drs. Lubert Stryer, Kristin Scott, Reuben Siraganian, Arlid Shirazi, and members of the Zuker lab for valuable help and advice. This work was supported in part by a grant from the National Institute on Deafness and Other Communication Disorders (to C. S. Z.). C. S. Z. is an investigator of the Howard Hughes Medical Institute.

Received February 4, 2000; revised February 25, 2000.

References

Abe, K., Kusakabe, Y., Tanemura, K., Emori, Y., and Arai, S. (1993). Primary structure and cell-type specific expression of a gustatory G protein-coupled receptor related to olfactory receptors. J. Biol. Chem. *268*, 12033–12039.

Adler, E., Hoon, M.A., Mueller, K.L., Chandrashekar, J., Ryba, N.J.P., and Zuker, C.S. (2000). A novel family of mammalian taste receptors. Cell *100*, this issue, 693–702.

Baker, E.K., Colley, N.J., and Zuker, C.S. (1994). The cyclophilin homolog NinaA functions as a chaperone, forming a stable complex in vivo with its protein target rhodopsin. EMBO J. *13*, 4886–4895.

Beck, J.A., Lloyd, S., Hafezparast, M., Lennon-Pierce, M., Eppig, J.T., Festing, M.F., and Fisher, E.M. (2000). Genealogies of mouse inbred strains. Nat. Genet. *24*, 23–55.

Beidler, L.M., and Smallman, R.L. (1965). Renewal of cells within taste buds. J. Cell Biol. *27*, 263–272.

Capeless, C.G., Whitney, G., and Azen, E.A. (1992). Chromosome mapping of Soa, a gene influencing gustatory sensitivity to sucrose octaacetate in mice. Behav. Genet. *22*, 655–663.

Chaudhari, N., Landin, A.M., and Roper, S.D. (2000). A metabotropic glutamate receptor variant functions as a taste receptor. Nat. Neurosci. *3*, 113–119.

Conneally, P.M., Dumont-Driscoll, M., Huntzinger, R.S., Nance, W.E., and Jackson, C.E. (1976). Linkage relations of the loci for Kell and phenylthiocarbamide taste sensitivity. Hum. Hered. *26*, 267–271.

Dwyer, N.D., Troemel, E.R., Sengupta, P., and Bargmann, C.I. (1998). Odorant receptor localization to olfactory cilia is mediated by ODR-4, a novel membrane-associated protein. Cell *93*, 455–466.

Frank, M.E. (1991). Taste-responsive neurons of the glossopharyngeal nerve of the rat. J. Neurophysiol. *65*, 1452–1463.

Frank, M.E., Contreras, R.J., and Hettinger, T.P. (1983). Nerve fibers sensitive to ionic taste stimuli in chorda tympani of the rat. J. Neurophysiol. *50*, 941–960.

Garcia, J., and Hankins, W.G. (1975). The evolution of bitter and the acquisition of toxiphobia. In Olfaction and Taste. V. Proceedings of the 5th International Symposium in Melbourne, Australia, D.A. Denton and J.P. Coghlan, eds. (New York: Academic Press), 39–45.

Glendinning, J.I. (1994). Is the bitter rejection response always adaptive? Physiol. Behav. *56*, 1217–1227.

Glendinning, J.I., Tarre, M., and Asaoka, K. (1999). Contribution of different bitter-sensitive taste cells to feeding inhibition in a caterpillar (Manduca sexta). Behav. Neurosci. *113*, 840–854.

Hargrave, P.A., Adamus, G., Arendt, A., McDowell, J.H., Wang, J., Szaby, A., Curtis, D., and Jackson, R.W. (1986). Rhodopsin's amino terminus is a principal antigenic site. Exp. Eye Res. *42*, 363–373.

Hoon, M.A., Northup, J.K., Margolskee, R.F., and Ryba, N.J.P. (1995). Functional expression of the taste specific G-protein, alpha-gustducin. Biochem. J. *309*, 629–636.

Hoon, M.A., Adler, E., Lindemeier, J., Battey, J.F., Ryba, N.J.P., and Zuker, C.S. (1999). Putative mammalian taste receptors: a class of taste-specific GPCRs with distinct topographic selectivity. Cell *96*, 541–551.

Kinnamon, S.C., and Cummings, T.A. (1992). Chemosensory transduction mechanisms in taste. Annu. Rev. Physiol. *54*, 715–731.

Krautwurst, D., Yau, K.W., and Reed, R.R. (1998). Identification of ligands for olfactory receptors by functional expression of a receptor library. Cell *95*, 917–926.

Kusano, T., Kasahara, Y., and Kawamura, Y. (1971). A study on taste effectiveness of cycloheximide as a repellent to rats. Appl. Exptl. Zool. *6*, 40–50.

Lefkowitz, R.J., Inglese, J., Koch, W.J., Pitcher, J., Attramadal, H., and Caron, M.G. (1992). G-protein-coupled receptors: regulatory role of receptor kinases and arrestin proteins. Cold Spring Harb. Symp. Quant. Biol. *57*, 127–133.

Lindemann, B. (1996a). Chemoreception: tasting the sweet and the bitter. Curr. Biol. *6*, 1234–1237.

Lindemann, B. (1996b). Taste reception. Physiol. Rev. *76*, 718–766.

Lush, I.E. (1984). The genetics of tasting in mice. III. Quinine. Genet. Res. *44*, 151–160.

Lush, I.E. (1986). The genetics of tasting in mice. IV. The acetates of raffinose, galactose and beta-lactose. Genet. Res. *47*, 117–123.

Lush, I.E., and Holland, G. (1988). The genetics of tasting in mice. V. Glycine and cycloheximide. Genet. Res. *52*, 207–212.

Masu, M., Tanabe, Y., Tsuchida, K., Shigemoto, R., and Nakanishi, S. (1991). Sequence and expression of a metabotropic glutamate receptor. Nature *349*, 760–765.

Matsuoka, I., Mori, T., Aoki, J., Sato, T., and Kurihara, K. (1993). Identification of novel members of G-protein coupled receptor superfamily expressed in bovine taste tissue. Biochem. Biophys. Res. Commun. *194*, 504–511.

McBurney, D.H., and Gent, J.F. (1979). On the nature of taste qualities. Psychol. Bull. *86*, 151–167.

Mehta, R.K., and Singh, J. (1999). Bridge-overlap-extension PCR method for constructing chimeric genes. Biotechniques *26*, 1082–1086.

Ming, D., Ruiz-Avila, L., and Margolskee, R.F. (1998). Characterization and solubilization of bitter-responsive receptors that couple to gustducin. Proc. Natl. Acad. Sci. USA *95*, 8933–8938.

Nejad, M.S. (1986). The neural activities of the greater superficial petrosal nerve of the rat in response to chemical stimulation of the palate. Chemical Senses *11*, 283–293.

Offermanns, S., and Simon, M.I. (1995). G alpha 15 and G alpha 16 couple a wide variety of receptors to phospholipase C. J. Biol. Chem. *270*, 15175–15180.

Reed, D.R., Nanthakumar, E., North, M., Bell, C., Bartoshuk, L.M., and Price, R.A. (1999). Localization of a gene for bitter-taste perception to human chromosome 5p15. Am. J. Hum. Genet. *64*, 1478–1480.

Reisine, T. (1995). Opiate receptors. Neuropharmacology *34*, 463–472.

Ryba, N.J.P., and Tirindelli, R. (1995). A novel GTP-binding protein gamma-subunit, G gamma 8, is expressed during neurogenesis in the olfactory and vomeronasal neuroepithelia. J. Biol. Chem. *270*, 6757–6767.

Sardi, A. (1984). Structure-activity relationship of a bitter compound: denatonium chloride. Naturwissenschaften *71*, 428–429.

Stewart, R.E., DeSimone, J.A., and Hill, D.L. (1997). New perspectives in a gustatory physiology: transduction, development, and plasticity. Am. J. Physiol. *272*, C1–C26.

Tsien, R.Y., Rink, T.J., and Poenie, M. (1985). Measurement of cytosolic free Ca^{2+} in individual small cells using fluorescence microscopy with dual excitation wavelengths. Cell Calcium *6*, 145–157.

Tsunoda, S., Sierralta, J., and Zuker, C.S. (1998). Specificity in signaling pathways: assembly into multimolecular signaling complexes. Curr. Opin. Genet. Dev. *8*, 419–422.

Warren, R.P., and Lewis, R.C. (1970). Taste polymorphism in mice involving a bitter sugar derivative. Nature *227*, 77–78.

Whitney, G., and Harder, D.B. (1986). Single-locus control of sucrose octaacetate tasting among mice. Behav. Genet. *16*, 559–574.

Wong, G.T., Gannon, K.S., and Margolskee, R.F. (1996). Transduction of bitter and sweet taste by gustducin. Nature *381*, 796–800.